CTR D-STOP

Technical Report 104

Project:
Transit Demand and Routing after Autonomous Vehicle Availability

Author
Stephen Boyles (CTR)

December 2015

Data-Supported Transportation Operations & Planning Center (D-STOP)

A Tier 1 USDOT University Transportation Center at The University of Texas at Austin

D-STOP is a collaborative initiative by researchers at the Center for Transportation Research and the Wireless Networking and Communications Group at The University of Texas at Austin.

1. Report No. D-STOP/2016/104	2. Government Accession No.	3. Recipient's Catalog No.
4. Title and Subtitle Transit Demand and Routing after Autonomous Vehicle Availability		5. Report Date December 2015
		6. Performing Organization Code
7. Author(s) Stephen Boyles, Michael W. Levin, Rahul Patel, Melissa Duell, S. Travis Waller		8. Performing Organization Report No. Report 104
9. Performing Organization Name and Address Data-Supported Transportation Operations & Planning Center (D-STOP) The University of Texas at Austin 1616 Guadalupe Street, Suite 4.202 Austin, Texas 78701		10. Work Unit No. (TRAIS)
		11. Contract or Grant No. DTRT13-G-UTC58
12. Sponsoring Agency Name and Address Data-Supported Transportation Operations & Planning Center (D-STOP) The University of Texas at Austin 1616 Guadalupe Street, Suite 4.202 Austin, Texas 78701		13. Type of Report and Period Covered
		14. Sponsoring Agency Code

15. Supplementary Notes

16. Abstract

Autonomous vehicles (AVs) create the potential for improvements in traffic operations as well as new behaviors for travelers such as car sharing among trips through driverless repositioning. Most studies on AVs have focused on technology or traffic operations, and the impact of AVs on planning is currently unknown. Development of a planning model integrating AV improvements to traffic operations and the impact of new traveler behavior options will soon be of practical interest as AVs are currently test-driven on public roads. The altered traveler preferences may affect mode choice, leading to changes in transit demand and transit provider cost. An analysis of the model on metropolitan planning data will provide predictions on the impact of general AV ownership on network conditions.

This project report combines five papers on this topic:

1. Effects of Autonomous Vehicle Behavior on Arterial and Freeway Networks
2. A Multiclass Cell Transmission Model for Shared Human and Autonomous Vehicle Roads
3. Intersection Auctions and Reservation-Based Control in Dynamic Traffic Assignment
4. The Impact of Autonomous Vehicles on Traffic Management: The Case of Dynamic Lane Reversal
5. Bus Routing Problem for KIPP Charter Schools

17. Key Words
Autonomous vehicles, AVs, dynamic traffic assignment, DTA
	18. Distribution Statement
	No restrictions. This document is available to the public through NTIS (http://www.ntis.gov):
	    National Technical Information Service
	    5285 Port Royal Road
	    Springfield, Virginia 22161		

19. Security Classif. (of this report) Unclassified	20. Security Classif. (of this page) Unclassified	21. No. of Pages 86	22. Price

Form DOT F 1700.7 (8-72)   **Reproduction of completed page authorized**

Disclaimer

The contents of this report reflect the views of the authors, who are responsible for the facts and the accuracy of the information presented herein. Mention of trade names or commercial products does not constitute endorsement or recommendation for use.

Acknowledgements

.

Table of Contents

Effects of autonomous vehicle behavior on arterial and freeway networks

Rahul Patel
Research Assistant
Department of Civil, Architectural and Environmental Engineering
The University of Texas at Austin
301 E. Dean Keeton St. Stop C1761
Austin, TX 78712-1172
Phone: 512-471-3548, Fax: 512-475-8744
E-Mail: rahul428@sbcglobal.net

Michael W. Levin (corresponding author)
Graduate Research Assistant
Department of Civil, Architectural and Environmental Engineering
The University of Texas at Austin
301 E. Dean Keeton St. Stop C1761
Austin, TX 78712-1172
Phone: 512-471-3548, Fax: 512-475-8744
E-Mail: michaellevin@mail.utexas.edu

Stephen D. Boyles
Assistant Professor
Department of Civil, Architectural and Environmental Engineering
The University of Texas at Austin
301 E. Dean Keeton St. Stop C1761
Austin, TX 78712-1172
Phone: 512-471-3548, Fax: 512-475-8744
E-Mail: sboyles@mail.utexas.edu

6263 words+ 5 figures + 3 tables

ABSTRACT
Autonomous vehicles offer new traffic behaviors that could revolutionize transportation, such as the reservation-based intersection control and reduced reaction times that result in greater road capacity. Most studies have used micro-simulation models of these new technologies to more realistically study their impacts. However, micro-simulation is not tractable for larger networks. Recent developments in simulating reservation-based controls and multiclass cell transmission models for autonomous vehicles in dynamic traffic assignment have allowed studies of larger networks. This paper presents analyses of several highly congested arterial and freeway networks to quantify how reservations and reduced reaction times affect travel times and congestion. Reservations were observed to improve over signals in most situations. However, signals outperformed reservations in a congested network with several close local road-arterial intersections because the capacity allocations of signals were more optimized for the network. Reservations also were less efficient than traditional merges/diverges for on- and off-ramps. On the other hand, the increased capacity due to reduced following headways resulted in significant improvements for both freeway and arterial networks. Finally, we studied a downtown network, including freeway, arterial, and local roads, and found that the combination of reservations and reduced following headways resulted in a 78% reduction in travel time.

1 INTRODUCTION

Autonomous vehicles (AVs) offer new traffic behaviors that could revolutionize city transportation. New intersection controls *(1, 2)* could reduce intersection delays *(3, 4)* and adaptive cruise control and/or reduced reaction times could similarly increase road capacity *(5, 6)*. On the other hand, AVs could offset these improvements by increasing travel demand. Levin & Boyles *(7)* found that allowing empty repositioning trips to avoid parking costs could result in overall *increases* in congestion. Furthermore, the Braess and Daganzo paradoxes *(8, 9)* demonstrate that improvements in capacity could increase congestion due to selfish route choice.

Most previous studies of AVs have relied on microsimulators to capture AV behavior differences, but micro-simulation is not tractable for large network analyses. Carlino et al. *(10)* simplified the reservation controls to simulate a city network, but the capacity of the reservation mechanism was reduced and they did not include route choice. Ideally, analyses of large networks would be based on dynamic traffic assignment (DTA), which includes the effects of selfish route choice. Levin & Boyles *(11)* developed a conflict region simplification of the reservation protocol that is tractable for dynamic traffic assignment (DTA), and Levin & Boyles *(12)* developed a multiclass version of the cell transmission model (CTM) by Daganzo *(13, 14)* with a corresponding car following model that predicts increases in capacity and backwards wave speed as reaction-time decreases. The purpose of this paper is to use these DTA models to study how AVs affect larger networks.

The contributions of this paper are to analyze the effects of reservation controls and increased capacity from AV technologies on freeway and arterial networks using DTA. We studied a variety of subnetworks from the 100 most congested roads in Texas, and drew conclusions that can be generalized to other locations. For most scenarios, reservations improved over traffic signals for arterial networks (and the freeway network that used signals to control access), but were not effective at replacing merges/diverges. Reduced reaction times, resulting in reduced following headways and increased capacity, improved travel times for all scenarios. We also studied the downtown Austin network, which includes many route choice options, and found that the combination of these AV technologies could reduce travel times by 78%.

The remainder of this paper is organized as follows. Section 2 describes models of reservation-based intersection control, and Section 3 summarizes the work of Levin & Boyles *(12)* on a reaction-time based multiclass CTM model for AVs. Both of these are used in Section 4, which analyzes the effects of AVs on several arterial and freeway networks. We conclude in Section 5.

2 INTERSECTION MODEL

Dresner & Stone *(1, 2)* proposed the reservation-based intersection protocol for AVs to use AV technologies to increase intersection utilization. Traffic signals are not the most efficient use of intersection capacity because during any phase, many turning movements are completely restricted. In moderate traffic, there may be gaps in the stream sufficient to move vehicles on conflicting turning movements. In addition, clearance intervals result in significant lost time per cycle. However, these are necessary for human drivers to ensure safety.

In reservation-based controls, vehicles communicate wirelessly with an *intersection manager* to request to move through the intersection at a specific time. The intersection manager simulates the request in a grid of space-time tiles and accepts or rejects it depending on whether it conflicts with other reservations. When conflicts occur, most studies *(1, 2, 3, 4)* have used a first-come-first-serve (FCFS) priority: the reservation of the vehicle that requested first is granted. However, alternative policies have also been studied, such as prioritizing emergency vehicles *(15)* or even holding an auction at each intersection to allow vehicles to bid to move first *(16, 17, 18)*, which was found to be an improvement over FCFS in some scenarios.

Results by Fajardo et al. *(3)* in Dresner & Stone's AIM4 simulator and Li et al. *(4)* in VISSIM indicated that FCFS reservations could reduce delays beyond optimized traffic signals. However, most network-based studies have been limited by the computational complexity of the simulation of vehicles through the intersection space-time tiles in the reservation protocol. Micro-simulation studies have therefore been limited to small networks *(19)* or made major simplifications to the reservation protocol that reduced its capacity *(10)*. Levin & Boyles *(11)* addressed the computational issues by aggregating the tiles into *conflict regions*, illustrated in Figure 1, and replacing the simultaneous occupancy checks of the tile-based reservation protocol with capacity constraints.

Each time step, the conflict region algorithm considers the list of vehicles that are waiting and able to enter the intersection, S. This is the set of vehicles that are at the intersection and in front of their lane (so they are not blocked from moving by other vehicles). The algorithm then sorts S according to some priority function $f(\cdot)$. (For FCFS, the priority function is their reservation request time.) Next, the algorithm iterates through S until it finds a vehicle v that can move through the intersection (moving could be obstructed by conflict region capacity or receiving flow in the downstream link). v's reservation request is granted, and the vehicle waiting behind v is added to S in sorted order. The algorithm continues to look through S until none of the vehicles in S are able to move.

The conflict region model was shown to be tractable for DTA on city networks while retaining the simultaneous-use characteristics of reservation controls. The purpose of this paper is to use the conflict region model, as well as the later multiclass CTM model of Levin & Boyles *(12)*, to study how increasing use of AVs will affect the traffic efficiency of arterial and freeway networks.
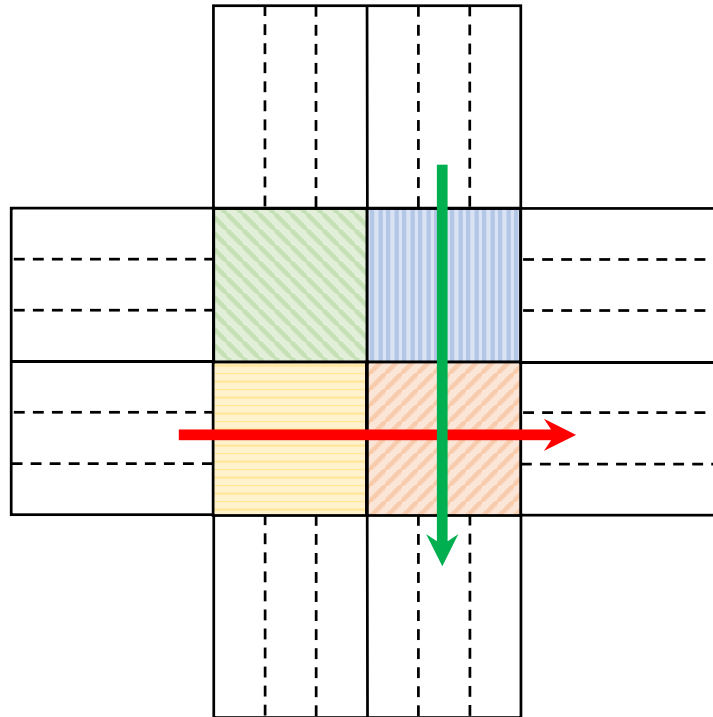
FIGURE 1 Conflict region representation of a four-way intersection, showing two conflicting turning movements

The reservation protocol may also be extended for human vehicles. Human vehicles have two potential issues when using a reservation system: two-way communication and following a reservation. For AVs, communication of reservation requests usually involves short-range wireless communications with the intersection manager. Humans might be able to inform the intersection manager of their request through a smart-phone app. However, vehicles typically must communicate their ETA at the intersection, which might not be known if there are vehicles in front. The protocol for using a smartphone app could be quite complex. To solve the communications issue, Dresner & Stone *(15, 20)* proposed inserting a cycling green light into the reservation protocol to allow human vehicles to move.

In addition, following the reservation is difficult for human vehicles because of the required precision in speed, acceleration, entrance time, and the vehicle's travel through the intersection to avoid conflicts with other vehicles. Humans following a smartphone app would have less precision and would therefore require greater safety margins than AVs. Bento et al. *(21)* and Qian et al. *(22)* studied methods of integrating human vehicles into the reservation protocol directly. Bento et al. *(21)* proposed reserving additional safety margins for human vehicles, and Levin et al. *(12)* implemented this into the conflict region model.

3 FLOW MODEL

In addition to new intersection controls, connected or autonomous vehicles could reduce reaction times, resulting in reduced following headways. Micro-simulation studies of adaptive cruise control have observed increases in capacity *(5, 6)* and stability *(23, 24)*. However, a micro-simulation model is not tractable for city network modeling. This section summarizes the multiclass CTM model and fundamental diagram developed by Levin & Boyles *(12)* to estimate capacity and backwards wave speed as a function of vehicle class proportions and their reaction

times. This model is used to propagate flow in our DTA analyses. For a complete discussion of the multiclass CTM conservation of flow and the effects of AV reaction times on capacity and backwards wave speed, see Levin & Boyles *(12)*.

Since the focus is on vehicles with identical or similar physical characteristics but different drivers, we assume that all vehicles have the same free flow speed. Note that although all vehicles have the same free flow speed, human vehicles and AVs respond differently to congestion due to different reaction times. AVs will maintain free flow speed at higher densities than human vehicles would be able to, and have correspondingly higher capacity. In addition, congested shockwaves propagate faster for AVs. In our cell discretization, we also assume a uniform distribution of class-specific density per cell, although of course those densities may change each time step. The model admits an arbitrary number of vehicle classes to be extensible to different levels of automation.

3.1 Multiclass cell transmission model

Let M be the set of vehicle classes with class-specific density $k_m(x,t)$ at space-time point (x,t) and class-specific flow $q_m(x,t) = u\left(\frac{k_1}{k}, \dots, \frac{k_{|M|}}{k}\right) k_m(x,t)$, a function of the speed $u(k_1, \dots, k_{|M|})$ possible with class proportions of $\frac{k_1}{k}, \dots \frac{k_{|M|}}{k}$. Similarly, let $w\left(\frac{k_1}{k}, \dots, \frac{k_{|M|}}{k}\right)$ be the backwards wave speed function. Then speed is limited by free flow speed, capacity, and backwards wave propagation:

$$u(k_1, \dots, k_{|M|}) = \min\left\{u^{\mathrm{f}}, \frac{q^{\max}\left(\frac{k_1}{k}, \dots, \frac{k_{|M|}}{k}\right)}{k}, w\left(\frac{k_1}{k}, \dots, \frac{k_{|M|}}{k}\right)\left(k^{\mathrm{jam}} - k\right)\right\} \tag{1}$$

where u^{f} is the free flow speed, $q^{\max}\left(\frac{k_1}{k}, \dots, \frac{k_{|M|}}{k}\right)$ is the capacity function, and k^{jam} is the jam density. For the cell discretization, let $n_i^m(t)$ be the number of vehicles of class m in cell i at time t and $y_i^m(t)$ be the transition flow of class m from cell i to cell $i+1$ at time t. We assume that the fundamental diagram is trapezoidal, bounded by the free flow speed u^{f}, cell-time specific capacity $Q_i(t)$, and cell-time specific backwards wave speed $w_i(t)$:

$$y_i^m(t) = \frac{n_{i-1}^m(t)}{n_{i-1}(t)} \min\left\{\sum_{m \in M} n_{i-1}^m(t), Q_i(t), \frac{w_i(t)}{u^{\mathrm{f}}}\left(N - \sum_{m \in M} n_i^m(t)\right)\right\} \tag{2}$$

$$= \min\left\{n_{i-1}^m(t), \frac{n_{i-1}^m(t)}{n_{i-1}(t)} Q_i(t), \frac{n_{i-1}^m(t)}{n_{i-1}(t)} \frac{w_i(t)}{u^{\mathrm{f}}}\left(N - \sum_{m \in M} n_i^m(t)\right)\right\} \tag{3}$$

which shows that flow of class m is restricted by three factors: first, class-specific cell occupancy; second, proportional share of the capacity; and third, proportional share of congested flow. $Q_i(t)$ and $w_i(t)$ are functions of the proportion of classes. These transition flows satisfy conservation of flow, consistent with the multiclass hydrodynamic theory *(12)*.

When implementing this CTM, it is necessary for $w_i(t) \leq u^{\mathrm{f}}$ so that the cell length is determined by the free flow speed and not the backwards wave speed. This is usually satisfied by single-class flow, and may be satisfied for multiclass flow depending on the reaction time chosen for the car following model. We also note that assuming uniformly distributed density results in

the possibility of non-FIFO behavior within cells. However, as discussed by Blumberg and Bar-Gera *(25)*, even single class CTMs may violate FIFO at intersections.

3.2 Link capacity and backwards wave speed

To determine $Q_i(t)$ and $w_i(t)$, we use the car following model from Levin & Boyles *(12)* based on kinematics that predicts the safe following distance as a function of reaction time.

Backwards wave speed increases as reaction time decreases, which is consistent with micro-simulation results by Schakel et al. *(24)*.

For heterogeneous flow, equation (8) must be satisfied by all vehicles:

Capacity is

$$q^{\max} = \frac{u^{\mathrm{f}}}{u^{\mathrm{f}}\sum_{m\in M}\frac{k_m}{k}\Delta t_m + \ell} \tag{4}$$

where Δt_m is the reaction time of class m and ℓ is vehicle length. Backwards wave speed is

$$w = -\frac{\frac{u^{\mathrm{f}}}{u^{\mathrm{f}}\sum_{m\in M}\frac{k_m}{k}\Delta t_m + \ell}}{\frac{1}{u^{\mathrm{f}}\sum_{m\in M}\frac{k_m}{k}\Delta t_m + \ell} - \frac{1}{\ell}} = \frac{\ell}{\sum_{m\in M}\frac{k_m}{k}\Delta t_m} \tag{5}$$

Backwards wave speed increases as reaction time decreases, which is consistent with micro-simulation results by Schakel et al. *(24)*. Figure 2 shows how the fundamental diagram changes with AV proportion when human drivers have a reaction time of 1 second *(26)* and autonomous vehicles have a reaction time of 0.5 second for a link with free flow speed of 60 miles per hour. Figure 2 illustrates the flow model used for all links in our experiments. The specific fundamental diagram for each link depends on its free flow speed and AV proportion.

As discussed in Levin & Boyles *(12)*, capacity is affected by other factors such as lane width and road condition. To integrate the capacity and backwards wave speed predictions in equations (4) and (5) into current CTM models, we scale the estimated current capacity $\bar{q}^{\max}$ and backwards wave speed $\bar{w}$ accordingly:

$$\tilde{q}^{\max} = \frac{u^{\mathrm{f}}\Delta t_{\mathrm{HM}} + \ell}{u^{\mathrm{f}}\sum_{m\in M}\frac{k_m}{k}\Delta t_m + \ell}\bar{q}^{\max} \tag{6}$$

$$\tilde{w} = \frac{\Delta t_{\mathrm{HM}}}{\sum_{m\in M}\frac{k_m}{k}\Delta t_m}\bar{w} \tag{7}$$

$\tilde{q}^{\max}$ and $\tilde{w}$ are then used to determine flow for the trapezoidal fundamental diagram in CTM.
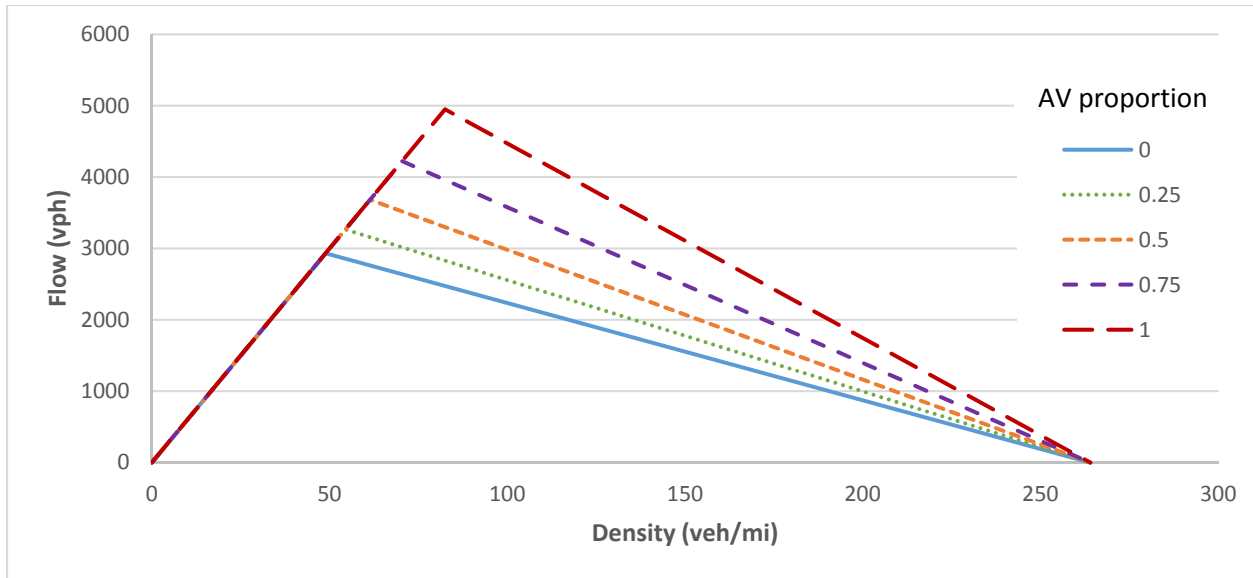
FIGURE 2 Fundamental diagram scaling with proportion of AVs with 0.5s reaction time and 60mph free flow speed

4 EXPERIMENTAL RESULTS

This section presents analyses on arterial, freeway, and downtown networks using the multiclass CTM to propagate flow in DTA. The key features of these results are the multiclass comparison of human and autonomous vehicles, and the analysis of how reservations compare to signals. The fundamental diagram changes with space and time in response to the proportion of AVs in each cell. When combined with discrete vehicles, the fundamental diagram varies significantly between cells and time steps despite an overall fixed proportion of AVs. Reservation-based intersection control also exhibited unusual characteristics. Contrary to the results of Fajardo et al. *(3)* and Li et al. *(4)*, reservations performed *worse* than signals in many scenarios due to suboptimal vehicle priority. In addition, Daganzo *(27)* showed that the increasing capacity due to AVs does not necessarily result in improved network performance.

The arterial and freeway networks do not have multiple available routes, so all improvements are due to AV technologies. However, the downtown networks include many alternate routes, which admits paradoxes in which capacity improvements increase congestion due to selfish route choice *(8, 9)*. The reaction times of AVs was set to 0.5 seconds, which significantly increases capacity (Figure 2). Smaller reaction times might be more realistic of automation, but could result in backwards wave speed exceeding free flow speed, causing technical issues with the cell transmission model. For all experiments, we recorded the total system travel time (TSTT) as well as the average travel time per vehicle.

4.1 Arterial Networks

We first present results on two arterial networks, shown in Figure 3. The first arterial network, Lamar & 38th Street, contains the intersection between the Lamar & 38th Street arterials, as well as 5 other local road intersections. This network contains 31 links, 17 nodes and 5 signals with a total demand of 16,284 vehicles over a 4 hour time period. We also studied Congress Avenue in Austin, with a total of 25 signals in the network, 216 links and 122 nodes with a total demand of

64,667 vehicles in a 4 hour period. These arterial networks used fixed-time signals for controlling flow along the entire corridor. These networks were chosen for this experiment because they are among the 100 most congested networks in Texas, which is useful for studying how AVs affect congestion. By changing the demand on these networks, our analyses can be generalized to less congested networks.

Lamar & 38ᵗʰ Street   Congress Avenue

FIGURE 3 Arterial networks

Travel time results for arterial networks are shown in Table 1. The general trend for the arterial networks is that the use of the reservation protocol reduced travel times. Although reservations helped most arterial networks such as Congress Avenue and, at high demands the reservations increased travel times for Lamar & 38ᵗʰ St. The lower 0.5 second reaction time for AVs compared to the 1 second reaction time for HV's decreased travel times for every network tested. As the proportion of AVs in the network was increased, the travel times would decrease. Reduced reaction times were more beneficial in some scenarios than in others, but all saw a benefit. The reaction time difference was analyzed by running simulations of each demand proportion at 0% and 100% AVs.

In the Lamar & 38ᵗʰ Street network, the reservation protocol significantly decreased travel times for a 50% demand simulation as compared to traffic signals at 50% demand; however, once the demand was increased to 75%, reservations began increase travel times relative to signals. This is most likely due to the close proximity of the local road intersections. On local road-arterial intersections, the fairness attribute of FCFS reservations, could give greater capacity to the local road than would traffic signals. Because these intersections are so close together, reservations likely induced queue spillback on the arterial. The longer travel times might also be influenced to reservations removing signal progression on 38ᵗʰ Street. In high congestion, FCFS reservations tended to be less optimized than signals for the local road-arterial intersections. On the other hand, in low demand, intersection saturation was sufficiently low for reservations to reduce delays.

The Lamar & 38th Street network responded well to an increase in the proportion of AVs with dramatic decreases in travel times, due to the AV reaction times. At 85% demand and at 25% AVs, the total travel time was reduced by 50%, and when all vehicles were AVs, the total travel time was reduced by 87%. As demand increased, the improvements from reduced reaction times also increased. At 50% demand, reduced reaction times decreased travel time by 44%, whereas at 100% demand, reduced reaction times decreased travel time by 93%. The effect of greater capacity improved as demand increased because as demand increased, the network became more limited by intersection capacity. At low congestion (50% demand), signal delays dominated travel times because reservations made significant improvements. At higher congestion, intersection capacity was the major limitation, and therefore reduced reaction times were of greater benefit.

Congress Avenue responded well to the introduction of reservations, showing decreases in travel times at all demand scenarios. These improvements are due to the large amount of streets intersecting Congress Avenue, each with a signal not timed for progression. The switch to reservations therefore reduced the intersection delay. However, the switch to reservations could result in greater demand on this arterial. We include the effects of route choice in the downtown Austin network (Section 4.3).

AVs also improved travel times and congestion due to reduced reaction times. At 85% demand, even a 25% proportion of AVs on roads decreased travel times by almost 60%. This increased to almost 70% when all vehicles were AVs. As with Lamar & 38th Street, as demand increased, the improvements from AV reaction times also increased. For example, at 50% demand, 100% AVs decreased travel time by about 10%, but at 100% demand, using all AVs reduced the travel time by nearly 82%. The reduced reaction times did not improve as much as the reservation protocol, except for the 100% demand scenario. This indicates that at lower demands, travel time was primarily increased by signal delay – but was still improved by AV reaction times.

Overall, these results consistently show significant improvements from reduced reaction times of AVs at all demand scenarios. As shown in Figure 2, reducing the reaction time to 0.5 seconds nearly doubles road and intersection capacity. However, the effects of reservations were mixed. At low congestion, traffic signal delays had a greater effect on travel time, and in these scenarios reservations improved. Reservations also improved when signals were not timed for progression (although this may be detrimental to the overall system). However, as seen on Lamar & 38th Street, at high demand reservations performed worse than signals, particularly around local road-arterial intersections.

TABLE 1 Arterial network results

Intersections	Demand	Proportion of AVs	TSTT (hr)	Travel time per vehicle (min)
Lamar & 38th Street				
Signals	50%	0	421.6	3.11
Signals	50%	1	237.2	1.75
Reservations	50%	1	157.8	1.16
Signals	75%	0	2566.7	12.61
Signals	75%	1	372.7	1.83
Reservations	75%	1	2212.5	10.87
Signals	85%	0	3890.2	16.86
Signals	85%	0.25	2097.2	9.09
Signals	85%	0.5	504.8	2.19
Signals	85%	0.75	477.8	2.07
Signals	85%	1	476.8	2.07
Reservations	85%	1	4472.8	19.39
Signals	100%	0	7043.1	25.95
Signals	100%	1	526.6	1.94
Reservations	100%	1	8678.7	31.98
Congress Avenue				
Signals	50%	0	1366.1	2.54
Signals	50%	1	1220	2.26
Reservations	50%	1	821.5	1.52
Signals	75%	0	4306.1	5.33
Signals	75%	1	1957.1	2.42
Reservations	75%	1	1545.1	1.91
Signals	85%	0	8976.8	9.8
Signals	85%	0.25	3661.4	4
Signals	85%	0.5	3303.3	3.61
Signals	85%	0.75	2936.2	3.21
Signals	85%	1	2956	3.23
Reservations	85%	1	2934	3.2
Signals	100%	0	21484.4	19.93
Signals	100%	1	4038.2	3.75
Reservations	100%	1	8673.6	8.05

4.2 Freeway Networks

Next, we studied three freeway networks, shown in Figure 4. The first freeway network is the I-35 corridor in the Austin region which includes 220 links and 220 nodes with a total demand of

128,051 vehicles within a 4 hour span. (Due to the length, the on- and off-ramps are difficult to see in the image.) All intersections are off-ramps or on-ramps. The I-35 network is by far the most congested of the freeway networks and one of the most congested freeways in all of Texas, especially in the Austin Region. We also studied the US-290 network in the Austin Region with 97 links, 62 nodes, 5 signals and a total demand of 11,098 vehicles within 4 hours. Finally, we studied the Mopac Expressway in the Austin Region with 45 links, 36 nodes, and 4 signals with a total demand of 27,787 vehicles within 4 hours. This network includes a mix of merging and diverging ramps and signals which allows some interesting analyses. This network was chosen due to the large number of signals around the freeway. All freeway networks are also among the 100 most congested roads in Texas.
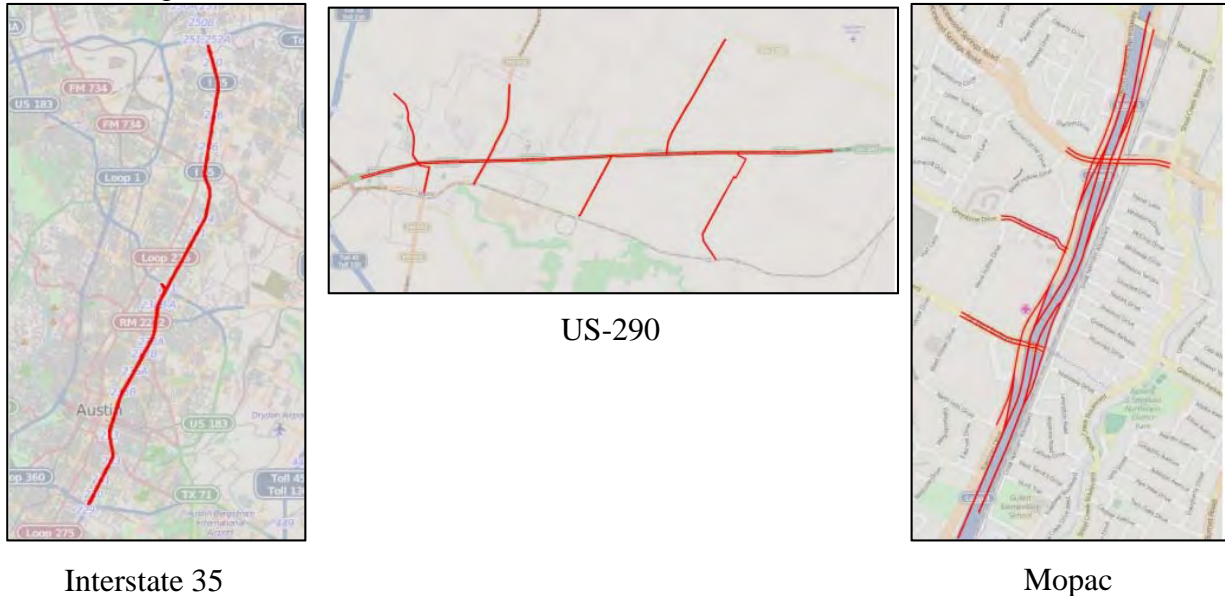

US-290

Interstate 35   Mopac

FIGURE 4 Freeway networks

Results for the freeway networks are presented in Table 2. Although there were some observed improvements in travel times for US-290 using reservations, the improvements were modest. For I-35 and Mopac, reservations made travel times worse for all demand scenarios. Most of the access on US-290 is controlled by signals, which explains the improvements observed when reservations were used there. Reservations seem to have worked more effectively with arterial networks, probably because on- and off-ramps do not have signal delays. Therefore the potential for improvement from reservations is smaller.

Overall, greater capacity from AVs' reduced reaction times improved travel times in all freeway networks tested, with better improvements at higher demands. Reduced reaction times improved travel times by almost 72% at 100% demand on I-35. On US-290 and I-35, as with the arterial networks, the improvement from AV reaction times increased as demand increased. This is because freeways are primarily capacity restricted. On Mopac, reaction times had a smaller impact, but the network overall appeared to be less congested.

We also analyzed several groups of links and nodes in depth. Links and nodes were chosen to study how reservations affected travel times at critical intersections, such as high demand on- or off-ramps. For these specific links, we compared average link travel times between 120 and 135 minutes into the simulation, at the peak of the demand. We compared human vehicles, AVs with signals, and AVs with reservations at 85% demand, which resulted in

moderate congestion. In the I-35 network, very few changes in travel times for the critical groups of links were observed from the different intersection controls.

The differences seemed to be greater in the US-290 corridor with more overall improvements in critical groupings of links near intersections. Interestingly, the largest improvements in travel times going from traffic signals to reservations occurred at queues for right turns onto the freeway. A possible explanation for this result is that making a right turn conflicts with less traffic than going straight or making a left turn. Although signals often combine right-turn and straight movements, reservations could combine turning movements in more flexible ways. Although larger improvements in travel times occurred at the observed right turns, improvements at left turns were also observed. Because US-290 has signals intermittently spaced throughout its span, vehicles are frequently stopping for signal delays. Using the reservations system, the flow of traffic is stopped less frequently, reducing congestion. The use of AVs rather than HVs also helped travel times but by less than reservations. In most cases, using reservations instead of signals doubled the improvements resulting from using AVs. Reservations appear to have a positive effect on traffic flow and congestion in networks (freeway and arterial) that use signals to control intersections.

TABLE 2 Freeway network results

I-35				
Intersections	**Demand**	**Proportion of AVS**	**TSTT (hr)**	**Travel time per vehicle (min)**
Traditional	50%	0%	3998.9	3.75
Traditional	50%	100%	3893.3	3.65
Reservations	50%	100%	3975.2	3.73
Traditional	75%	0%	10087	6.3
Traditional	75%	100%	5934.2	3.71
Reservations	75%	100%	9861.1	6.16
Traditional	85%	0%	16127.7	8.89
Traditional	85%	25%	16023.5	8.83
Traditional	85%	50%	15944.3	8.79
Traditional	85%	75%	14545.3	8.02
Traditional	85%	100%	14101.6	7.77
Reservations	85%	100%	16084.7	8.87
Traditional	100%	0%	31611.7	14.81
Traditional	100%	100%	9063.3	4.25
Reservations	100%	100%	30211.3	14.16

Mopac				
Intersections	**Demand**	**Proportion of AVs**	**TSTT (hr)**	**Travel time per vehicle (min)**
Traditional	50%	0%	373.9	1.61
Traditional	50%	100%	363.6	1.57
Reservations	50%	100%	409.9	1.77
Traditional	75%	0%	576.6	1.66
Traditional	75%	100%	554.9	1.6
Reservations	75%	100%	616.1	1.77
Traditional	85%	0%	667.9	1.7
Traditional	85%	25%	651.1	1.65
Traditional	85%	50%	647.8	1.65
Traditional	85%	75%	645.2	1.64
Traditional	85%	100%	644.1	1.64
Reservations	85%	100%	698.7	1.77
Traditional	100%	0%	1288.3	2.78
Traditional	100%	100%	752.1	1.62
Reservations	100%	100%	825.4	1.78
US-290				
Intersections	**Demand**	**Proportion of AVs**	**TSTT (hr)**	**Travel time per vehicle (min)**
Traditional	50%	0%	557.8	6.03
Traditional	50%	100%	547.5	5.92
Reservations	50%	100%	505.4	5.47
Traditional	75%	0%	845.7	6.1
Traditional	75%	100%	827.7	5.97
Reservations	75%	100%	759.8	5.48
Traditional	85%	0%	997.6	6.35
Traditional	85%	25%	952	6.06
Traditional	85%	50%	945.3	6.01
Traditional	85%	75%	942.5	6
Traditional	85%	100%	939.8	5.98
Reservations	85%	100%	860.6	5.47
Traditional	100%	0%	1518.5	8.21
Traditional	100%	100%	1108.8	5.99
Reservations	100%	100%	1014.1	5.48

4.3 Downtown Networks

We tested the downtown network of Austin, shown in Figure 5, with 100% demand, at different proportions of AVs. Downtown Austin differs from the previous networks in that there are many route choices available. Therefore, we solved dynamic traffic assignment using the method of successive averages. All scenarios were solved to a 2% gap, which was defined as the ratio of

average excess cost to total system travel time. Route choice admits issues such as the Braess and Daganzo paradoxes *(8, 9)*, in which capacity improvements induce selfish route choice that increase travel times for all vehicles. The downtown network also contains both freeway and arterial links, with part of I-35 on the east side, a grid structure, and several major arterials.

Reservations greatly helped travel times and congestion in the downtown network, cutting travel times by an additional 55% at 100% demand. When combined with reduced reaction times, the total reduction in travel time was 78%. Reservations were highly effective in downtown Austin – more effective than in the freeway or arterial networks – even with the high congestion. In downtown Austin, most intersections are controlled by signals, with significant potential for improvement from reservations. Although many intersections are close together, congested intersections might be avoided by dynamic user equilibrium route choice decisions, avoiding the issues seen with reservations in Lamar & 38th Street. The increased capacity from 100% AVs also contributed, reducing travel times by around 51%.

TABLE 3 Downtown Austin results

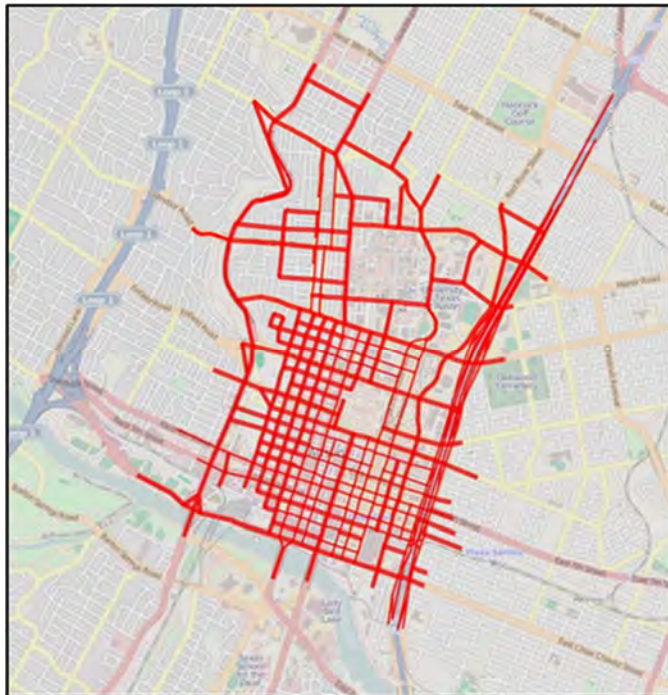| Downtown Austin				
Intersections	**Demand**	**Proportion of Avs**	**TSTT (hr)**	**Travel time per vehicle (min)**
Traditional	100%	0	18040.2	17.23
Traditional	100%	0.25	13371.4	12.77
Traditional	100%	0.5	11522.3	11
Traditional	100%	0.75	9905.1	9.46
Traditional	100%	1	8824.7	8.43
Reservations	100%	1	3984.3	3.8

FIGURE 5 Downtown Austin network

5 CONCLUSIONS
This paper is the first study using the cell transmission model to study the effects of reservation-based intersection control and reduced following headways for AVs on large networks. We studied several arterial and freeway networks among the 100 most congested roads in Texas to study how AVs affected congestion on different types of roads. For arterial regions, reservations were beneficial in some situations but not in others. On Congress Avenue, a long arterial without progression, reservations improved travel times. However, on Lamar & 38th Street, reservations gave greater priority to vehicles entering from local roads. Since intersections were so close together, this created queue spillback and *greater congestion* from using reservation controls. This was due to the FCFS policy: vehicles were prioritized according to how long they had been waiting. In contrast, signals allowed more freedom in capacity allocation, and were optimized to give arterials a greater share of the capacity. On freeway networks, the effects of reservations were again mixed. On US-290, which uses signals to control access, reservations were an overall improvement. In other freeway networks, reservations were worse than merges/diverges. In the downtown Austin grid network, reservations resulted in great reductions in travel times.

The negative results for FCFS reservations are surprising considering the work of Fajardo et al. *(3)* and Li et al. *(4)*. However, the major issue with FCFS reservations is that FCFS allocates capacity in different proportions and at different times than signals. On arterials, in high demand this resulted in greater capacity given to local or collector roads. Furthermore, the lack of consistent timing for reservations disrupted progression along arterials, increasing queues and causing queue spillback at high demand.

Overall, we conclude that reservations using the FCFS policy have great potential for replacing signals. However, in certain scenarios – local road-arterial intersections that are close together, and at high demand – signals outperform FCFS reservations. This might be improved by a reservation priority policy more suited for the specific intersection. However, reservations were detrimental when used in place of merges/diverges. Since merges/diverges do not require the same delays as signals, reservations have limited ability to improve their use of capacity. Furthermore, the FCFS policy could adversely affect the capacity allocation. Therefore, FCFS reservations should not be used in place of merges/diverges, but other priority policies for reservations might be considered.

The capacity increases due to reduced reaction times improved travel times significantly on all networks. Furthermore, regardless of the intersection control, intersection bottlenecks mostly benefited from increased capacity. These capacity increases arise from permitting AVs to use computer reaction times to safely reduce following headways. Although this might be disconcerting to human drivers in a shared-road scenario, the potential benefits demonstrated here are a significant incentive.

In future work, we would like to develop more analytical methods to determine when reservations will improve over signals, merges, and diverges. We would also like to study priority policies other than FCFS for reservations to optimize them for different intersections. Furthermore, reservations move vehicles more similarly to adaptive signal controls than fixed-time signals, and should therefore be compared with adaptive signals. Although adaptive signals still have lost time due to clearance intervals, the differences between reservations and adaptive signals should be explored. With regards to reduced reaction times, we would like to determine typical reaction times for autonomous and connected vehicles. Connected (partially automated) vehicles might require greater safety margins than AVs, but still reduce reaction times sufficiently to achieve significant improvements in capacity. Finally, more thorough analyses of

how AVs affect link queues and intersection flow would be beneficial for policy on when to use reservations and how to plan for widespread use of AVs.

ACKNOWLEDGEMENTS

REFERENCES

(1) Dresner, K., & Stone, P. (2004, July). Multiagent traffic management: A reservation-based intersection control mechanism. In *Proceedings of the Third International Joint Conference on Autonomous Agents and Multiagent Systems-Volume 2* (pp. 530-537). IEEE Computer Society.

(2) Dresner, K., & Stone, P. (2006, July). Traffic intersections of the future. In *Proceedings of the National Conference on Artificial Intelligence* (Vol. 21, No. 2, p. 1593). Menlo Park, CA; Cambridge, MA; London; AAAI Press; MIT Press; 1999.

(3) Fajardo, D., Au, T. C., Waller, S., Stone, P., & Yang, D. (2011). Automated intersection control: Performance of future innovation versus current traffic signal control. *Transportation Research Record: Journal of the Transportation Research Board*, (2259), 223-232.

(4) Li, Z., Chitturi, M., Zheng, D., Bill, A., & Noyce, D. (2013). Modeling Reservation-Based Autonomous Intersection Control in VISSIM. *Transportation Research Record: Journal of the Transportation Research Board*, (2381), 81-90.

(5) Kesting, A., Treiber, M., & Helbing, D. (2010). Enhanced intelligent driver model to access the impact of driving strategies on traffic capacity. *Philosophical Transactions of the Royal Society of London A: Mathematical, Physical and Engineering Sciences*, *368*(1928), 4585-4605.

(6) Shladover, S., Su, D., & Lu, X. Y. (2012). Impacts of cooperative adaptive cruise control on freeway traffic flow. *Transportation Research Record: Journal of the Transportation Research Board*, (2324), 63-70.

(7) Levin, M. W., & Boyles, S. D. (2015). Effects of Autonomous Vehicle Ownership on Trip, Mode, and Route Choice. In press in *Transportation Research Record.*

(8) Braess, P. D. D. D. (1968). Über ein Paradoxon aus der Verkehrsplanung. *Unternehmensforschung*, *12*(1), 258-268.

(9) Daganzo, C. F. (1998). Queue spillovers in transportation networks with a route choice. *Transportation Science*, *32*(1), 3-11.

(10) Carlino, D., Depinet, M., Khandelwal, P., & Stone, P. (2012, September). Approximately orchestrated routing and transportation analyzer: Large-scale traffic simulation for autonomous vehicles. In *Intelligent Transportation Systems (ITSC), 2012 15th International IEEE Conference on* (pp. 334-339). IEEE.

(11) Levin, M. W., & Boyles, S. D. (2015). Intersection Auctions and Reservation-Based Control in Dynamic Traffic Assignment. In press in *Transportation Research Record.*

(12) Levin, M.W., & Boyles, S.D. (2015c). A multiclass cell transmission model for human and autonomous vehicle roads. Accepted for publication in *Transportation Research Part C: Emerging Technologies.*

(13) Daganzo, C. F. (1994). The cell transmission model: A dynamic representation of highway traffic consistent with the hydrodynamic theory. *Transportation Research Part B: Methodological*, *28*(4), 269-287.

(14) Daganzo, C. F. (1995). The cell transmission model, part II: network traffic. *Transportation Research Part B: Methodological*, *29*(2), 79-93.

(15) Dresner, K., & Stone, P. (2006, May). Human-usable and emergency vehicle-aware control policies for autonomous intersection management. In *Fourth International Workshop on Agents in Traffic and Transportation (ATT), Hakodate, Japan*.

(16) Schepperle, H., & Böhm, K. (2008, July). Auction-based traffic management: towards effective concurrent utilization of road intersections. In *E-Commerce Technology and the Fifth IEEE Conference on Enterprise Computing, E-Commerce and E-Services, 2008 10th IEEE Conference on* (pp. 105-112). IEEE.

(17) Vasirani, M., & Ossowski, S. (2010). *A market-based approach to accommodate user preferences in reservation-based traffic management*. Technical Report ATT.

(18) Carlino, D., Boyles, S. D., & Stone, P. (2013, October). Auction-based autonomous intersection management. In *Intelligent Transportation Systems-(ITSC), 2013 16th International IEEE Conference on* (pp. 529-534). IEEE.

(19) Hausknecht, M., Au, T. C., & Stone, P. (2011, September). Autonomous intersection management: Multi-intersection optimization. In *Intelligent Robots and Systems (IROS), 2011 IEEE/RSJ International Conference on* (pp. 4581-4586). IEEE.

(20) Dresner, K. M., & Stone, P. (2007, January). Sharing the Road: Autonomous Vehicles Meet Human Drivers. In *IJCAI* (Vol. 7, pp. 1263-1268).

(21) Bento, L., Parafita, R., Santos, S., & Nunes, U. (2013, October). Intelligent traffic management at intersections: Legacy mode for vehicles not equipped with v2v and v2i communications. In *Intelligent Transportation Systems-(ITSC), 2013 16th International IEEE Conference on* (pp. 726-731). IEEE.

(22) Qian, X., Gregoire, J., Moutarde, F., & De La Fortelle, A. (2014, October). Priority-based coordination of autonomous and legacy vehicles at intersection. In *Intelligent Transportation Systems (ITSC), 2014 IEEE 17th International Conference on* (pp. 1166-1171). IEEE.

(23) Li, P. Y., & Shrivastava, A. (2002). Traffic flow stability induced by constant time headway policy for adaptive cruise control vehicles. *Transportation Research Part C: Emerging Technologies*, *10*(4), 275-301.

(24) Schakel, W. J., van Arem, B., & Netten, B. D. (2010, September). Effects of cooperative adaptive cruise control on traffic flow stability. In *Intelligent Transportation Systems (ITSC), 2010 13th International IEEE Conference on* (pp. 759-764). IEEE.

(25) Blumberg, M., & Bar-Gera, H. (2009). Consistent node arrival order in dynamic network loading models. *Transportation Research Part B: Methodological*, *43*(3), 285-300.

(26) Johansson, G., & Rumar, K. (1971). Drivers' brake reaction times. *Human Factors: The Journal of the Human Factors and Ergonomics Society*, *13*(1), 23-27.

(27) Daganzo, C. F. (1998). Queue spillovers in transportation networks with a route choice. *Transportation Science*, *32*(1), 3-11.

A multiclass cell transmission model for shared human and autonomous vehicle roads

Michael W. Levin
Graduate Research Assistant
Department of Civil, Architectural, and Environmental Engineering
The University of Texas at Austin
Ernest Cockrell, Jr. Hall (ECJ) 6.202
301 E. Dean Keeton St. Stop C1761
Austin, TX 78712-1172
Ph. (512) 471-3548
Fax (512) 475-8744
michaellevin@utexas.edu

Stephen D. Boyles
Assistant Professor
Department of Civil, Architectural, and Environmental Engineering
The University of Texas at Austin

October 12, 2015

Abstract

Autonomous vehicles have the potential to improve link and intersection traffic behavior. Computer reaction times may admit reduced following headways and increase capacity and backwards wave speed. The degree of these improvements will depend on the proportion of autonomous vehicles in the network. To model arbitrary shared road scenarios, we develop a multiclass cell transmission model that admits variations in capacity and backwards wave speed in response to class proportions within each cell. The multiclass cell transmission model is shown to be consistent with the hydrodynamic theory. This paper then develops a car following model incorporating driver reaction time to predict capacity and backwards wave speed for multiclass scenarios. For intersection modeling, we adapt the legacy early method for intelligent traffic management (Bento et al., 2013) to general simulation-based

1

dynamic traffic assignment models. Empirical results on a city network show that intersection controls are a major bottleneck in the model, and that legacy early method improves over traffic signals when the autonomous vehicle proportion is sufficiently high.

Keywords: autonomous vehicles, dynamic traffic assignment, cell transmission model, multiclass, shared road

Highlights

- We develop a multiclass cell transmission model consistent with hydrodynamic theory

- Capacity and backwards wave speed are modeled as functions of reaction times

- A shared intersection model is adapted for dynamic traffic assignment

- Reservation-based intersection controls improve over traffic signals when the proportion of AVs on the road is sufficiently high

1 Introduction

Autonomous vehicle (AV) technology is rapidly maturing with testing permitted on public roads in several states. When AVs become available to the public, computer precision and communications may allow new behaviors to increase network capacity. For instance, Dresner & Stone (2004) proposed the tile-based reservation (TBR) intersection policy which reduces delay beyond optimized traffic signals (Fajardo et al., 2011). Besides offering new intersection behaviors, AVs may also increase link capacity because reduced reaction times requires smaller following distances, and AVs may be less affected than human-driven vehicles (HVs) by certain adverse road conditions. However, capacity improvements are complicated by sharing roads with HVs, which will likely be the case for many years before AVs are sufficiently available and affordable to be driven by all travelers.

TBR is compatible with shared roads (Dresner & Stone, 2007), and link behaviors may be performed safely with a mixed fleet of vehicles. However, modeling link and intersection capacity improvements from shared road policies is still an open problem. Most current models of AVs are micro-simulations, which are not computationally tractable for the traffic assignment typically used to determine route choice. Levin & Boyles (2015a) modified static link performance functions model to predict capacity improvements as a function of the proportion of AVs on each link based on Greenshields' (1935) capacity model. However, in reality the proportion of AVs on each link will vary over time. Dynamic traffic assignment (DTA) models flow more accurately than static models and can include the varying-time effects of capacity. Kesting et al. (2010) predicted theoretical capacity for adaptive cruise control and use linear regression to extrapolate for various proportions of connected vehicles (CVs) and non-CVs. For consistency with DTA, we use a constant acceleration model to analytically predict capacity and wave speed as a function of the proportion of each vehicle class on the road, and generalize to multiple classes with different reaction times. Whereas

2

many previous papers on CVs use micro-simulation experiments, we use DTA on a city network to study the impacts of AVs under dynamic user equilibrium (DUE) route choice.

This paper makes several contributions with the aim of developing a shared road DTA model: First, a multiclass cell transmission model (CTM) is proposed that admits space-time variations of capacity and wave speed. Second, a link capacity model based on a collision avoidance car following model with different reaction times is presented. The link capacity assumptions lead to the triangular fundamental diagram assumed by Newell (1993) and Yperman et al. (2005). To facilitate shared intersections, the conflict region (CR) algorithm from Levin & Boyles (2015b) for general SBDTA models is modified using Bento et al. (2013)'s control policy. Intersection efficiency scales dynamically with the proportion of AVs using the intersection. Results from studies on a single intersection and the downtown Austin city network suggest that travel time reductions when using reservation-based controls scale linearly with the proportion of AVs, but do not improve over signals until 80% AV penetration or greater.

The remainder of this paper is organized as follows. Section 2 discusses literature relevant to multiclass DTA and AV flow. Section 3 presents the multiclass DTA model and shows consistency with the hydrodynamic theory of traffic flow. Section 4 develops a dynamic capacity and wave speed model based on driver reaction times. A shared intersection model for general SBDTA is developed in Section 5. In Section 6, we present a case study on a city network involving varying levels of human-driven and autonomous vehicles, and Section 7 discusses conclusions.

2   Literature review

This literature review starts by discussing multiclass DTA in Section 2.1 to provide a context for the AV models discussed in Section 2.2.

2.1   Dynamic traffic assignment

DTA includes a number of different flow models, some of which are solved analytically and others which are simulation-based (SBDTA). For an overview of DTA, we refer to Chiu et al. (2011). This paper focuses on the cell transmission (CTM) SBDTA model (Daganzo, 1994; 1995a), which is a discrete approximation of the Lighthill-Whitham-Richards (LWR) model (Lighthill & Whitham, 1955; Whitham, 1956). The partial differential equations of the LWR model are generally more difficult to solve when multiple vehicle classes result in varying capacities. However, the discretized space and time in CTM simplifies the multiclass solution method. The multiclass CTM presented in Section 3 is shown to be compatible with the conservation equations of LWR.

Multiclass DTA has previously been studied in the literature although primarily with a focus on heterogeneous vehicles of length and speed. Wong & Wong (2002) allowed vehicles to have a class-specific speed and demonstrate that their model adheres to flow conservation. However, they use a new discrete space-time approximation to solve their model, and it is

not clear whether it is compatible with the most common simulation-based approximations, which is desirable for integration with existing DTA models. Tuerprasert & Aswakul (2010) formulated a multiclass CTM with different speeds per class, including how different speeds affect cell propagation. It is not clear, though, whether their model solves a multiclass form of LWR, or is a modification of CTM with useful properties.

2.2 Autonomous vehicle flow

The model presented in this paper is concerned with varying capacities and wave speeds due to the multiple classes of human-driven and autonomous vehicles. We assume that speed does not depend on vehicle class, which is reasonable because some AVs are programmed to exceed the speed limit to maintain the same speed as surrounding traffic (Miller, 2014) for improved safety (Aarts & Van Schagen, 2006).

Potential improvements in traffic flow from CVs and AVs have begun to receive attention in the literature. Adaptive cruise control (ACC) (Marsden et al., 2001) has been developed to improve link capacity and, if it is not incorporated into AVs, will likely influence AV car-following behavior. Van Arem et al. (2006) used a micro-simulation to show that cooperative ACC can improve efficiency. Kesting et al. (2010) developed a continuous acceleration behavior model of CVs to predict theoretical capacity. They use a linear regression to extrapolate for different proportions of CVs and non-CVs. We generalize by including multiple vehicle classes with different reaction times in our constant acceleration model and predict both capacity and wave speed as a function of the proportion of each vehicle class. Schakel et al. (2010) used simulation to study traffic flow stability, finding that ACC increases stability and also increases shockwave speed. This is consistent with the theoretical wave speed we develop in Section 3. Although much of the literature uses micro-simulation to study CVs and AVs, we use the predicted capacities and wave speeds in a DTA model to study the impacts on a city network with DUE.

A major topic in the literature is new intersection policies for AVs. Dresner & Stone (2004) developed a reservation-based policy (TBR) using the greater precision and more complex communications possible with AVs. Fajardo et al., (2011) found that TBR improved over optimized traffic signals. Because TBR subsumes traffic signals, signals can be combined with an intersection agent controller to make TBR compatible with shared roads through an alternate reservation-granting policy (Dresner and Stone, 2007). Bento et al. (2013) proposed to extend TBR to non-communication equipped vehicles by reserving additional space to account for reduced precision and unknown destination, and Qian et al. (2014) developed a provably collision-free shared-intersection system. Other reservation prioritization policies with the goal of reducing intersection delay have been explored, such as intersection auctions (Schepperle & Bhm, 2007; Vasirani & Ossowski, 2012; Carlino et al., 2013). Analyzing TBR on city-size networks has been a major challenge as most AV traffic models have used micro-simulation. Carlino et al. (2012) used a simplified non-tile-based reservation policy to simulate a large network in reasonable time. However, the intersection capacity of this model was significantly reduced. Because of the number of simulations involved in solving DTA for user equilibrium, a micro-simulation model of intersections is

not sufficient. Levin & Boyles (2015b) used a conflict region (CR) simplification to make TBR computationally tractable for DTA, and an extension of the CR model is used for intersections in this paper.

3 Multiclass cell transmission model

This section presents a multiclass extension of CTM. The focus of this paper is on for roads with both human and autonomous personal vehicles; we do not include the speed differences between heavy trucks and personal vehicles. The models in Sections 3 and 4 are defined for continuous flows, which some DTA models use. Because this paper is also concerned with node models, and because reservation-based intersection controls are defined for discrete vehicles, Sections 5 and 6 will discretize the flow model defined here. In this paper, we make the following assumptions.

1. All vehicles travel at the same speed. Although in reality vehicle speeds differ, in DTA models the vehicle speed behavior model is often assumed to be identical for all vehicles. This is reasonable even with multiple vehicle classes because AVs may match the speed of surrounding vehicles even if it requires exceeding the speed limit (Miller, 2014). Although Tuerprasert & Aswakul (2010) consider different vehicle speeds in CTM, in this study of HVs and AVs much of the differences in speed would come from variations in HV behavior that are often not considered in DTA models.

2. Uniform distribution of class-specific density per cell. Single-class CTM assumes the density within a cell is uniformly distributed. We extend that assumption to class-specific densities.

3. Arbitrary number of vehicle classes. Although this study focuses on the transition from HVs to AVs, different types of AVs may be certified for different reaction times, and thus may respond differently in their car-following behavior.

4. Backwards wave speed is less than or equal to free flow speed. This is necessary to determine cell length by free flow speed. Although this is a common assumption in DTA models, in Section 4 we show that a sufficiently low reaction time might break this assumption.

We first define the multiclass hydrodynamic theory in Section 3.1. Then, following the presentation of Daganzo (1994), we state the cell transition equations in Section 3.2 and show that they are consistent with the multiclass hydrodynamic theory in Section 3.3.

3.1 Multiclass hydrodynamic theory

Let M be the set of vehicle classes. Let $k_m(x,t)$ be the density of vehicles of class m at space-time point (x,t) with total density denoted by $k(x,t) = \sum\limits_{m \in M} k_m(x,t)$. Similarly, let

$q_m(x,t) = u(\frac{k_1}{k}, \ldots, \frac{k_{|M|}}{k})k_m(x,t)$ be the class-specific flow, with the total flow given by $q(x,t) = \sum\limits_{m \in M} q_m(x,t)$, and let the function $u\left(\frac{k_1}{k}, \ldots, \frac{k_{|M|}}{k}\right)$ denote the speed possible with class proportions of $\frac{k_1}{k}, \ldots, \frac{k_{|M|}}{k}$.

Speed is limited by free flow speed, capacity, and backwards wave propagation:

$$u(k_1, \ldots k_{|M|}) = \min\left\{ u^{\mathrm{f}}, \frac{q^{\max}\left(\frac{k_1}{k}, \ldots, \frac{k_{|M|}}{k}\right)}{k}, w\left(\frac{k_1}{k}, \ldots, \frac{k_{|M|}}{k}\right)\frac{k^{\mathrm{jam}} - k}{k} \right\} \tag{1}$$

where u^{f} is free flow speed, $w\left(\frac{k_1}{k}, \ldots, \frac{k_{|M|}}{k}\right)$ is the backwards wave speed, $q^{\max}\left(\frac{k_1}{k}, \ldots, \frac{k_{|M|}}{k}\right)$ is the capacity when the proportions of density in each class are $\frac{k_1}{k}, \ldots, \frac{k_{|M|}}{k}$, and k^{jam} is jam density. k^{jam} is assumed not to depend on vehicle type, as the physical characteristics (such as length and maximum acceleration) of human-driven and autonomous vehicles are assumed to be the same. For consistency, conservation of flow must be satisfied, i.e. $\frac{\partial q_m(x,t)}{\partial x} = -\frac{\partial k_m(x,t)}{\partial t}$ for all $m \in M$ (Wong and Wong, 2012).

3.2 Cell transition flows

As with Daganzo (1994), to form the multiclass CTM we discretize time into timesteps of dt. Links are then discretized into cells labeled by $i = 1, , I$ such that vehicles traveling at free flow speed will travel exactly the distance of one cell per timestep. Let $n_i^m(t)$ be vehicles of class m in cell i at time t, where $n_i(t) = \sum\limits_{m \in M} n_i^m(t)$. Let $y_i^m(t)$ be vehicles of class m entering cell i from cell $i - 1$ at time t. Then cell occupancy is defined by

$$n_i^m(t+1) = n_i^m(t) + y_i^m(t) - y_{i+1}^m(t) \tag{2}$$

with total transition flows given by

$$y_i(t) = \sum_{m \in M} y_i^m(t) = \min\left\{ \sum_{m \in M} n_{i-1}^m(t), Q_i(t), \frac{w_i(t)}{u^{\mathrm{f}}}\left(N - \sum_{m \in M} n_i^m(t)\right) \right\} \tag{3}$$

where N is the maximum number of vehicles that can fit in cell i and $Q_i(t)$ is the maximum flow.

Equation (3) defines the total transition flows, which will now be defined specific to vehicle class. To avoid dividing by zero, assume $n_{(i-1)}(t) > 0$. (If $n_{(i-1)}(t) = 0$, there is no flow to propagate). As stated in Assumption 2, class-specific density is assumed to be uniformly distributed throughout the cell. Then class-specific transition flows are proportional to $\frac{n_{i-1}^m(t)}{n_{i-1}(t)}$:

$$y_i^m(t) = \frac{n_{i-1}^m(t)}{n_{i-1}(t)} \min\left\{ \sum_{m \in M} n_{i-1}^m(t), Q_i(t), \frac{w_i(t)}{u^{\mathrm{f}}}\left(N - \sum_{m \in M} n_i^m(t)\right) \right\} \tag{4}$$

Equation (4) may be simplified to

$$y_i^m(t) = \min \left\{ n_{i-1}^m(t), \frac{n_{i-1}^m(t)}{n_{i-1}(t)} Q_i(t), \frac{n_{i-1}^m(t)}{n_{i-1}(t)} \frac{w_i(t)}{u^{\mathrm{f}}} \left(N - \sum_{m \in M} n_i^m(t) \right) \right\} \qquad (5)$$

which shows that flow of class m is restricted by three factors: 1) class-specific cell occupancy; 2) proportional share of the capacity; and 3) proportional share of congested flow.

In the general hydrodynamic theory, class proportions may vary arbitrarily with space and time, which includes the possibility of variations within a cell. Therefore, assuming uniformly distributed density results in the possibility of non-FIFO behavior within cells. One class may have a higher proportion at the end of the cell, and thus might be expected to comprise a higher proportion of the transition flow. However, as discussed by Blumberg & Bar-Gera (2009), even single class CTMs may violate FIFO. The numerical experiments in this paper use discretized flow to admit reservation-based intersection models. The discretized flow also allows vehicles within a cell to be contained within a FIFO queue, which ensures FIFO behavior at the cell level. Total transition flows for discrete vehicles are determined as stated above for continuous flow.

3.3   Consistency with hydrodynamic theory

As with Daganzo (1994) we show that these transition flows are consistent with the multiclass hydrodynamic theory defined in Section 3.1. Assume class-specific flow is proportional to density, i.e. $\frac{k_m}{k}$, and all classes travel at the same speed. Also assume that $k > 0$, because if $k = 0$ then flow is also 0. Then

$$q_m(x,t) = \frac{k_m}{k} \min \left\{ u^{\mathrm{f}} k, q^{\mathrm{max}} \left(\frac{k_1}{k}, \ldots, \frac{k_{|M|}}{k} \right), w \left(\frac{k_1}{k}, \ldots, \frac{k_{|M|}}{k} \right) (k^{\mathrm{jam}} - k) \right\} \qquad (6)$$

Let dt be the timestep and choose cell length such that $u^{\mathrm{f}} \cdot dt = 1$. Then cell length is 1, u^{f} is 1, $x = i$, $k^{\mathrm{jam}} = N$, $q^{\mathrm{max}}(t) = Q(t)$, and $k(x,t) = n_i(t)$. Cell length is chosen so that flow may traverse at most one cell per timestep to satisfy the Courant-Friedrichs-Lewy conditions (Courant et al., 1928). Then

$$q_m(x,t) = \frac{n_i^m(t)}{n_i(t)} \min \left\{ n_i(t), q_i^{\mathrm{max}}(t), \frac{w_i(t)}{v} (N - n_i(t)) \right\} = y_{i+1}^m(t) \qquad (7)$$

except for the subindex of n the last term, which should be $i+1$. As with Daganzo (1994) this difference is disregarded. (See Daganzo, 1995b for more discussion on this issue.) Therefore $\frac{\partial q_m(x,t)}{\partial x} = y_{i+1}^m(t) - y_i^m(t)$. Since $\frac{\partial k_m(x,t)}{\partial t} = n_i^m(t+1) - n_i^m(t)$ is the rate of change in cell occupancy with respect to time, the conservation of flow equation $\frac{\partial q_m(x,t)}{\partial x} = -\frac{\partial k_m(x,t)}{\partial t}$ is satisfied by the cell propagation function of equation (2).

4 Link capacity and backwards wave speed

We now present a car following model based on kinematics to predict the speed-density relationship as a function of the reaction times of multiple classes. Car following models can be divided into several types as described by Brackstone et al. (1999) and Gartner et al. (2005). For instance, some predict fluctuations in the acceleration behavior of an individual driver in response to the vehicle ahead. However, for DTA a simpler model is more appropriate to predict the speed of traffic at a macroscopic level. Newell (2002) greatly simplified car following to be consistent with the hydrodynamic theory, but the model does not include the effects of reaction time. Instead, the car following model used here builds from the collision avoidance theory of Kometani & Sasaki (1959) to predict the allowed headway for a given speed, which varies with driver reaction time. The inverse relationship predicts speed as a function of the headway, which is determined by density. This car following model results in the triangular fundamental diagram used by Newell (1993) and Yperman et al. (2005).

Although this car following model is useful in predicting the effects of a heterogeneous vehicle composition on capacity and wave speed, other effects such as roadway conditions are not included. Furthermore, CTM assumes a trapezoidal fundamental diagram that admits a lower restriction on capacity. Therefore, the effect of reaction times on capacity and backwards wave speed are used to appropriately scale link characteristics for realistic city network models. Although AVs may be less affected by adverse roadway conditions than human drivers, this paper assumes similar effects for the purposes of developing a DTA model of shared roads. Other estimations of capacity and wave speed may also be included in the multiclass CTM model developed in Section 3.

4.1 Safe following distance

Suppose that vehicle 2 follows vehicle 1 at speed u with vehicle lengths ℓ. Vehicle 1 decelerates at a to a full stop starting at time $t = 0$, and vehicle 2 follows suit after a reaction time of Δt. The safe following distance, L, is determined by kinematics.

The position of vehicle 1 is given by

$$x_1(t) = \begin{cases} ut - \frac{1}{2}at^2 & t \leq \frac{u}{a} \\ \frac{u^2}{2a} & t > \frac{u}{a} \end{cases} \tag{8}$$

where $\frac{u}{a}$ is the time required to reach a full stop. For $t > \frac{u}{a}$, the position of vehicle 1 is constant after its full stop. The position of vehicle 2, including the following distance of L, is

$$x_2(t) = \begin{cases} ut - L & t \leq \Delta t \\ ut - \frac{1}{2}a(t - \Delta t)^2 - L & t > \Delta t \end{cases} \tag{9}$$
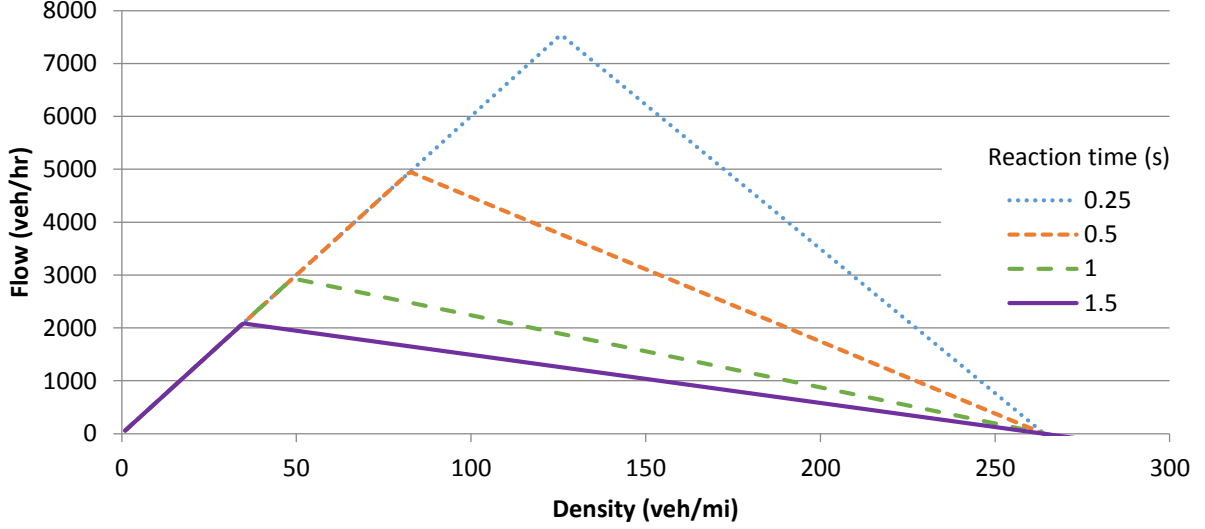
8

Figure 1: Flow-density relationship as a function of reaction time

The difference is

$$x_1(t) - x_2(t) = \begin{cases} u - \frac{1}{2}at^2 + L & t \le \Delta t \\ -at\Delta t + \frac{1}{2}a(\Delta t)^2 + L & \Delta t < t \le \frac{u}{a} \\ \frac{u^2}{2a} - ut + \frac{1}{2}a(t - \Delta t)^2 + L & t > \frac{u}{a} \end{cases} \tag{10}$$

and the minimum distance occurs when both vehicles are stopped, at $\frac{u}{a} + \Delta t$. To avoid a collision,

$$L \ge -\frac{u^2}{2a} + u\left(\frac{u}{a} + \Delta t\right) - \frac{1}{2}a\left(\frac{u}{a}\right)^2 + \ell = u\Delta t + \ell \tag{11}$$

4.2 Flow-density relationship

Equivalently, equation (11) may be expressed as

$$u \le \frac{L - \ell}{\Delta t} \tag{12}$$

which restricts speed based on following distance (from density). Flow may be determined from the relationship $q = \left(\frac{L-\ell}{\Delta t}\right) k$ with $L = \frac{1}{k}$, which is linear with respect to density. Figure 1 shows the resulting relationship between flow and density for different reaction times for a characteristic vehicle of length 20 feet that decelerates at 9 feet per second per second for a free flow speed of 60 miles per hour. Since speed is bounded by free flow speed and available following distance, the triangle is formed by $q = \min\left\{uk, \left(\frac{L-\ell}{\Delta t}\right) k\right\}$. Reaction times of 1 to 1.5 seconds correspond to human drivers (Johansson & Rumar, 1971).

9

The maximum density at which a speed of u is possible is $\frac{1}{u\Delta t + \ell}$ from equation (12), and therefore capacity for free flow speed of u^f is

$$q^{\max} = u^f \frac{1}{u^f \Delta t + \ell} \tag{13}$$

Backwards wave speed is

$$w = -\frac{\frac{u^f}{u^f \Delta t + \ell}}{\frac{1}{u^f \Delta t + \ell} - \frac{1}{\ell}} = \frac{\ell}{\Delta t} \tag{14}$$

which increases as reaction time decreases. The direction of this relationship is consistent with micro-simulation results by Schakel et al. (2010). Note that if $\Delta t < \frac{\ell}{u^f}$, which may be possible for computer reaction times, then backwards wave speed exceeds free flow speed. If $w > u^f$ for CTM, then the cell lengths would need to be derived from the backward wave speed, not the forward. That would complicate the cell transition flows. To avoid this issue, this paper assumes that $w \leq u^f$.

4.3 Flow for heterogeneous vehicles

The car following model in Section 4.2 is designed to estimate the capacity and backwards wave speed when the reaction time varies, but is uniform across all vehicles. This section expands the model for heterogeneous flow with different vehicles having different reaction times. Let the density be disaggregated into k_m for each vehicle class m. Consider the case where speed is limited by density. Assuming that all vehicles travel at the same speed, for all vehicle classes,

$$u = \frac{L_m - \ell}{\Delta t_m} \tag{15}$$

where L_m is the headway allotted and Δt_m is the reaction time for vehicles of class m. Also, with appropriate units,

$$\sum_{m \in M} k_m L_m = 1 \tag{16}$$

is the total distance occupied by the vehicles. Thus

$$\sum_{m \in M} k_m (L_m - \ell) = 1 - k\ell \tag{17}$$

By equation (15), $\sum_{m \in M} k_m u \Delta t_m = 1 - k\ell$, and

$$u = \frac{1 - k\ell}{\sum_{m \in M} k_m \Delta t_m} \tag{18}$$

Equation (18) may be rewritten as $u \sum_{m \in M} k_m \Delta t_m = 1 - k\ell$. Dividing both sides by k yields

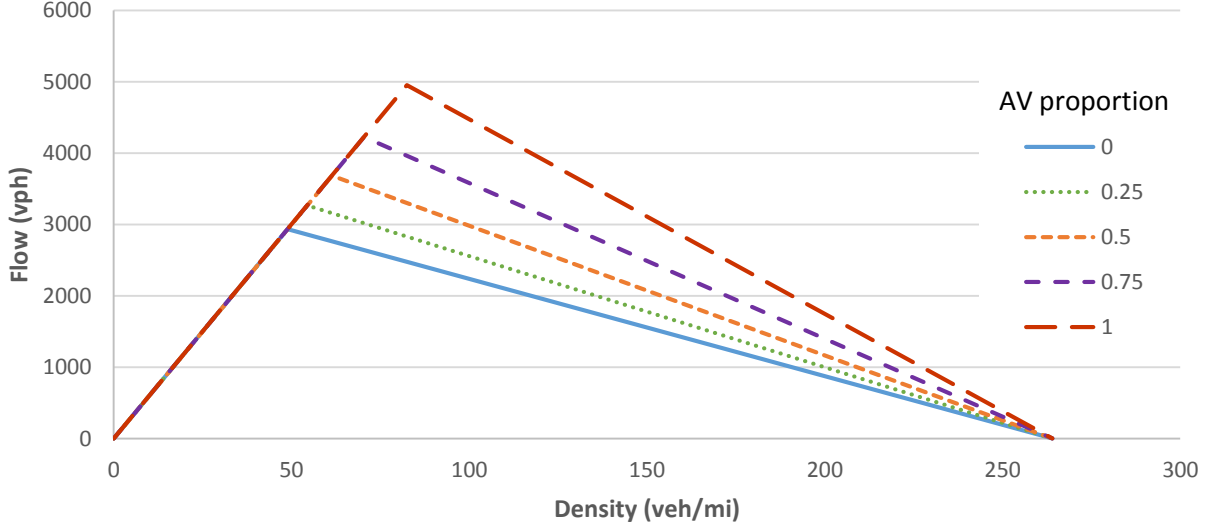$$u \sum_{m \in M} \frac{k_m}{k} \Delta t_m + \ell = \frac{1}{k} \tag{19}$$

10

Figure 2: Flow-density relationship as a function of AV proportion.

Assuming that vehicle class proportions $\frac{k_m}{k}$ remain constant because all vehicles travel at the same speed, the maximum density for which a speed of u^{f} is possible is

$$k = \frac{1}{u^{\mathrm{f}} \sum_{m \in M} \frac{k_m}{k} \Delta t_m + \ell} \tag{20}$$

which follows by taking the reciprocal of equation (19). Capacity is

$$q^{\mathrm{max}} = u^{\mathrm{f}} \frac{1}{u^{\mathrm{f}} \sum_{m \in M} \frac{k_m}{k} \Delta t_m + \ell} \tag{21}$$

Backwards wave speed is thus

$$w = -\frac{\frac{u^{\mathrm{f}}}{u^{\mathrm{f}} \sum_{m \in M} \frac{k_m}{k} \Delta t_m + \ell}}{\frac{1}{u^{\mathrm{f}} \sum_{m \in M} \frac{k_m}{k} \Delta t_m + \ell} - \frac{1}{\ell}} = \frac{\ell}{\sum_{m \in M} \frac{k_m}{k} \Delta t_m} \tag{22}$$

Equations (18) through (22) reduce to the model in Section 4.2 in the single vehicle class scenario. Figure 2 shows an example of how capacity and wave speed increase as the AV proportion increases when human drivers have a reaction time of 1 second and autonomous vehicles have a reaction time of 0.5 second. The cases of 0% AVs and 100% AVs are identical to the 1 second reaction time and 0.5 second reaction time fundamental diagrams in Figure 1, respectively.

4.4 Other factors affecting capacity

In reality, factors such as narrow lanes and road conditions affect capacity as well. These factors are usually in Highway Capacity Manual estimates of roadway capacity used for city network models. The model above, however, does not include factors beyond speed limit. To include these factors in the experimental results in Section 5, we scale existing estimates on capacity and wave speed in accordance with equations (21) and (22). Although the model in Section 4.3 predicts a triangular fundamental diagram as used by Newell (1993) and Yperman et al. (2005), other flow-density relationships are often used. CTM, the basis for multiclass DTA in this paper, uses a trapezoidal fundamental diagram.

Assume estimated roadway capacity and wave speed are $\hat{q}^{\max}$ and $\hat{w}$, respectively, and that the reaction time for human drivers is Δt_{HV}. Human reaction times may vary depending on the location of the road; for instance reaction times on rural roads are often greater than those in the city. Because capacity is affected by reaction time through equation (21), scaled capacity $\tilde{q}^{\max}$ is

$$\tilde{q}^{\max} = \frac{u^{\mathrm{f}} \Delta t_{\mathrm{HV}} + \ell}{u^{\mathrm{f}} \sum\limits_{m \in M} \frac{k_m}{k} \Delta t_m + \ell} \hat{q}^{\max} \tag{23}$$

Similarly, wave speed is affected by reaction time through equation (22), so scaled wave speed $\tilde{w}$ is

$$\tilde{w} = \frac{\Delta t_{\mathrm{HV}}}{\sum\limits_{m \in M} \frac{k_m}{k} \Delta t_m} \hat{w} \tag{24}$$

Equations (23) and (24) provide a method to integrate the capacity and backwards wave speed scaling of Section 4.3 with other factors and realistic data.

5 Intersection control policy

For shared road models, the intersection control policy is an important question. With 100% human vehicles, optimized traffic signals are the best option available. With 100% AVs, TBR can reduce delay beyond that of optimized signals (Fajardo et al., 2011). The difficulty is the choice of intersection control policy for shared roads. Dresner & Stone (2007) show that TBR subsumes traffic signals because the signal essentially reserves parts of the intersection. They propose link- and lane-cycling signals, where each link or lane successively receives full access to the intersection, and vehicles in other links or lanes may reserve non-conflicting paths. However, blocking out large portions of the intersection for a signal greatly restricts reservations from other links due to the possibility of conflict, even when most vehicles are AVs. As a result, this may not scale well when the proportion of AVs on the road becomes large. It is also an open question whether link- or lane-cycling signals even outperform optimized traffic signals.

Bento et al. (2013) propose the legacy early method for intelligent traffic management (LEMITM) policy of reserving space-time for all possible turning movements and increasing the safety margins for non-AVs to allow them to use the TBR infrastructure. AVs still use

conventional TBR, reserving only the requested path. This may be less efficient than traffic signals at small proportions of AVs because of the extra space-time reserved to ensure safety. However, as the proportion of AVs increases, TBR/LEMITM will devote less space-time to safety of human vehicles because it is not constrained by protecting turning movements allowed by traffic signals. As a result, TBR/LEMITM may scale at a higher rate. Therefore, TBR/LEMITM is used in this paper to study how link *and intersection* capacity scales with the proportion of AVs.

TBR/LEMITM makes two assumptions that we elaborate on here for the purposes of describing the DTA model of TBR/LEMITM. First, it separates vehicles into two groups: those that can establish digital communications on reservation acceptance and adherence, and those that cannot. The latter group consists of all non-AVs, although some AVs could conceivably fall into that group as well. This is possible in practice because current technology can already determine whether a vehicle is waiting at the intersection for actuated signals. Given that a vehicle is waiting, the intersection controller need only check whether the vehicle has established digital communications, which can be determined if vehicles transmit their position to the intersection controller along with reservation requests. Second, due to the unpredictably of human behavior, the intersection controller must be able to cancel granted reservations for AVs if a human is delayed in reacting to permission to enter the intersection. Because this DTA model does not include potential human errors and takes a more aggregate view of the intersection, canceled reservations are not included in the model.

Most studies on reservation-based controls use micro-simulation and are therefore not computationally tractable for the number of simulations required to solve DTA. Levin & Boyles (2015b) simplify TBR using the idea of larger conflict regions (CR) to distribute intersection capacity and receiving flows to sending flows for compatibility with general SBDTA models. Although the CR model is designed for arbitrary vehicle prioritization, TBR/LEMITM requires the intersection controller to reserve additional space and therefore make additional availability checks. Section 5.1 details the modifications to the CR algorithm to accommodate TBR/LEMITM.

5.1 Modified conflict region model

The conflict region model is a polynomial-time algorithm performed at each intersection each timestep to determine intersection movement. Vehicle movement is restricted by capacity of each conflict region it passes through during its turning movement. The purpose of the conflict region algorithm (Algorithms 1 & 2) is to determine which vehicles move subject to the constraints of sending flow, receiving flow, and conflict region capacity. The development of the conflict region algorithm is described in greater detail by Levin & Boyles (2015b). This section focuses on the modifications necessary to implement LEMITM.

The conflict region model requires discretized flow because of the priority function. For instance, Dresner & Stone (2004) propose a first-come-first-serve priority, and Dresner & Stone (2006) suggest priority for emergency vehicles. Modeling such prioritization functions with continuous flow is an open question, so discretized flow is used instead. These prioritization functions are orthogonal to the TBR/LEMITM control policy, although the

communications required for more complex prioritization functions such as auctions may be difficult for human drivers.

Let Γ^{-1} be the set of incoming links and Γ be the set of outgoing links for the intersection. The intersection is divided into a set of non-overlapping conflict regions C, with C_{ij} the subset of C through which vehicles turning from $i \in \Gamma^{-1}$ to $j \in \Gamma$ will pass. Let $y_{ij}(t)$ be the number of vehicles that have moved from i to j and y_c be the equivalent flow that has entered conflict region c in timestep t. Let Q_i be the capacity of link i and $Q_{ij} = \min\{Q_i, Q_j\}$ be the capacity of the turning movement from i to j. Every conflict region has some capacity

$$Q_c = \max_{(i,j)|c \in C_{ij}} \{Q_{ij}\} \tag{25}$$

to allow flow of $\min\{Q_i, Q_j\}$ for any (i,j) such that $c \in C_{ij}$ if no other demand is present, and vehicles traveling from i to j consume $\frac{Q_c}{Q_{ij}}$ of the capacity of c. $\frac{Q_c}{Q_{ij}} > 1$ refers to the case in which a vehicle from one approach reserves a capacity equivalent to more than 1 vehicle from another approach. For example, in a local road-arterial intersection, 1 vehicle crossing the intersection from the local road might prevent 2 vehicles on the arterial from moving.

Let l_i be the number of lanes and $S_i(t)$ the sending flow of link i at time t, i.e. the set of vehicles that could leave i at t if no other constraints were present. Each vehicle v has some priority defined by the arbitrary function $f(v, i)$. Let $R_j(t)$ be the receiving flow of link j, i.e. the number of vehicles that could enter j at t if incoming flow was infinite. Sending and receiving flows are general characteristics of dynamic flow models and allow the CR model to be applied to general SBDTA models. Denote by δ_v^{AV} whether vehicle v is autonomous.

Two modifications to the control algorithm are required to implement TBR/LEMITM. First, for non-AVs, movement from i to j across the intersection requires available capacity for all possible turning movements from i because the vehicle cannot communicate its destination to the intersection controller. The set of conflict regions a vehicle leaving link i *could* pass through is $\cup_{j' \in \Gamma} C_{ij'}$. It is not specific to j because for a human vehicle, the intersection manager does not know the vehicle's destination link. Therefore the intersection controller must check whether all such turning movements have space available. Second, when such a reservation is accepted, space for all possible turning movements from i must be reserved. The modified CR model is formalized in Algorithms 1 & 2.

5.2 Adjusted flows for vehicle classes

As shown in Section 4, cell capacities can be adjusted based on the reaction times of vehicles in the cell. However, CR capacities cannot similarly be adjusted because it is not known in advance which vehicles will pass through. Instead, the equivalent flow is adjusted based on the vehicle reaction time. Levin & Boyles (2015b) adjust the equivalent flow to account for differences in speeds from incoming links. Here we define an adjustment to equivalent flow because of differences in density due to reaction times. Vehicles with lower reaction times consume a smaller amount of the capacity. Based on equation (23), when the base capacity $\hat{q}^{\text{max}}$ is used to determine CR capacity, a vehicle v with reaction time Δt_v should have an

Algorithm 1 Conflict region algorithm (see Algorithm 2 for canMove procedure)

1: Set $V = \emptyset$
2: **for** all $i \in \Gamma^{-1}$ **do**
3:     Sort $S_i(t)$ by arrival time at i
4:     Remove first l_i vehicles in $S_i(t)$ and add them to V
5:     **for** all $j \in \Gamma$ **do**
6:         Set $y_{ij}(t) = 0$
7:     **end for**
8: **end for**
9: Sort V by $f(v)$
10: **for** all $v \in V$ **do**
11:     Let (i, j) be the turning movement of v
12:     **if** $\texttt{canMove}(\delta_v^{\mathrm{AV}}, i, j)$ **then**
13:         Set $y_{ij}(t) = y_{ij}(t) + 1$
14:         **if** $\delta_v^{\mathrm{AV}} = 1$ **then**
15:             **for** all $c \in C_{ij}$ **do**
16:                 Set $y_c(t) = y_c(t) + \frac{Q_c}{Q_{ij}}$
17:             **end for**
18:         **else**
19:             **for** all $c \in \cup_{j' \in \Gamma} C_{ij'}$ **do**
20:                 Set $y_c(t) = y_c(t) + \frac{Q_c}{Q_{ij}}$
21:             **end for**
22:         **end if**
23:         Remove next vehicle in $S_i(t)$ and add it to V in sorted order
24:         Go to line 10
25:     **end if**
26: **end for**

Algorithm 2 `canMove` procedure

1: **function** CANMOVE$\left(\delta_v^{\mathrm{AV}}, i \in \Gamma^{-1}, j \in \Gamma\right)$
2:     **if** $R_j - \sum\limits_{i' \in \Gamma^{-1}} y_{i'j}(t) < \frac{u_i^{\mathrm{f}}\Delta t_v + \ell}{u_i^{\mathrm{f}}\Delta t_{\mathrm{HV}} + \ell}$ **then**
3:         Return False
4:     **end if**
5:     **if** $\delta_v^{\mathrm{AV}} = 1$ **then**
6:         **for** all $c \in C_{ij}$ **do**
7:             **if** $Q_c - y_c(t) < \frac{u_i^{\mathrm{f}}\Delta t_v + \ell}{u_i^{\mathrm{f}}\Delta t_{\mathrm{HV}} + \ell} \frac{Q_c}{Q_{ij}}$ **then**
8:                 Return False
9:             **end if**
10:         **end for**
11:     **else**
12:         **for** all $c \in \cup_{j' \in \Gamma} C_{ij'}$ **do**
13:             **if** $Q_c - y_c(t) < \frac{u_i^{\mathrm{f}}\Delta t_v + \ell}{u_i^{\mathrm{f}}\Delta t_{\mathrm{HV}} + \ell} \frac{Q_c}{Q_{ij}}$ **then**
14:                 Return False
15:             **end if**
16:         **end for**
17:     **end if**
18:     Return True
19: **end function**

---

equivalent flow of

$$\frac{u_i^{\mathrm{f}}\Delta t_v + \ell}{u_i^{\mathrm{f}}\Delta t_{\mathrm{HV}} + \ell} \tag{26}$$

where u_i^{f} is the free flow speed of link i.

6　Experimental results

This section describes the results of two experiments using multiclass CTM and TBR/LEMITM. All experiments used a custom DTA software implemented in Java. First we study a single intersection to determine how TBR/LEMITM affects intersection delay as the proportion of AVs increases. Second, we implement the shared road model in DTA on the downtown Austin city network with varying proportions of AVs to study the effects on total travel time and compare with traffic signals. Although TBR/LEMITM was introduced by Bento et al. (2013), their experiments are focused on the efficiency of the various intersection controls they study rather than their use in combination. Therefore the experiments in this section are a first look at using TBR/LEMITM as needed in a shared road scenario. These are also the first results for shared roads with DUE routing behavior.

For these experiments, flow is discretized so reservation-based intersection controls may be used. As a result, vehicles within a cell are contained in a FIFO queue, and FIFO is ensured within cells except at intersections. Cell transition flows are restricted by capacity and cell density as functions of class proportions as discussed in Sections 3 and 4.

To study a gradual shift from HVs to AVs, flow is separated into two classes: HVs with a reaction time of 1 second, and AVs with a reaction time of 0.5 seconds. ℓ is 20 feet for the purposes of car following and jam density. The experiments hold the total demand fixed while changing the proportion of AVs. Based on equation (26), with the parameters of this study, AVs require 0.593 of the capacity that HVs require. The vehicular demand places, on average, $1400\left(p^{\mathrm{HV}} + 0.593 p^{\mathrm{AV}}\right) + 1300\left(p^{\mathrm{HV}}\right)$ vehicles per hour demand on the intersection in each direction.

6.1　Single intersection

First, we study the four link, single lane intersection shown in Figure 3 with capacity and demand chosen to demonstrate two observed conditions for the effects of TBR/LEMITM on single intersections. Each approach has demand of 1200 vehicles per hour through traffic, 200 vehicles per hour right-turning, and 100 vehicles per hour left-turning traffic. Each link is 1 mile long and has capacity of 1800 vehicles per hour, which does not allow all demand to be satisfied on average when a significant proportion of vehicles are HVs. Links have a free flow speed of 60 miles per hour and a backwards wave speed of half the free flow speed — 30 miles per hour. Capacity and backwards wave speed increase with the proportion of AVs as defined in Section 4.4.

Experiments were performed at 10% intervals of AV proportion. Each experiment had 1 hour of demand with vehicle departure times randomly chosen. Experiments were repeated
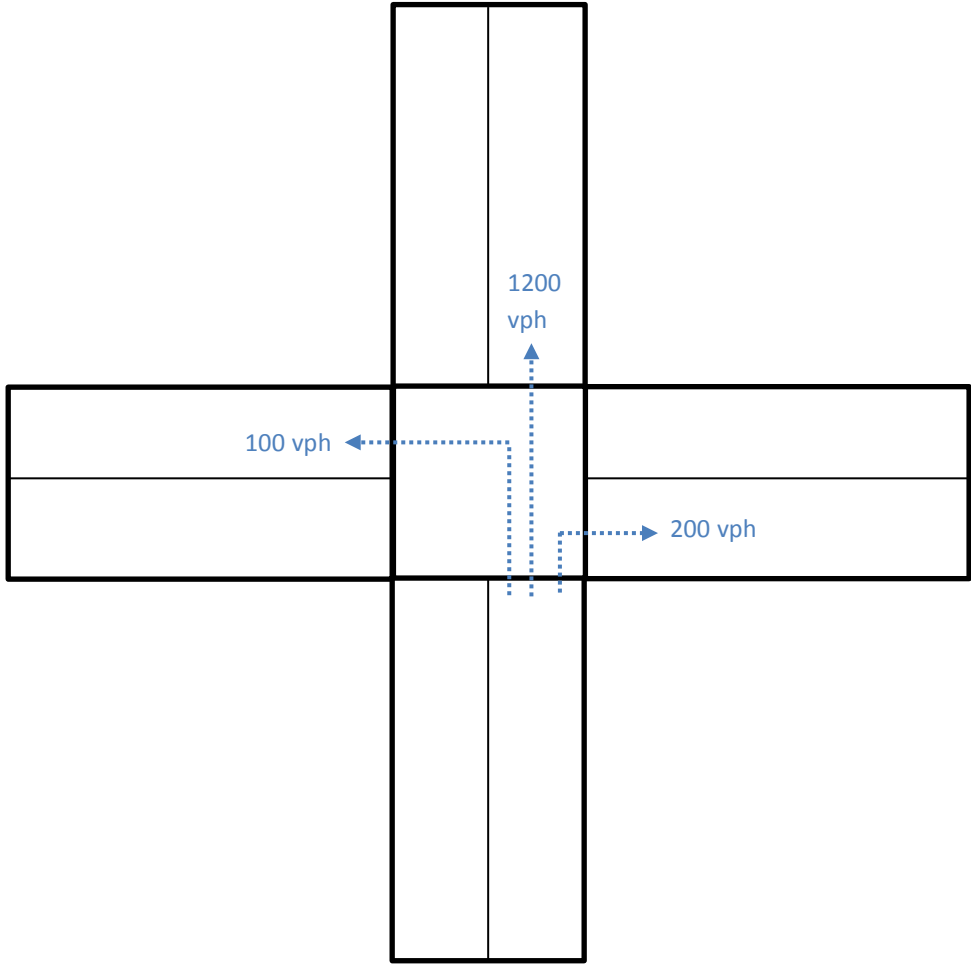
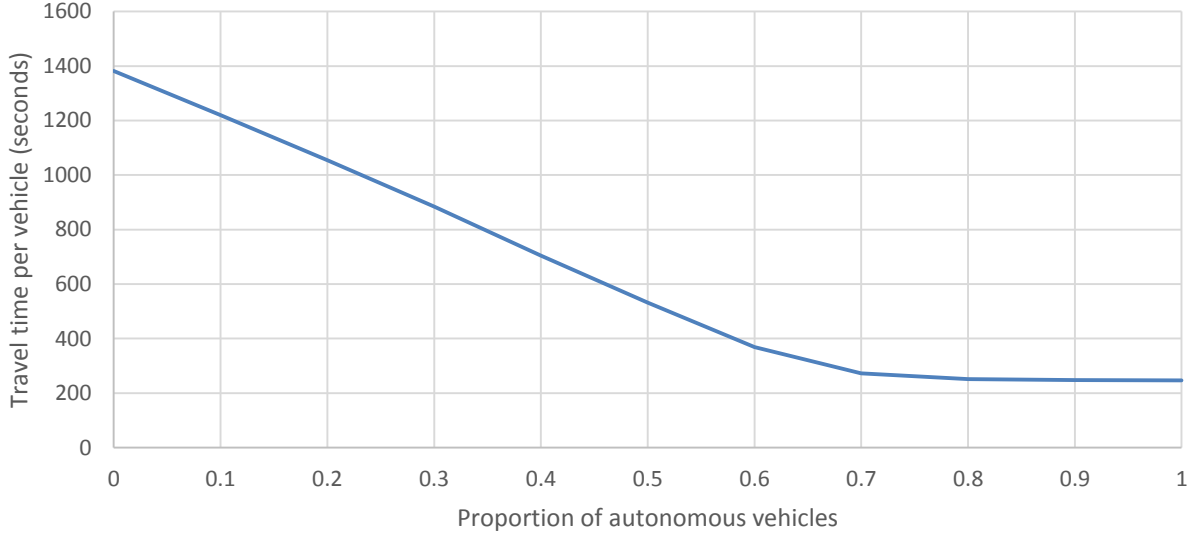Figure 3: Single intersection case study

Figure 4: Average travel time per vehicle at different proportions of AVs

10 times and average travel times per vehicle are shown in Figure 3. Between 0% and 60% AVs, average travel time decreases linearly with the proportion of AVs. Between 70% and 100% AVs, travel time is almost unchanged. At this point, the capacity of the intersection, increased by reduced headways from AVs, is sufficient for the demand. Slight delays for a few vehicles are observed due to the randomness in the distribution of departure times and of AVs but overall the effect is small. This is consistent with the TBR/LEMITM model: the additional capacity required to reserve all turning movements for HVs is proportional to the percentage of HVs. In practice, this may be used to predict the intersection delay for arbitrary proportions of AVs and thus determine the point at which TBR/LEMITM improves over signals. Of course, intersection delay also affects intersection demand through route choice, which is the subject of the DTA model of the rest of this section.

6.2   Shared road dynamic traffic assignment

We now consider a DTA model using the multiclass CTM and TBR/LEMITM intersection controls to study the predictions of the shared road model with DUE routing. The model was run on the downtown Austin network, which has 171 zones, 546 intersections, 1247 links, and 62836 trips, shown in Figure 5. This network was chosen because many links are arterials or part of the downtown grid and terminate at (currently) signal-controlled intersections. Convergence was measured by comparing travel time with the shortest paths for 15 minute assignment intervals. Let t^*_{rst} be the travel time of the shortest path from r to s departing within $t \in \mathcal{T}$, where $\mathcal{T}$ is the set of all assignment intervals. Let t_v be the travel time of
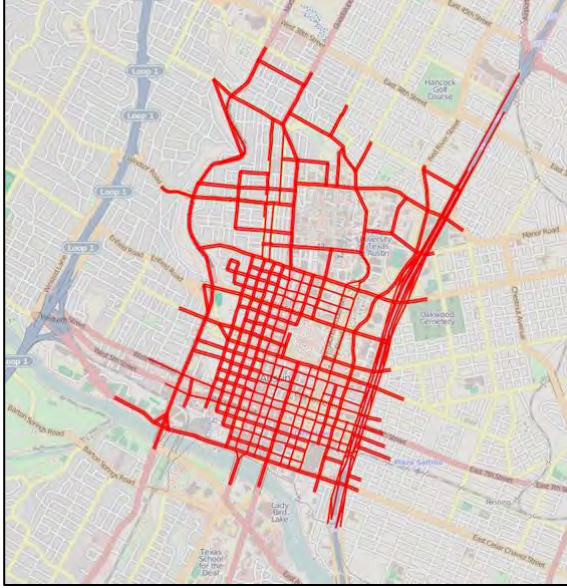
Figure 5: Downtown Austin network

vehicle v. The convergence measure of average excess cost (AEC) is then defined as

$$AEC = \frac{\displaystyle\sum_{(r,s,t)\in Z^2\times\mathscr{T}} \sum_{v\in V_{rst}} t(v) - t_{rst}^*}{\displaystyle\sum_{(r,s,t)\in Z^2\times\mathscr{T}} |V_{rst}|} \qquad (27)$$

where Z is the set of zones and V_{rst} is the demand from r to s departing within $t \in \mathscr{T}$. DTA used the MSA solution algorithm (see Levin et al., 2014), but more complex techniques could improve convergence. Computation times for 50 iterations of MSA on an Intel Xeon processor running at 3.33 GHz are shown in Figure 6. Since greater proportions of autonomous vehicles increase the network efficiency, and vehicles exit sooner, greater proportions of autonomous vehicles also decrease computation times. The computation times of less than 18 minutes per scenario allow a suite of scenarios to be run on the downtown Austin city network within a few hours.

6.3 Convergence

Figure 7 shows the average excess cost per iteration for the 50% AVs scenario. The solution quickly reaches an AEC of less than 50 seconds, but the convergence pattern is slow and non-monotone afterwards. However, that is expected for SBDTA (Levin et al., 2014).

Although convergence is difficult to prove for multiclass formulations even with static traffic assignment (Marcotte & Wynter, 2004), the multiclass DTA appears to converge to an equilibrium on the downtown Austin city network for all studied proportions of AVs. These results empirically demonstrate that the multiclass dynamic flow and intersection models developed in this paper may be used with DTA on city networks.
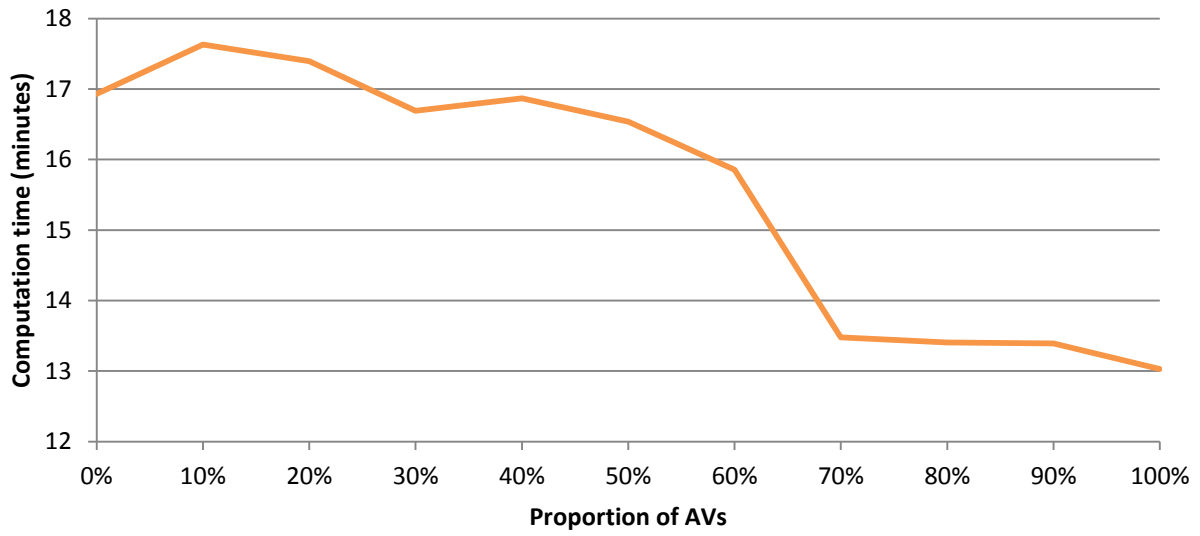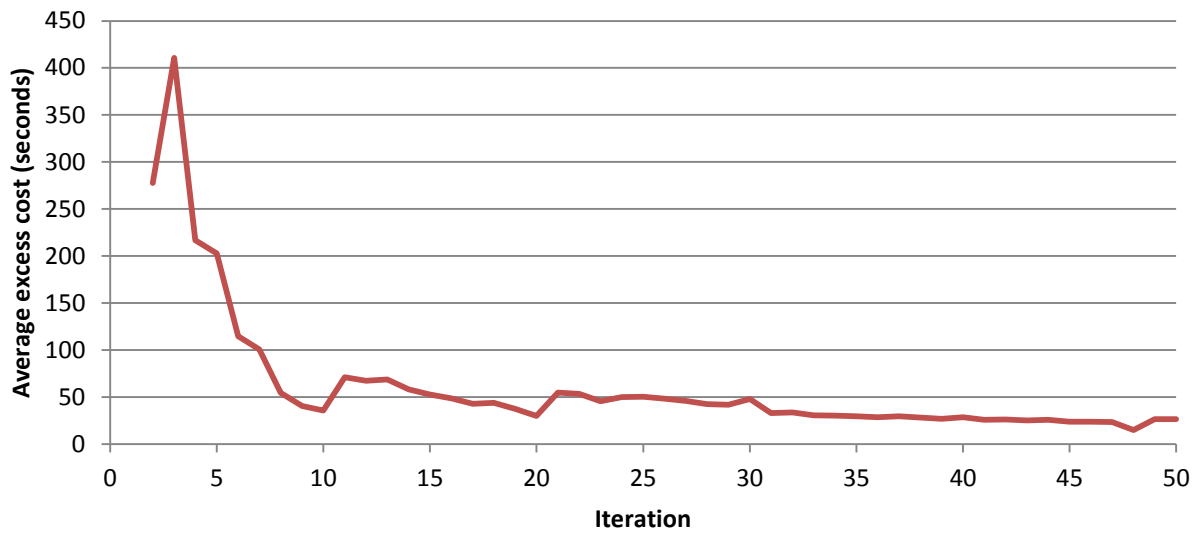
20

Figure 6: Downtown Austin network

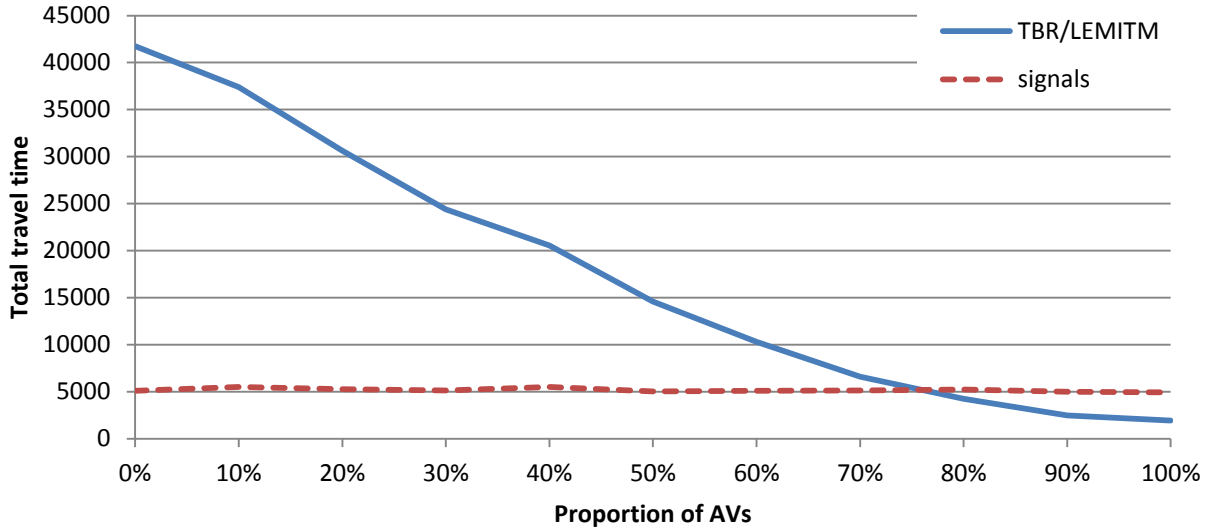Figure 7: Average excess cost for 50% AVs scenario

21

Figure 8: Total travel time as proportion of AVs increases

6.4 Travel time predictions

Total travel time (TTT) with TBR/LEMITM are compared with traffic signals at intersections in Figure 8. DTA was solved for each scenario, so vehicles are considering the average travel times from the correct AV proportion in their route choice. Traffic signals benefit from reduced headways for AVs but delay may be improved by TBR for 100% AVs (Fajardo et al., 2011). However, this experiment explores the effects of these intersection controls for shared roads. The downtown Austin network (shown in Figure 4) is mostly arterials and downtown grid region. Therefore intersections are the major source of congestion for many links. This is supported by the results: when traffic signals are used, TTT decreases only slightly. Although AVs increase capacity per signal phase, vehicles are still delayed waiting for a phase that allows their turning movement. In contrast, TBR/LEMITM performs much worse when the proportion of AVs is low. For HVs, LEMITM is less efficient than signals because it reserves more of the intersection to ensure safe movement. However, intersection delay and TTT appear to decrease linearly at a significant rate with the proportion of AVs, as with the single intersection results in Section 6.1.

These results suggest that TBR/LEMITM improves over signals after AV penetration reaches around 80%. However, the exact proportion of AVs at which TBR/LEMITM becomes advantageous may vary depending on the city network topology. Note that although Dresner & Stone (2007) and Bento et al. (2013) study a single shared intersection, route choice may be affected by the proportion of AVs. Intersections with a higher proportion of AVs will experience lower delay and may encourage greater use. Therefore, to estimate the effect of intersection controls on route choice, a DTA framework such as the one presented here should be used.

22

7   Conclusions

Maturing AV technology suggests that AVs will be publicly available within the next few decades. To provide a framework for studying the effects of AVs on city networks, this paper develops a shared road DTA model for human and autonomous vehicles. A multiclass CTM is presented for vehicles traveling at the same speed with capacity and backwards wave speed a function of class proportions. A collision avoidance car following model incorporating vehicle reaction time is used to predict how reduced reaction times might increase capacity and backwards wave speed. These models are generalized to an arbitrary number of classes because different AVs may be certified for different reaction times. These models also use continuous flow so that SBDTA models built on continuous flows may incorporate these multiclass predictions.

The second part of a shared road DTA model is the intersection control. We modify the CR model proposed by Levin et al. (2015b) to include the LEMITM reservation model for non-AVs (Bento et al., 2013) while using conventional TBR for AVs. This TBR/LEMITM combination with multiclass CTM flow model is studied in a DTA framework on a single intersection and on a city network. Results verify that use of TBR/LEMITM decreases intersection delay linearly with the proportion of AVs, as is expected from the intersection model. This may be used to predict what AV penetration is required for TBR/LEMITM to improve over traffic signals. Although results on downtown Austin suggest that 80% AV penetration is required, this may depend on the network topology.

In future work, the capacity and backwards wave speed predicted here should be verified with microsimulation and/or real vehicles. Other such estimations may still be incorporated into the multiclass CTM model presented in this paper. The model of LEMITM should also be calibrated. On a larger scale, determining an efficient shared intersection controls is still an open question to bridge the gap between optimized traffic signals for HVs and TBR for AVs. New shared intersection controls may be implemented in this multiclass framework to study how their performance under DUE routing. This framework might also be used to study the impact of mixed intersection controls (some signals, some TBR/LEMITM) on DUE routing in a traffic network.

Acknowledgements

References

Aarts, L., & Van Schagen, I. (2006). Driving speed and the risk of road crashes: A review. Accident Analysis & Prevention, 38(2), 215–224.

Bento, L. C., Parafita, R., Santos, S., & Nunes, U. Intelligent Traffic Management at Intersections: Legacy Mode for Vehicles not Equipped with V2V and V2I Communications.

COMMUNICATIONS, 2, V2I.

Brackstone, M., & McDonald, M. (1999). Car-following: a historical review. Transportation Research Part F: Traffic Psychology and Behaviour, 2(4), 181–196.

Blumberg, M., & Bar-Gera, H. (2009). Consistent node arrival order in dynamic network loading models. Transportation Research Part B: Methodological, 43(3), 285–300.

Carlino, D., Depinet, M., Khandelwal, P., & Stone, P. (2012, September). Approximately orchestrated routing and transportation analyzer: Large-scale traffic simulation for autonomous vehicles. In Intelligent Transportation Systems (ITSC), 2012 15th International IEEE Conference on (pp. 334–339). IEEE.

Carlino, D., Boyles, S. D., & Stone, P. (2013, October). Auction-based autonomous intersection management. In Proceedings of the 16th IEEE Intelligent Transportation Systems Conference (ITSC).

Chiu, Y. C., Bottom, J., Mahut, M., Paz, A., Balakrishna, R., Waller, T., & Hicks, J. (2011). Dynamic traffic assignment: A primer. Transportation Research E-Circular, (E-C153).

Daganzo, C. F. (1994). The cell transmission model: A dynamic representation of highway traffic consistent with the hydrodynamic theory. Transportation Research Part B: Methodological, 28(4), 269–287.

Daganzo, C. F. (1995a). The cell transmission model, part II: network traffic. Transportation Research Part B: Methodological, 29(2), 79–93.

Daganzo, C. F. (1995b). A finite difference approximation of the kinematic wave model of traffic flow. Transportation Research Part B: Methodological, 29(4), 261–276.

Dresner, K., & Stone, P. (2004, July). Multiagent traffic management: A reservation-based intersection control mechanism. Procgs of 3rd International Joint Conference on Autonomous Agents & Multiagent Systems-Vol. 2 (pp. 530–537). IEEE Computer Society.

Dresner, K., & Stone, P. (2006, May). Human-usable and emergency vehicle-aware control policies for autonomous intersection management. In Fourth International Workshop on Agents in Traffic and Transportation (ATT), Hakodate, Japan.

Dresner, K. M., & Stone, P. (2007, January). Sharing the Road: Autonomous Vehicles Meet Human Drivers. In IJCAI (Vol. 7, pp. 1263–1268).

Fajardo, D., Au, T. C., Waller, S. T., Stone, P., & Yang, D. (2011). Automated Intersection Control. Transportation Research Record: Journal of the Transportation Research Board, 2259(1), 223–232.

Gartner, N. H., Messer, C. J., & Rathi, A. K. (2005). Revised monograph on traffic flow theory: a state-of-the-art report. Special Report by the Transportation Research Board of the National Research Council.

Greenshields, B. D., Channing, W., & Miller, H. (1935). A study of traffic capacity. In Highway research board proceedings (Vol. 1935). National Research Council (USA), Highway Research Board.

Johansson, G., & Rumar, K. (1971). Drivers' brake reaction times. Human Factors: The Journal of the Human Factors and Ergonomics Society, 13(1), 23–27.

Kesting, A., Treiber, M., & Helbing, D. (2010). Enhanced intelligent driver model to

access the impact of driving strategies on traffic capacity. Philosophical Transactions of the Royal Society A: Mathematical, Physical and Engineering Sciences, 368(1928), 4585–4605.

Kometani, E., & Sasaki, T. (1959). Dynamic behaviour of traffic with a nonlinear spacing-speed relationship. In Proceedings of the Symposium on Theory of Traffic Flow , Research Laboratories, General Motors (pp. 105–119). New York: Elsevier.

Levin, M. W., Pool, M., Owens, T., Juri, N. R., & Waller, S. T. (2014). Improving the Convergence of Simulation-based Dynamic Traffic Assignment Methodologies. Networks and Spatial Economics, 1–22.

Levin, Michael W. & Stephen D. Boyles (2015a). Effects of Autonomous vehicle ownership on trip, mode, and route choice. Publication pending in Transportation Research Record.

Levin, Michael W. & Stephen D. Boyles (2015b). Intersection auctions and reservation-based control in dynamic traffic assignment. Publication pending in Transportation Research Record.

Lighthill, M. J., & Whitham, G. B. (1955). On kinematic waves. II. A theory of traffic flow on long crowded roads. Proceedings of the Royal Society of London. Series A. Mathematical and Physical Sciences, 229(1178), 317-345.

Marcotte, P., & Wynter, L. (2004). A new look at the multiclass network equilibrium problem. Transportation Science, 38(3), 282–292.

Marsden, G., McDonald, M., & Brackstone, M. (2001). Towards an understanding of adaptive cruise control. Transportation Research Part C: Emerging Technologies, 9(1), 33–51.

Miller, Joe. "Google Cars 'designed to Speed'" BBC News. BBC, n.d. Web. 25 Aug. 2014.

Newell, G. F. (1993). A simplified theory of kinematic waves in highway traffic, part I: general theory. Transportation Research Part B: Methodological, 27(4), 281–287.

Newell, G. F. (2002). A simplified car-following theory: a lower order model. Transportation Research Part B: Methodological, 36(3), 195–205.

Qian, X., Gregoire, J., Moutarde, F., & De La Fortelle, A. (2014). Autonomous Intersection Management for Mixed Traffic Flow. arXiv preprint arXiv:1407.5813. Richards, P. I. (1956). Shock waves on the highway. Operations research, 4(1), 42–51.

Schakel, W. J., van Arem, B., & Netten, B. D. (2010). Effects of cooperative adaptive cruise control on traffic flow stability. In Intelligent Transportation Systems (ITSC), 2010 13th International IEEE Conference on (pp. 759–764). IEEE.

Schepperle, H., & Bhm, K. (2007). Agent-based traffic control using auctions. In Cooperative Information Agents XI (pp. 119–133). Springer Berlin Heidelberg.

Tuerprasert, K., & Aswakul, C. (2010). Multiclass cell transmission model for heterogeneous mobility in general topology of road network. Journal of Intelligent Transportation Systems, 14(2), 68–82.

Van Arem, B., van Driel, C. J., & Visser, R. (2006). The impact of cooperative adaptive cruise control on traffic-flow characteristics. Intelligent Transportation Systems, IEEE Transactions on, 7(4), 429–436.

Vasirani, M., & Ossowski, S. (2012). A market-inspired approach for intersection management in urban road traffic networks. Journal of Artificial Intelligence Research, 43(1), 621-659.

Wong, G. C. K., & Wong, S. C. (2002). A multi-class traffic flow modelan extension of LWR model with heterogeneous drivers. Transportation Research Part A: Policy and Practice, 36(9), 827–841.

Yperman, I., Logghe, S., & Immers, B. (2005, September). The Link Transmission Model: An efficient implementation of the kinematic wave theory in traffic networks. In Proceedings of the 10th EWGT Meeting, Poznan, Poland.

Intersection auctions and reservation-based control in dynamic traffic assignment

Michael W. Levin

Stephen D. Boyles

Abstract

Autonomous vehicle (AV) technology is maturing, with AVs test-driving on public roads. A promising intersection control policy (TBR) proposed by Dresner and Stone (2004) offers the potential to improve intersection capacity beyond the capabilities of optimized traffic signals. Although TBR has been studied in several micro-simulation models, it has yet to be analyzed under user equilibrium behavior. Towards this goal, we model TBR in dynamic traffic assignment to draw on its extensive literature on vehicle routing behaviors. The proposed model makes TBR computationally feasible to be simulated on large city networks with the goal of solving traffic assignment. TBR also offers benefits through arbitrarily prioritizing vehicle movement; high value-of-time travelers may be able to gain priority through intersection auctions, as suggested by previous literature. We perform an in-depth study of simple intersection auctions and find that much of its benefits (over first-come-first-serve prioritization) result from the randomizing effect of auctions giving larger queues of vehicles greater shares of the intersection capacity.

1. Introduction

Autonomous vehicle (AV) technology is quickly maturing, and AVs are already test-driving on the public roads of several states (Oakley, 2014). AVs have the potential to improve the road network in several ways, such as by increasing intersection capacity through the tile-based reservation (TBR) control policy proposed by Dresner and Stone (2004). TBR divides the intersection into tiles in space-time to monitor conflicts. Vehicles wishing to cross the intersection request to reserve tiles to ensure safe passage. Their request is accepted only if their path does not conflict with other vehicles, illustrated in Figure 1. The net result is that vehicles making conflicting movements (such as cross traffic) can simultaneously use the intersection through proper timing. Fajardo et al. (2011) demonstrated that TBR reduces delay beyond optimized traffic signals for a variety of demand scenarios.

Although TBR has been implemented in several custom micro-simulators, modeling this control over large city networks has yet to be accomplished due to the computational requirements. This is expected because micro-simulation is less appropriate for modeling city networks. However, this motivates the need for TBR integration into more aggregate flow models such as dynamic traffic assignment (DTA). A DTA model of TBR allows analyzing traffic flow under user equilibrium (UE) behavior. Although previous network-wide models of autonomous vehicles, such as Carlino et al. (2012), assumed routing to avoid congestion, predictions may differ when UE routing is considered. For instance, the greater capacity afforded by TBR-controlled intersections may also result in an increase in demand. UE behavior becomes more important when considering prioritization strategies besides FCFS in TBR. Studies by Schepperle and Böhm (2007) and Carlino et al. (2013) propose intersection auction schemes that reduce average intersection delay under heuristic routing behavior. However, the mechanisms leading to improvements are not fully understood; Carlino et al. (2013) use heuristic system bids to boost

delay reductions, but how to choose optimal system bids is not clear. Moreover, the benefits may change due to vehicle routing behaviors. For instance, low-bidding vehicles may route to avoid auctions dominated by high-bidding vehicles. The primary obstruction to a more rigorous analysis of TBR is its micro-simulation definition, which has thus far prevented it from being studied in DTA. Improving computational feasibility and compatibility with DTA is the goal of this paper.

The contributions of this paper are to develop a conflict region (CR) intersection model of TBR, compatible with general simulation-based DTA (SBDTA) models for solving for UE. The CR algorithm reduces the computational complexity of TBR but retains its properties of allowing simultaneous use of the intersection by potentially conflicting vehicles. The proposed model is also compatible with arbitrary vehicle prioritization schemes, including FCFS and auctions. We compare the CR model with results from micro-simulations of the TRB policy and analyze capacity on a single intersection case study. Finally, we implement the model in SBDTA to analyze the effect of auctions on traffic flow. Under UE behavior, much of the benefits of auctions appear to result from its randomizing effect. We compare results with a pure random policy and observe similar reductions in average travel time.

The remainder of this paper is organized as follows. Section 2 reviews literature on congestion pricing and intersection auctions to motivate the CR model proposed in section 3. Section 4 compares the CR model with micro-simulation results from Fajardo et al. (2011) on a single intersection. Section 5 discusses results from implementation of the CR model on test networks, and conclusions are presented in section 6.

2. Literature review

We first discuss the considerable literature on congestion pricing and intersection auctions in Section 2.1. This leads to a review of the tile-based reservation (TBR) policy in Section 2.2 which enables intersection auctions. The review of TBR is a background for the methods developed in Section 3 to allow modeling of intersection auctions in DTA under UE behavior.

2.1 Congestion pricing

The potential inefficiencies of UE relative to system optimal (SO) solutions, demonstrated best through the Braess (1968) paradox, can be eliminated through marginal cost pricing (Smith, 1979). de Palma and Lindsey (2011) give a comprehensive review of pricing methodologies and technologies, but we discuss some literature here to motivate the proposed model. Although implementations in practice typically do not toll all links, May et al. (2008) found that tolling 10% of the links could achieve 60% to 70% of the benefits. However, partial tolling can lead to traffic diversion, increasing congestion on non-tolled links (Swan and Belzer, 2010). Another consideration is variations in congestion over time, which can be addressed by time-of-day tolling, as with Yin and Lou (2009)'s study on managed toll lanes.

The goal of reducing use of the limited resource of road capacity results in a grouping of travelers by value-of-time (VOT). Only travelers with sufficiently high VOT are willing to pay the toll for the benefit of reduced travel time. Determining pricing to maximize capacity of the tolled road is difficult; Lou et al. (2011) studied a self-learning approach based on loop detector data for setting

dynamic tolls. However, the US National Surface Transportation Infrastructure Financing Commission (2009) report raised the issue that complex or real-time toll schemes require travelers to have more information about tolls. Lack of information may lead to unintended or suboptimal behavior.

Auctions may be an alternative to the problems of complex or changing tolls and determining toll prices. Due to the communication requirements of implementing auctions, most studies have considered auctions in the context of autonomous vehicles. Schepperle and Böhm (2007, 2008) studied the use of auctions to control vehicle priority in traveling through intersections, and found that average delay weighted by VOT was reduced. Vasirani and Ossowski (2010) similarly found reductions in average travel time from auctions on a network of such intersections. Carlino et al. (2013) added system bids to improve equity and travel time, and found that auctions reduced average travel time for some of the scenarios. However, route choice differences due to UE behavior have yet to be incorporated into network comparisons of intersection auctions.

Although auctions have greater communication requirements, existing technologies come close to meeting them. de Palma and Lindsey (2011) note that most tolling facilities in the United States use dedicated short range communications technology to identify vehicles. In addition to transmitting vehicle identification, these technologies could be modified to transmit an auction bid as well. Of greater difficulty is communicating to drivers whether they have won the auction and are permitted to use the facility. Since no such system yet exists, as with Schepperle and Böhm (2007, 2008), Vasirani and Ossowski (2010), and Carlino et al. (2013), we study auctions in the context of autonomous vehicle intersection controls. Auctions at intersections may offer further advantages in terms of congestion reduction. First, they are integrated with autonomous vehicle intersection controllers, obviating the need for investment in separate facilities. Second, intersections (both arterial and highway merge/diverge) are often major sources of congestion. Although tolling links will reduce the backwards propagation of congestion, pricing the source of the congestion could be more effective.

2.2 Tile-based reservation intersection control

Tile-based reservation (TBR) controls were proposed by Dresner and Stone (2004, 2006a) to take advantage of the computer precision and communications abilities of autonomous vehicles. Vehicles request permission from the intersection controller to follow a specific path through the intersection in space-time. The intersection controller divides the intersection into a grid of tiles to check whether vehicles collide, accepting or rejecting requests depending on whether the tiles are occupied at the requested time. This is best illustrated by Fajardo et al. (2011), reproduced in Figure 1.
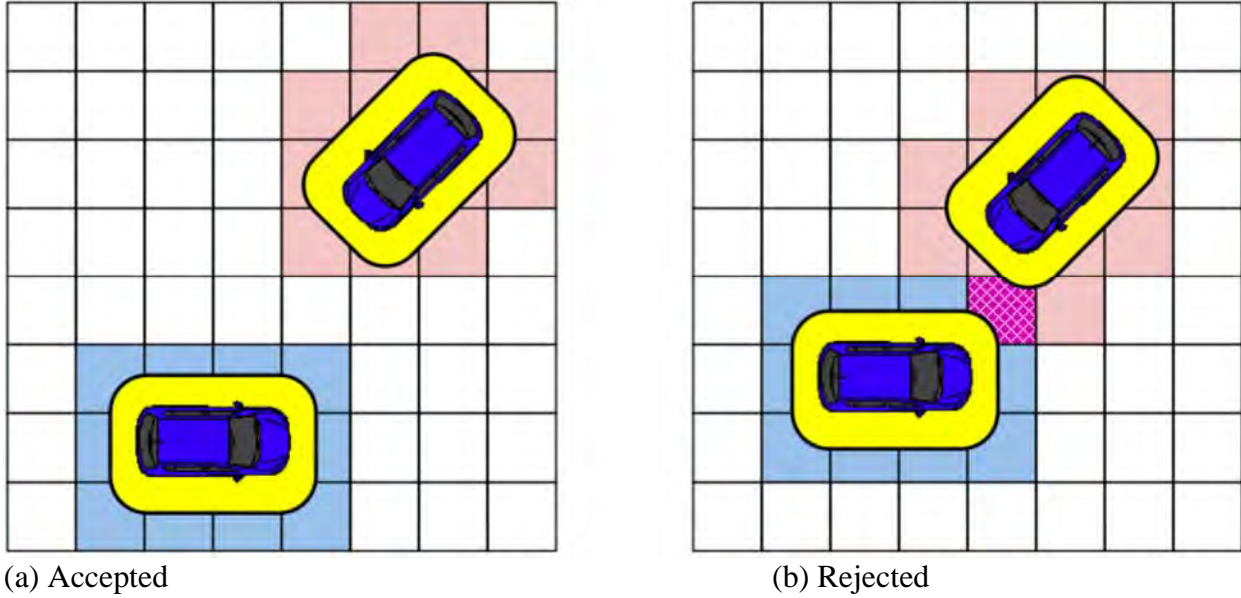
(a) Accepted   (b) Rejected

FIGURE 1 (a) The two vehicles do not conflict at the specified time. (b) The vehicles conflict in a single tile at the specified time, so the request is rejected (Fajardo et al., 2011).

Fajardo et al. (2011) also demonstrate reductions in delay from TBR over SYNCHRO-optimized traffic signals for a variety of demands. Since autonomous vehicle market penetration is likely to occur gradually, Dresner and Stone (2007) modified TBR to permit use of the intersection by human drivers.

One challenge in modeling the reservation policy is the computational complexity of simulating vehicles over a grid of tiles over time per intersection. When implemented for real vehicles, each intersection may have a separate computerized controller, but in dynamic traffic assignment models all intersections share the same computing power. These requirements are in addition to the baseline of vehicle movement or propagation. To reduce computation requirements for city-size networks, Carlino et al. (2012) implemented reservations on the entire intersection as opposed to specific tiles to make single simulations of vehicles on city-size networks tractable. However, this restricts the simultaneous use of the intersection to non-conflicting vehicles. Vehicles can only enter the intersection if the paths of vehicles that already hold or are executing a reservation do not conflict. This differs from the TBR proposed by Dresner and Stone (2004), and this may reduce the benefits demonstrated in AIM4 (Fajardo et al., 2011) of TBR over traffic signals. Furthermore, solving SBDTA to account for user equilibrium behavior typically requires many simulations. Therefore, implementing TBR directly in DTA is too computationally demanding. At the same time, the DTA model of TBR should preserve its simultaneous use and arbitrary prioritization characteristics. This leads to the model proposed in Section 3.

3. Reservation control model for dynamic traffic assignment

To motivate the reservation control model in DTA presented in section 3.2, we first describe the requirements we seek to achieve in section 3.1. As with TBR, the proposed model requires some

knowledge about vehicle path through the intersection, which may be dependent on intersection geometry. We develop a method to automate finding these paths in section 3.3.

3.1 Requirements of the model

To reduce the computational requirements of TBR sufficient for many simulations on city-size networks, we propose a simplified model to meet the following requirements:

1) The reservation policy model should be compatible with SBDTA in general, not restricted to a specific flow model. To accomplish this, the proposed algorithm builds on characteristics of general intersection models studied by Tampère et al. (2011).
2) The model should admit arbitrary prioritization schemes, such as FCFS and auctions. This is necessary to compare the effects of arbitrary prioritization strategies such as emergency vehicle-aware policies (Dresner and Stone, 2006b) or auctions with system bids (Carlino et al., 2013).
3) The model should retain the simultaneous-use behavior of TBR, even by vehicles with potentially conflicting paths, to model the benefits of AV intersections. Without this, the model may not accurately predict vehicle behaviors and capacities of reservation policy intersections.
4) The model should be independent of specific intersection characteristics. Due to the number of intersections in city networks, tuning the model per intersection would be a time-consuming process as noted by Tampère et al. (2011). TBR requires tracing the path of a vehicle through a grid of tiles, which is dependent on intersection geometry. The proposed model reduces this to tracing the path through larger *conflict regions*. Section 3.3 presents an algorithm to divide intersections into conflict regions based on link angles.

In the development of this model, we make the following assumptions:

1) Flow is discretized to model vehicle-specific prioritization such as auctions. Applying such prioritizations to continuous flow requires additional study.
2) Vehicles are identical in terms of tiles occupied during turning movements. Many aggregate DTA models assume a characteristic, identical passenger vehicle, and we do the same here.
3) In the absence of other demand, flow between any incoming link to any outgoing link is restricted only by capacity of the two links. This is necessary to be as independent as possible from specific intersection geometry, as suggested by Tampère et al. (2011).

3.2 Intersection flow algorithm

The CR solution method is formalized in Algorithm 1 and described here in more detail. Consider an intersection with outgoing links Γ and incoming links Γ^{-1}. Divide the intersection into a set of non-overlapping *conflict regions* C. These conflict regions are intended to be much larger than tiles used in TBR, and are discussed in more detail in section 3.3. Denote by C_{ij} the subset of C through which vehicles turning from $i \in \Gamma^{-1}$ to $j \in \Gamma$ will pass. Let $y_{ij}(t)$ be the number of vehicles that have moved from i to j and y_c be the equivalent flow that has entered conflict region c in timestep t. Let Q_i be the capacity of link i and $Q_{ij} = \min\{Q_i, Q_j\}$ be the capacity of the turning movement from i to j. Every tile has some capacity

$$Q_c = \max_{\{(i,j)|c \in C_{ij}\}} (Q_{ij}) \tag{1}$$

to allow flow of $\min\{Q_i, Q_j\}$ for any (i,j) such that $c \in C_{ij}$ if no other demand is present. This definition of conflict region capacity, however, may overestimate vehicle movement if two turning movements that share a conflict region have different capacities. More specifically, consider the case where turning movements $(1,2)$ and $(3,4)$ with capacities $Q_{12} < Q_{34}$ share conflict point c. (The reduced capacities could be due to lower speeds or fewer lanes). Flow of Q_{12} from 1 to 2 should consume all supply of c, but valuing each vehicle as 1 flow through c leaves $Q_{34} - Q_{12}$ capacity unused – capacity that might incorrectly be applied to flow from 3 to 4. Instead, each vehicle should consume $\frac{Q_c}{Q_{ij}}$ of the capacity of c.

Let ℓ_i be the number of lanes and $S_i(t)$ the sending flow of link i at time t, i.e. the set of vehicles that could leave i at t if no other constraints were present. Each vehicle v has some priority defined by the arbitrary function $f(v, i)$. The link is a parameter because vehicle priority could be different at different intersections. Let $R_j(t)$ be the receiving flow of link j, i.e. the number of vehicles that could enter j at t if incoming flow was infinite. Sending and receiving flows are general characteristics of dynamic flow models.

The algorithm works as follows: sort $S_i(t)$ by the time the vehicle entered link i. At time t, the first $\min\{\ell_i, |S_i(t)|\}$ vehicles from each $i \in \Gamma^{-1}$ are at the front of the queue and ready to enter the intersection. Let the set V_i comprise these vehicles for i. This preserves the first-in-first-out (FIFO) property: vehicles that arrived first reach the end of the link first. Note that these vehicles are not guaranteed to exit the link first because entering the intersection is dependent on the prioritization function. This is not a limiting assumption as it is potentially true for intersection controls in general; under traffic signals, left-turning vehicles may have to wait while later-arriving through traffic proceeds through the intersection.

We do not make a distinction for turning lanes because determining permitted turning movements for each lane could require intersection-specific information. As Tampere et al. (2011) note, such specific information could be difficult to acquire for each intersection in a city network.

Select the highest priority vehicle $v = \arg\max_{v' \in \cup_{i \in \Gamma^{-1}} V_i} f(v')$ that can move, i.e. where capacity in all $c \in C_{ij}$ and receiving flow of j is sufficient considering vehicles that have already moved. This is the equivalent to reservations: each vehicle at the front of the queue for their link requests to enter the intersection. The highest priority request that is compatible with vehicles that have already entered is accepted.

Let (i', j') be the incoming and outgoing link of v. Move v from i' to j'. This is the equivalent to blocking out tiles. Accepting the reservation of v reduces the remaining capacity of conflict regions in C_{ij} and remaining receiving flow of j. If $S_i(t)$ has remaining vehicles, add the earliest arrival time vehicle from $S_i(t)$ to V_i. Repeat selection of a vehicle until no vehicles can move.

Algorithm 1. Simplified model of tile-based reservations for DTA

1. Set $V = \emptyset$
2. For all $i \in \Gamma^{-1}$
3.   Sort $S_i(t)$ by arrival time at i
4.   Remove first ℓ_i vehicles in $S_i(t)$ and add them to V
5. End For
6. Sort V by $f(v)$
7. For $v \in V$ traveling from i to j
8.   If canMove(i, j)
9. $y_{ij}(t) := y_{ij}(t) + 1$
10.   For $c \in C_{ij}$
11. $y_c(t) := y_c(t) + \dfrac{Q_{ij}}{Q_c}$
12.   End For
13.   Remove first vehicle in $S_i(t)$ and add it to V
14.   Go to 6
15.   End If
16. End For

17. function canMove$(i \in \Gamma^{-1}, j \in \Gamma)$
18.   If $R_j - \sum_{i' \in \Gamma^{-1}} y_{i'j} < 1$
19.   Return False
20.   End If
21.   For all $c \in C_{ij}$
22.   If $Q_c - y_c < \dfrac{Q_{ij}}{Q_c}$
23.   Return False
24.   End If
25.   End For

3.3 Invariance principle

A major concern of Tampère et al. (2011)'s work on general intersection models is satisfaction of the invariance principle. When flow is less than sending flow, the demand at some infinitesimal point in time transitions to link capacity. If distribution of supply depends on demand, the flow allotted to a demand of link capacity may be different and therefore contradictory. An analogous situation may occur for supply.

The invariance principle for supply is satisfied because the solution distributes the supply (Tampère et al., 2011). However, the prioritization schemes by necessity consider demand in their allocation of supply, warranting a closer look at the invariance principle for demand. Due to lane blocking behavior, supply is distributed through vehicle prioritization on the vehicles at the front of the queue. If flow is constrained by supply, a change in demand on i from $|S_i(t)|$ to Q_i would not change the allocated supply because the priority of vehicles at the front of the queue on i would

not change, and thus any demand behind those vehicles would be blocked from moving. Therefore the invariance principle of demand is also satisfied.

3.4 Division of intersections into conflict regions

A proper division of the intersection into conflict regions is vital to the proposed algorithm. Division into a grid of small tiles is more computationally demanding, and also requires more precise predictions of vehicle paths to determine which conflict regions are occupied. Tampere et al. (2011) in particular note the necessity of intersection models to be as independent as possible of specific intersection geometry due to the potentially high number of intersections in city networks. Division into tiles of high granularity, for example one tile at the intersection of every two lanes, requires lane-specific vehicle paths. At the other extreme, no division at all (i.e. the entire intersection is one conflict region) may not properly capture vehicle interactions between specific turning movements. Capacity may be incorrectly "borrowed" from other areas of the intersection.

We propose a *radial division* into conflict regions at incoming and outgoing links, as shown in Figures 2 and 3. This division does not require lane-specific turning movements but limits supply of specific areas of the intersection. This division can also be determined geometrically when link angles are known by the method below. Link angles can be determined through node coordinates, which are readily available from internet-based geographic information systems.

The radial division method divides a circle into conflict regions through radii along incoming and outgoing link angles. Therefore any angle θ can be mapped to a conflict region; let $d(\theta)$ be this mapping. Let θ_i be the angle of directed link i. The path from $i \in \Gamma^{-1}$ to $j \in \Gamma$ is assumed to be composed of two lines. Starting and ending coordinates of are shifted to the right by ε (for countries in which vehicles travel on their right), so that the paths do not follow conflict region boundaries. This results in starting coordinate $\boldsymbol{x}_i$ and ending coordinate $\boldsymbol{x}_j$ defined by

$$\boldsymbol{x}_i = (\cos(\theta_i + \pi), \sin(\theta_i + \pi)) + \varepsilon\left(\cos\left(\theta_i - \frac{\pi}{2}\right), \sin\left(\theta_i - \frac{\pi}{2}\right)\right) \tag{2}$$

$$\boldsymbol{x}_j = \left(\cos(\theta_j), \sin(\theta_j)\right) + \varepsilon\left(\cos\left(\theta_j - \frac{\pi}{2}\right), \sin\left(\theta_j - \frac{\pi}{2}\right)\right) \tag{3}$$

Paths are defined by the intersection of the lines $\boldsymbol{l}_i(\delta_i) = \boldsymbol{x}_i + \delta_i(\cos(\theta_i), \sin(\theta_i))$ and $\boldsymbol{l}_j(\delta_j) = \boldsymbol{x}_j + \delta_j(\cos(\theta_j), \sin(\theta_j))$.

All conflict regions crossed by the turning movement path (determined through angles to the center of the circle) are added to C_{ij}. Choose δ_i^* and δ_j^* such that $\boldsymbol{l}_i(\delta_i^*) = \boldsymbol{l}_j(\delta_j^*)$. Then $C_{ij} = \left\{ d\left(\tan^{-1}\left(\frac{y}{x}\right)\right) \mid (x,y) \in \{\boldsymbol{l}_i(\delta) \mid 0 \leq \delta \leq \delta_i^*\} \cup \{\boldsymbol{l}_j(\delta) \mid 0 \leq \delta \leq \delta_j^*\} \right\}$. Although this path does not model the curves traced by real vehicles, such curves are unnecessary for this division because conflict regions are not lane-specific. Figure 2 demonstrates this method applied to a typical three approach intersection.
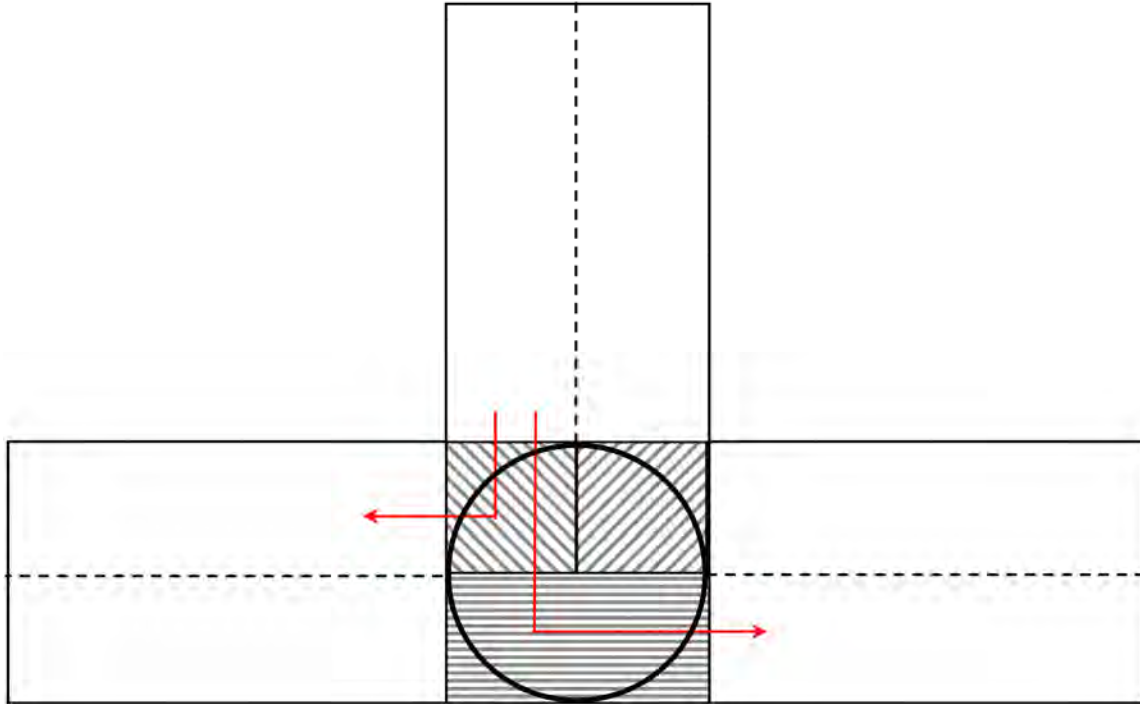
FIGURE 2. Illustration of radial division on a three approach intersection. The inner circle is divided by radii to the incoming and outgoing links.

4. Single intersection case study

To analyze predictions of the CR model, the four approach, three lane intersection studied by Fajardo et al. (2011) was encoded. The link transmission model (Yperman, 2005) with a timestep of 10 seconds was used for flow propagation on links. The intersection was divided into four conflict regions, each the intersection of two directed links, as illustrated in Figure 3. Traffic passes through one, two, or three of these regions, depending on whether it is making a right turn, going through the intersection, or making a left turn, respectively. Since capacities were not specified by Fajardo et al. (2011), conservative estimates of 1200 vehicles per hour per lane were chosen. This results in each conflict region having a capacity of 3600 vehicles per hour. However, that is shared among all traffic passing through the region, including turning traffic.
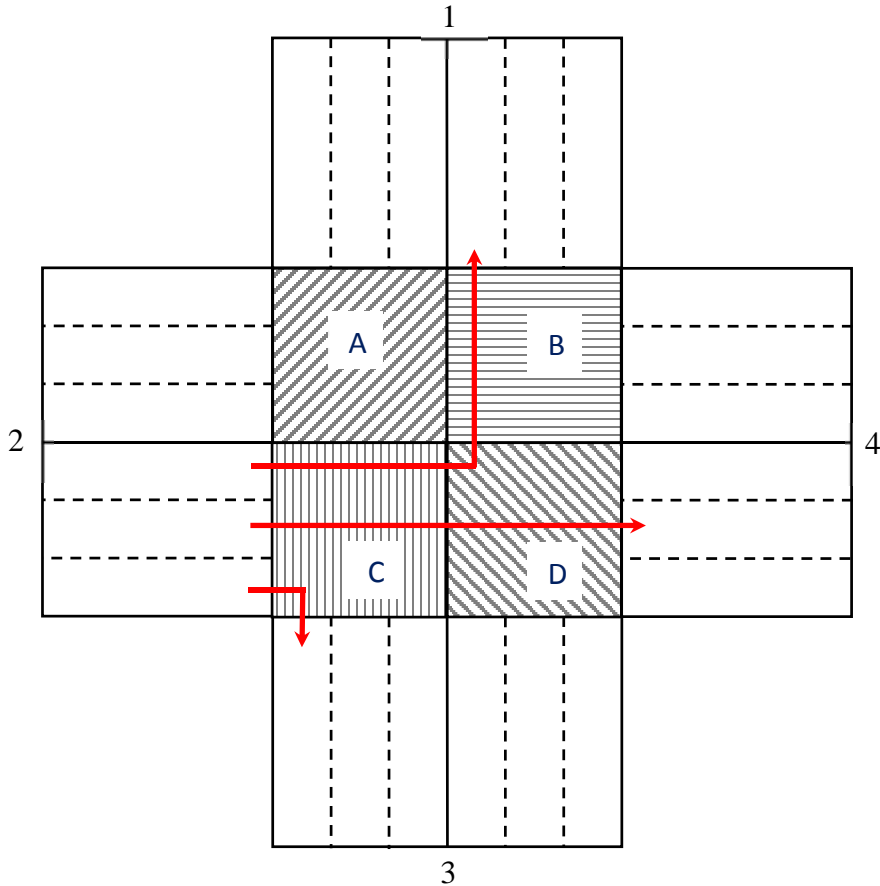
FIGURE 3. Single intersection case study. The 4 conflict regions are shaded, and turning movements from 2 are drawn to indicate which conflict regions they pass through. (Turning movements from other incoming links are symmetric).

The maximum demand cases were tested. Fajardo et al. (2011) reported average delay of 0.67 seconds per vehicle using their smallest buffer settings for demand of 1000 through vehicles, 200 right turning vehicles, and 100 left turning vehicles for each approach. The CR model predicted a similar average delay of 0 seconds (all vehicles that reached the end of the intersection moved through in the next timestep). Considering the relatively low total demand of 1300 vehicles per hour over 3 lanes, this is not surprising. As each conflict region in the case study is shared by two through movements, one right-turn movement, and three left-turn movements, the demand on each conflict region is 2400 vehicles per hour – much less than the 3600 vehicle per hour capacity predicted. The small average delay of 0.67 seconds reported by Fajardo et al. (2011) could be due to small waiting times for tiles to clear. However, as the delay was much less than the 10 second timestep, it was not observed in the more aggregate CR model. The smallest buffer settings are most appropriate for comparison with the CR model because additional spacing requirements between vehicles was not assumed. Nevertheless, at all studied buffer settings the average delay was less than

Similarly, Fajardo et al. (2011)'s left turn experiment, incorporating volumes of 1000 vehicles turning from approach 1 to 4, 1000 vehicles traveling through from approach 3 to 1 (as shown in

10

Figure 2), and 500 vehicles on all other through movements and 100 vehicles on all other turning movements, resulted in observed average delay of 0.69 seconds per vehicle using the smallest buffer settings. The maximum demand on any conflict region occurs in region D on Figure 2, which has a total demand of 2800 vehicles per hour – still less than the 3600 vehicle per hour capacity. As a result, 0 delay is predicted for this scenario as well, which is similar to 0.69 seconds.

Unfortunately, intersection delay or capacity statistics for larger demands were not found in the literature. These would have been useful for validation purposes. Nevertheless, the CR model is built on capacity-restricted tiles, with capacity determined by incoming and outgoing links, and is therefore a reasonable approximation of TBR with reduced computational requirements.

5. Auction-based intersection control

The CR model was implemented in SBDTA to analyze the impact of auctions on travel time under UE behavior. Section 5.1 discusses the details of the implementation, including the VOT-aware routing. Section 5.2 presents empirical evidence for convergence of SBDTA with reservation intersections in a city network. In section 5.3, a detailed analysis of auctions is performed on a test network. Results indicate that reductions in travel time are due to the randomizing effect of auctions, and a comparison with a pure random policy yields similar results.

5.1 Implementation in DTA

The CR model was implemented in a link transmission model (LTM) SBDTA (Yperman et al., 2005) with a 10 second timestep. Vehicles were discretized because of the requirements of the prioritization function in the intersection model. To reduce the number of shortest paths found, demand was divided into assignment intervals of 15 minutes. UE was defined as the state in which no vehicle can reduce their travel time by choosing a shorter path. To measure convergence, the gap function from Levin et al. (2014) was used. Let $\tau(v)$ be the travel time of v and τ_{rst}^* be the travel time of the shortest path from r to s departing within the assignment interval t. The cost gap as a percent of the total travel time is then

$$\frac{\sum_{(r,s,t) \in Z^2 \times T} \sum_{v \in V_{rst}} (\tau(v) - \tau_{rst}^*)}{\sum_{(r,s,t) \in Z^2 \times T} \sum_{v \in V_{rst}} (\tau(v))} \tag{4}$$

where Z is the set of zones, T is the set of assignment intervals, and V_{rst} is the set of demand from r to s departing within $t \in T$.

Although previous work has studied more complex auction schemes, such as bidding on behalf of vehicles blocking the front of the queue and second price auctions, this paper instead studies the benefits resulting from a simple auction scheme in depth. Specifically, the auction algorithm worked as follows. At each intersection, each vehicle v chooses a bid for themselves (bidding for other vehicles was not permitted). Then, the bid chosen becomes the value of the prioritization function $f(v)$. Vehicles are sorted by $f(\cdot)$ in descending order, and the highest bidding vehicle that can move (given capacity constraints) is allowed to move. This repeats until capacity or lane blocking prevents all vehicles from moving.

Each vehicle was assigned a VOT and assumed to bid that VOT at each intersection. Although realistically vehicles might be limited by an overall trip budget or bid differently at intersections depending on demand, this simpler bidding model was chosen because literature on more accurate bidding behavior is not available. Bidding the VOT at each intersection will exaggerate any benefits for higher VOT vehicles. Because a distribution of VOTs throughout the driver population was not found, we instead assumed that VOT is proportional to income. Vehicle VOT was chosen from

Because higher VOT vehicles may experience lower delay at intersections, the shortest path algorithm was modified to include VOT. Intersection delay was averaged for *VOT intervals* of $5, and shortest paths accounting for average intersection delay were found per VOT interval. As with assignment intervals, the trade-off of choosing smaller intervals is greater accuracy but also higher computation time. This modification was used to find more accurate shortest paths for vehicle assignment and cost gap analyses.

5.2 Convergence of FCFS

The method of successive averages (MSA) algorithm was used for convergence. On the kth iteration, $\frac{1}{k}$ vehicles were randomly chosen and moved to their shortest path. Using improved algorithms or heuristics (see Levin et al., 2014) could further reduce the computation time. Since the purpose of this section is to demonstrate the computational tractability of SBDTA with the CR model, basic MSA was used.

Figure 4 shows the cost gap per iteration from running MSA on the downtown Austin network, which has 171 zones, 546 intersections, 1247 links, and 62836 demand. MSA exhibited a general trend of decreasing the cost gap despite occasional spikes. Running on a Core i7-3770k at 4.2GHz, MSA required 922.5 seconds for 50 iterations, or an average of 18.5 seconds per iteration. This indicates that SBDTA with the CR model can be solved in a reasonable amount of time.
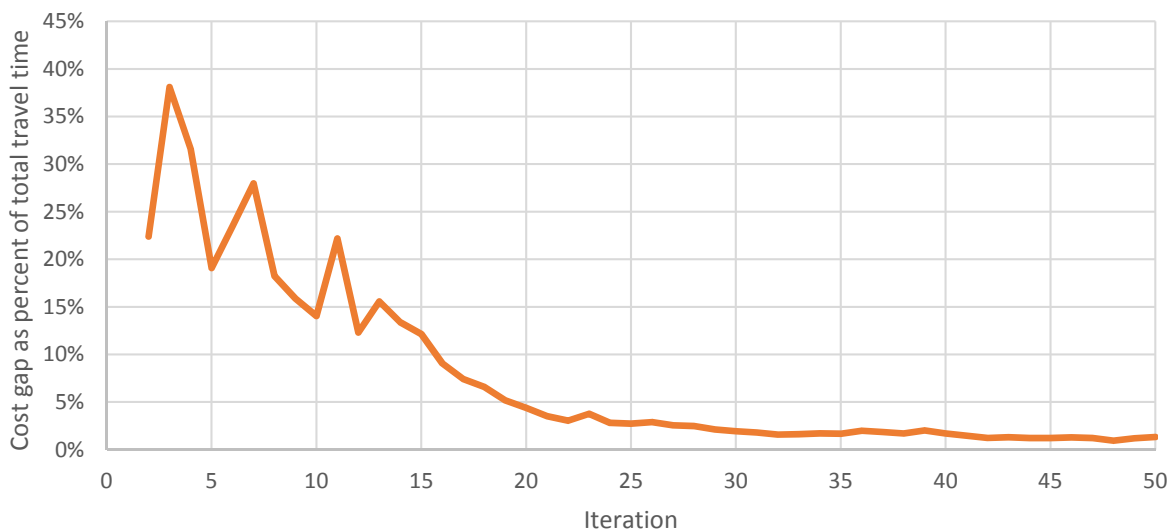

FIGURE 4. Convergence of MSA in the downtown Austin network.

5.3 Effect of auctions on travel time

The CR model was used for an in-depth study of the effect of basic auctions on travel time on the Sioux Falls network with 24 nodes/zones, 72 links, and 28836 demand. Computation time averaged 0.58 seconds per iteration. Vehicles bid their VOT at each intersection, and the highest bidding vehicle was given priority.

On average, auctions reduced travel time (TT) by 495.9 seconds, or just over 8 minutes. However, the reduction was not significantly greater for most above-average-VOT vehicles, as shown in the histogram in Figure 5. Only at $69 VOT or higher did some vehicles experience significantly larger decreases in overall travel time. These changes had high variance though because few vehicles had such high VOTs.
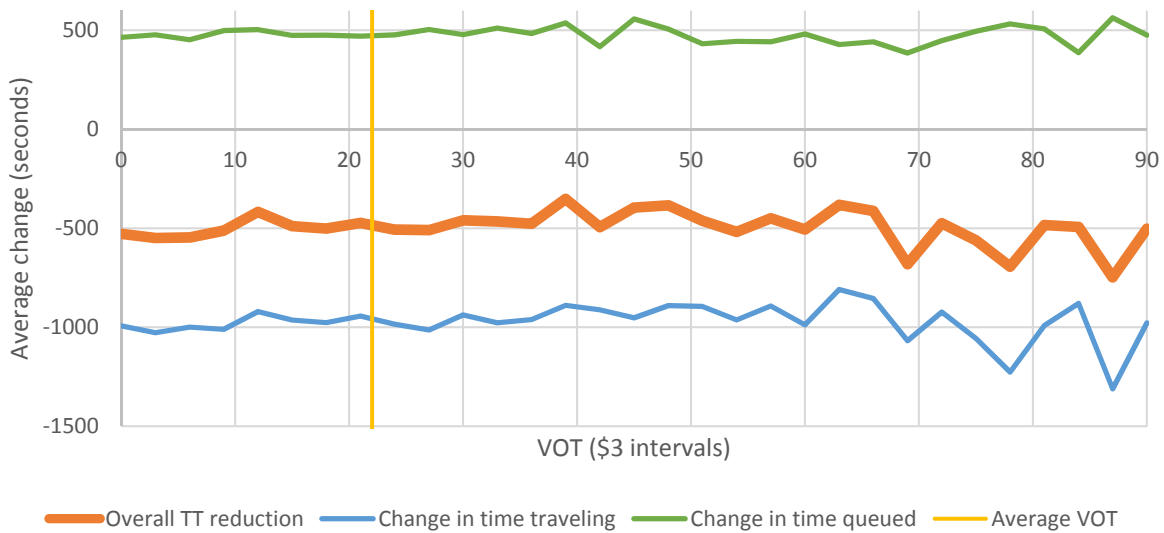
FIGURE 5. Histogram of effect of auctions (no subsidies) on overall travel time, time spent waiting at intersections, and time actually traveling on links.

Figure 5 also divides the change in time into two parts: time traveling on a link, and time waiting at an intersection. Time waiting was defined as the difference between when a vehicle entered the sending flow of a link, and when it entered the next link in its path. Time spent traveling was the remainder, and could increase due to link congestion.

Figure 5 shows that most of the decreases in travel time were due to reduced congestion on the links. Vehicles of all VOTs experienced, on average, higher waiting times at intersections. Although higher VOT vehicles were more likely to win auctions, they were often unable to enter the intersection due to the lane being blocked by lower VOT vehicles. To address this, Schepperle and Böhm (2007) proposed auctions with subsidies, in which vehicles could bid for vehicles queued ahead. When implemented with UE behavior, as shown in Figure 6, average waiting time at intersections decreased sharply, but still did not improve for higher VOT vehicles. This is because the cumulative bidding of a large queue of vehicles can overcome a single high VOT

vehicle. On the other hand, time spent traveling increased as well, and therefore overall travel time benefits disappeared. Therefore, the remainder of the analysis is focused on understanding the auction without subsidies policy, which had significant observed benefits.
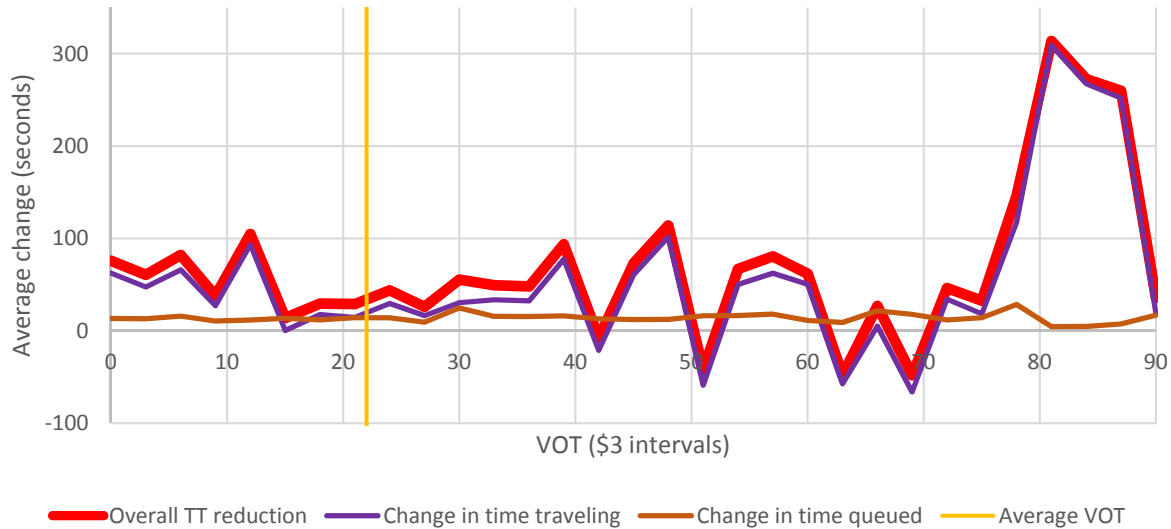

FIGURE 6. Histogram of effect of auctions (*with subsidies*) on overall travel time, time spent waiting at intersections, and time actually traveling on links.

Auctions greatly reduced time spent traveling in contrast to FCFS because it reduced queue lengths. Under FCFS, large numbers of vehicles became queued on the link, causing congestion due to capacity limitations. To demonstrate, Figure 7 compares queues on one link – the number of vehicles that would have been sending flow if capacity was unlimited. On average, FCFS resulted in a congestion queue of 58.1 vehicles whereas auctions reduced that to 30.2 vehicles. Despite the much larger queues, FCFS exiting flow oscillated between capacity, or near capacity, and 0 vehicles leaving. Exiting flow for auctions, in contrast, never reached capacity during the same period, and the queue was nonexistent.

The reason for the flow oscillations, and resulting larger queues, in FCFS, is due to its fairness attribute. For a congested intersection, with queues on two or more incoming links competing for limited intersection capacity, FCFS distributes it according to arrival time. If vehicles from link 1 cause vehicles from link 2 to wait, then those vehicles that waited will have priority in the next timestep due to earlier arrival time even if link 1 has greater demand for the intersection. The result is increasing queue lengths as observed in Figure 7: exiting flow oscillates because priority is given to another link, resulting in a large queue.

Auctions do not have this issue because they effectively serve as a randomizer. Each vehicle, once it reaches the downstream end of its link, has a chance to move depending on its VOT. If it wins the auction and moves, another vehicle from its link takes its place. As a result, links with larger queues have a greater chance to send more vehicles through the intersection, and large queues are less likely to build up. Although it is possible for a long queue of low VOT vehicles to be blocked by higher VOT vehicles from a competing approach, this is unlikely to be sustained because a queue of high VOT vehicles will win auctions and quickly dissipate, and the inflow rate of high

VOT vehicles is limited due to the VOT distribution. With smaller queues on average, there is less backwards propagation of congestion, and time traveling on links correspondingly decreases.
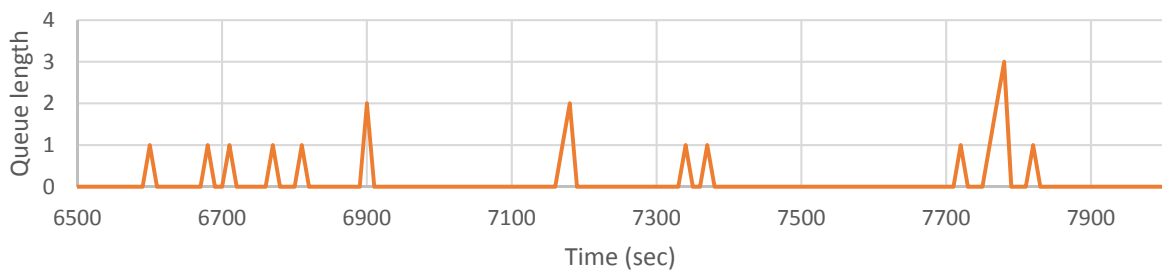
Queue length - FCFS
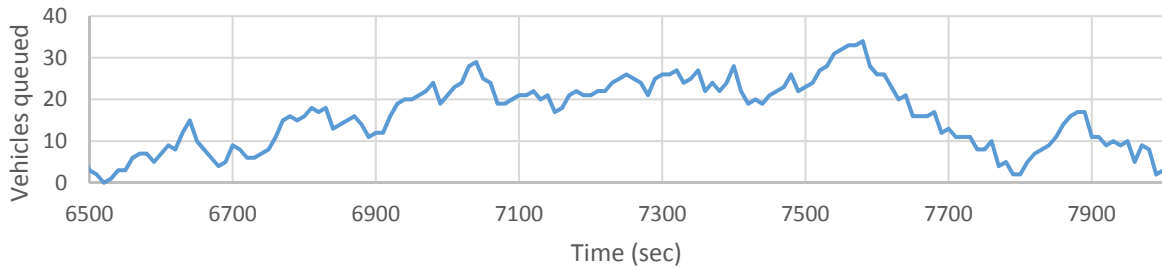
Vehicles exiting - FCFS
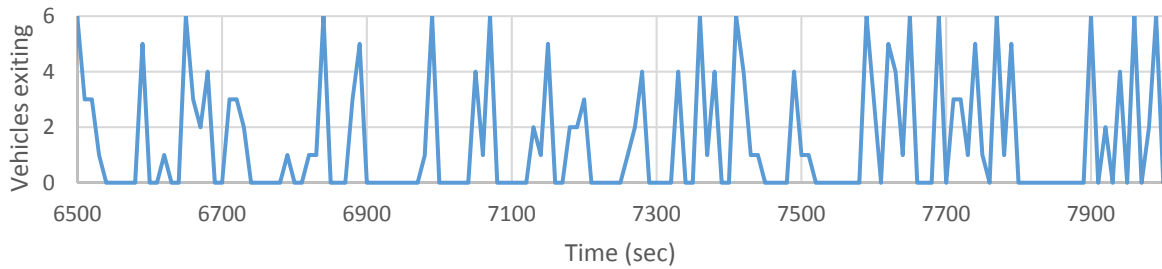
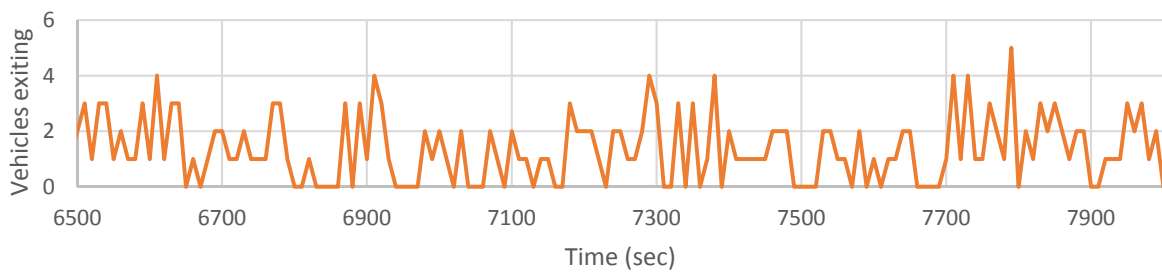### Queue length - auction

Vehicles exiting - auction

FIGURE 7. Comparison of queue lengths and number of vehicles exiting between auctions and FCFS prioritization.

To verify, a lottery prioritization was tested. In this policy, at each intersection, a random vehicle was chosen as the winner from the set of vehicles at the front of their lanes. Unlike the auction policy, each vehicle had an equal chance to win the lottery. This resulted in similar benefits as the auction policy – an average travel time reduction of 476 seconds, with an average increase in waiting time at intersections but a much higher decrease in time spent traveling on links. Figure 8 shows a histogram over VOT of change in overall travel time, time queued, and time spent traveling, for comparison with Figure 5. Average queue length was 25 vehicles, lower than FCFS and auctions. This is not surprising because auctions randomized based on a Dagum distribution, as opposed to a uniform distribution in the lotteries.
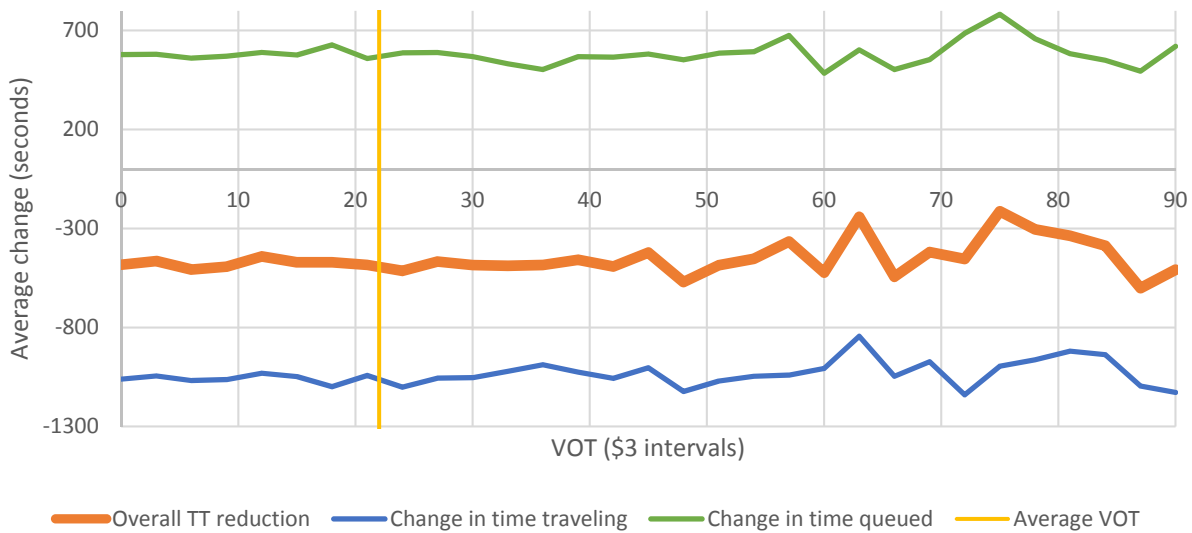

FIGURE 8. Histogram of effect of lotteries on overall travel time, time spent waiting at intersections, and time actually traveling on links.

6. Conclusions

This paper developed a SBDTA conflict region (CR) model of the tile-based reservation (TBR) intersection control policy for autonomous vehicles (AV) proposed by Dresner and Stone (2004, 2006a). The CR model reduces computation time yet retains the simultaneous-use characteristics of TBR. The model divides the intersection into *conflict regions* and restricts flow based on their capacity. Although the CR model requires some information about intersection geometry (as does TBR), we propose an algorithm to automate the division into conflict regions based on link angles. This allows large numbers of intersections in city networks to be modeled. By building on Tampère et al. (2011)'s work on general DTA intersection models, the CR model is independent of the SBDTA flow model and satisfies characteristics such as first-in-first-out and the invariance principle. The computational tractability allows for the analysis of TBR controls under UE behavior, which previous studies on AV intersection controls have not considered.

The CR model was used to compare auctions with and without subsidies to first-come-first-serve (FCFS) prioritization. Little benefit was observed for auctions with subsidies. Auctions without subsidies effectively randomized the prioritization, reducing queue lengths and link congestion. In contrast, the fairness attribute of FCFS led to higher queue lengths and congestion on high demand links. Surprisingly, auctions offered little benefit to favor high bidding vehicles, but reduced travel times similarly for all vehicles. To verify, a pure random lottery prioritization was compared with auctions, and found to have similar effects.

In future work, the effects of TBR instead of traffic signals should be verified under UE behavior. Although Fajardo et al. (2011) demonstrated capacity improvements of TBR over optimized traffic signals, that does not exclude the possibility of Braess (1968) paradox-like phenomena due to higher capacities. Optimal prioritization functions for TBR should also be studied in greater depth, as results in this paper suggest that a lottery prioritization may offer similar benefits to auctions.

References
Braess, D. (1968). Uber ein Paradoxon der Verkehrsplanung. *Unternehmensforschung*, 12, 258–268.

Carlino, D., Depinet, M., Khandelwal, P., & Stone, P. (2012, September). Approximately orchestrated routing and transportation analyzer: Large-scale traffic simulation for autonomous vehicles. In *Intelligent Transportation Systems (ITSC), 2012 15th International IEEE Conference on* (pp. 334-339). IEEE.

Carlino, D., Boyles, S. D., & Stone, P. (2013, October). Auction-based autonomous intersection management. In *Proceedings of the 16th IEEE Intelligent Transportation Systems Conference (ITSC)*.

Chiu, Y. C., Bottom, J., Mahut, M., Paz, A., Balakrishna, R., Waller, T., & Hicks, J. (2011). Dynamic traffic assignment: A primer. *Transportation Research E-Circular*, (E-C153).

de Palma, A., & Lindsey, R. (2011). Traffic congestion pricing methodologies and technologies. *Transportation Research Part C: Emerging Technologies*, *19*(6), 1377-1399.

Dresner, K., & Stone, P. (2004, July). Multiagent traffic management: A reservation-based intersection control mechanism. In *Proceedings of the Third International Joint Conference on Autonomous Agents and Multiagent Systems-Volume 2* (pp. 530-537). IEEE Computer Society.

Dresner, K., & Stone, P. (2006a, July). Traffic intersections of the future. In *PROCEEDINGS OF THE NATIONAL CONFERENCE ON ARTIFICIAL INTELLIGENCE* (Vol. 21, No. 2, p. 1593). Menlo Park, CA; Cambridge, MA; London; AAAI Press; MIT Press; 1999.

Dresner, K., & Stone, P. (2006b, May). Human-usable and emergency vehicle-aware control policies for autonomous intersection management. In *Fourth International Workshop on Agents in Traffic and Transportation (ATT), Hakodate, Japan*.

Dresner, K. M., & Stone, P. (2007, January). Sharing the Road: Autonomous Vehicles Meet Human Drivers. In *IJCAI* (Vol. 7, pp. 1263-1268).

Fajardo, D., Au, T. C., Waller, S. T., Stone, P., & Yang, D. (2011). Automated Intersection Control. *Transportation Research Record: Journal of the Transportation Research Board*, *2259*(1), 223-232.

Henderson, J. V. (1974). Road congestion: a reconsideration of pricing theory. *Journal of Urban Economics*, *1*(3), 346-365.

Levin, M. W., Pool, M., Owens, T., Juri, N. R., & Waller, S. T. (2014). Improving the Convergence of Simulation-based Dynamic Traffic Assignment Methodologies. *Networks and Spatial Economics*, 1-22.

Lou, Y., Yin, Y., & Laval, J. A. (2011). Optimal dynamic pricing strategies for high-occupancy/toll lanes. *Transportation Research Part C: Emerging Technologies*, *19*(1), 64-74.

Łukasiewicza, P., Karpioa, K., & Orłowskia, A. (2012). The Models of Personal Incomes in USA.

May, A. D., Shepherd, S. P., Sumalee, A., & Koh, A. (2008). 7. Design tools for road pricing cordons. *Road congestion pricing in Europe: Implications for the United States*, 138.

Oakley, E. The Race to the Autonomous Car. *Berkeley Political Review*. UC Berkeley, n.d. Web. 07 Feb. 2014.

Schepperle, H., & Böhm, K. (2007). Agent-based traffic control using auctions. In *Cooperative Information Agents XI* (pp. 119-133). Springer Berlin Heidelberg.

Schepperle, H., & Böhm, K. (2008, July). Auction-based traffic management: Towards effective concurrent utilization of road intersections. In *E-Commerce Technology and the Fifth IEEE Conference on Enterprise Computing, E-Commerce and E-Services, 2008 10th IEEE Conference on* (pp. 105-112). IEEE.

Smith, M. J. (1979). The marginal cost taxation of a transportation network. *Transportation Research Part B: Methodological*, *13*(3), 237-242.

Swan, P. F., & Belzer, M. H. (2010). Empirical evidence of toll road traffic diversion and implications for highway infrastructure privatization. *Public Works Management & Policy*, *14*(4), 351-373.

Tampère, C. M., Corthout, R., Cattrysse, D., & Immers, L. H. (2011). A generic class of first order node models for dynamic macroscopic simulation of traffic flows. *Transportation Research Part B: Methodological*, *45*(1), 289-309.

US National Surface Transportation Infrastructure Financing Commission, 2009. *Paying our way: A new framework for transportation finance*.

Vasirani, M., & Ossowski, S. (2010). *A market-based approach to accommodate user preferences in reservation-based traffic management*. Technical Report ATT.

Yin, Y., & Lou, Y. (2009). Dynamic tolling strategies for managed lanes. *Journal of Transportation Engineering*, *135*(2), 45-52.

Yperman, I., Logghe, S., & Immers, B. (2005, September). The Link Transmission Model: An efficient implementation of the kinematic wave theory in traffic networks. In *Proceedings of the 10th EWGT Meeting, Poznan, Poland*.

THE IMPACT OF AUTONOMOUS VEHICLES ON TRAFFIC MANAGEMENT: THE CASE OF DYNAMIC LANE REVERSAL

Melissa Duell (corresponding)
Research Associate
School of Civil and Environmental Engineering
University of New South Wales
Sydney, NSW, 2052, Australia
Phone: (+61 2) 9385 5721 Fax: (+61 2) 9385 6139
E-Mail: melissaduell@gmail.com

Michael W. Levin
Graduate Research Assistant
Department of Civil, Architectural and Environmental Engineering
The University of Texas at Austin
301 E. Dean Keeton St. Stop C1761
Austin, TX 78712-1172
Phone: 512-471-3548, Fax: 512-475-8744
E-Mail: michaellevin@mail.utexas.edu

Stephen D. Boyles
Assistant Professor
Department of Civil, Architectural and Environmental Engineering
The University of Texas at Austin
301 E. Dean Keeton St. Stop C1761
Austin, TX 78712-1172
Phone: 512-471-3548, Fax: 512-475-8744
E-Mail: sboyles@mail.utexas.edu

S. Travis Waller
Professor
School of Civil and Environmental Engineering
University of New South Wales
Sydney, NSW, 2052, Australia
Phone: (+61 2) 9385 5721 Fax: (+61 2) 9385 6139
E-Mail: s.waller@unsw.edu.au

5,594 words + 6 Figures + 3 Tables = 7,844 total words

ABSTRACT

Transformative technologies such as autonomous vehicles (AVs) create an opportunity to reinvent features of the traffic network to improve efficiency. The focus of this work is dynamic lane reversal: using AV communications and behavior to change the direction vehicles are allowed to travel on a road lane with much greater frequency than would be possible with human drivers. This work presents a novel methodology based on the linear programming formulation of dynamic traffic assignment using the cell transmission model for solving the system optimal (SO) problem. The SO assignment is chosen because the communications and behavior protocols necessary to operate AV intersection and lane reversal controls could be used to assign routes and optimize network performance. This work expands the model to determine the optimal direction of lanes at small space-time intervals. Model assumptions are outlined and discussed. Results demonstrate the model on a single link and a grid network, exploring the dynamic demand scenarios which are most conducive to increasing system efficiency with dynamic lane reversal.

1. INTRODUCTION

Technological advances in autonomous vehicles (AVs) introduce the possibility of new communication and behavior protocols that could significantly improve traffic efficiency. For example, researchers have shown that the reservation-based control *(1)* reduces intersection delays under a variety of traffic demand scenarios *(2)*. Another proposed protocol with great potential, and the focus of the current work, is *dynamic lane reversal* (DLR), which can be described as frequent changes to the direction vehicles are permitted to travel on a lane in response to dynamic traffic conditions.

The concept of DLR stems from contraflow lanes used in evacuation scenarios and reversible lanes which are used to alleviate peak hour congestion in many locations. One example is the Sydney Harbour Bridge, which has eight lanes, of which three change direction daily for morning and evening peak traffic. The greatest challenge for contraflow lanes that limits the timeframe of application is the reaction of human drivers. Drivers who do not respond appropriately will at best negate the benefits, and at worse could cause a head-on collision. Consequently, rapid direction changes are not available for contraflow lanes.

Most previous work focuses on evacuation *(3, 4, 5)*, although some literature addresses contraflow lanes for peak hour demand. Zhou et al. *(6)* and Xue and Dong *(7)* use machine learning techniques to decide when to use contraflow for a bottleneck link. Meng et al. *(8)* use a bi-level formulation, with traffic assignment as the subproblem, because the driver response to contraflow lanes results affects the user equilibrium (UE).

To address the limitations of contraflow lanes, Hausknecht et al. *(9)* proposed DLR for AVs. They studied two models: first, DLR in a micro-simulation with lane direction decided by road saturation; and second, a bi-level problem for deciding lane direction in static flow context with traffic assignment as the subproblem. However, both of these models focused on stationary demand. The goal of this paper therefore is to develop a DLR model responsive to time-varying demand. In scenarios such as a congested downtown grid, different directions may become oversaturated at different times in the AM or PM peak. Depending on network topology, demand does not necessarily prefer a single direction. These conditions warrant a more adaptive policy to dynamic lane reversal as well as an aggregate but dynamic flow model for studying larger networks.

To address these objectives, this paper uses the cell transmission model (CTM) proposed by Daganzo *(10, 11)*. CTM is frequently applied in dynamic traffic assignment (DTA) models. CTM captures traffic waves while being computationally tractable for larger networks. It also admits space-time dependent fundamental diagrams, which are necessary for modeling DLR. Because efficiency may be improved by partial lane reversal, such as through a temporary turning bay, lane reversal is decided at the cell level.

Because UE behavior can be a significant obstacle to improving system efficiency, as demonstrated by the Braess paradox *(12)*, we assume that route choice is assigned by a system manager resulting in system optimal (SO) conditions. For AVs in communication with intersection managers to facilitate intersection reservations and DLR, it is feasible for AVs to follow assigned routes. In a future where all vehicles are autonomous, policymakers may require vehicles to follow SO routes. UE behavior also makes the problem more complex: to find the optimal DLR policy when vehicles route themselves requires solving DTA as a subproblem to DLR. Therefore, this work focuses on the SO version of the problem.

The contributions of this paper are summarized by the following:

- We develop a system optimal dynamic traffic assignment model incorporating dynamic lane reversal (DLR-SODTA) in order to demonstrate the potential and feasibility of DLR
- We formulate the model using a mixed integer linear program (MILP) based on a well-established SODTA model *(13)*. This application solves the optimization problem for lane allocation as part of the combined DLR and SO assignment problem.
- We use this model to find the optimal lane allocation at different times for varying demand scenarios and compare these results with the fixed lane scenario.

The remainder of this paper is organized as follows. In Section 2, we describe the AV technologies necessary for DLR and review other AV behaviors using these technologies. Section 3 introduces the DLR constraints and decision variables to develop the MILP model. Section 4 presents the potential improvement on a bottleneck link with varying demand, and Section 5 studies improvements on a grid network with alternative routes. Conclusions are discussed in Section 6.

2. BACKGROUND

Although the technology and protocols necessary for frequent reversal of lane direction are far beyond the capabilities of human drivers, they are well within the possibilities proposed for AVs. Previous studies on AV traffic behaviors have generally relied on two advantages that AVs possess: 1) wireless two-way communications with other vehicles (V2V) or infrastructure (V2I); and 2) precise driving allowing reduced margins on safety. Connected adaptive cruise control (CACC), which is available for connected vehicles (CVs) with V2V but still partially controlled by humans, has been shown to reduce following headways due to decreased reaction times from the CACC controller. As a result, CACC improves capacity *(24, 29)* as well as traffic flow stability *(27, 30)*. These studies demonstrate the potential of even partial automation. However, Levin & Boyles *(33)* demonstrated that additional demand induced by AV behaviors could result in greater congestion despite capacity improvements.

Reservation-based intersection control *(20, 21)* is a more radical protocol that uses V2I and precision to improve intersection capacity. Vehicles request a *reservation* from the *intersection manager*, which simulates vehicles' requested trajectories on a grid of space-time tiles. Non-conflicting requests are approved, whereas conflicting requests must be denied until a later time. This protocol relies on two-way communication with the infrastructure and vehicles following precise paths through the intersection to avoid collisions. Most studies have used a first-come-first-serve priority for resolving conflicting reservation requests. However, Dresner & Stone *(22)* proposed prioritizing emergency vehicles, and later work *(19, 28, 31, 32)* has studied auctions at each intersection to allow vehicles to pay to move first. Microsimulation studies on reservation protocols have demonstrated that they can reduce delays beyond optimized traffic signals *(23, 26)*. Reservation controls demonstrate the possibilities for AV technology.

Hausknecht et al. *(9)* extended the reservation protocol for a full-lane dynamic lane reversal (DLR). They used the tight constraints on specific-lane turning movements in the reservation protocol to control which lanes vehicles could use. We propose to extend their lane control to a more complex DLR in which each link is divided into predetermined cells, and lane direction may differ in each section. Furthermore, the direction of lanes may change at small time intervals. This requires only a small modification to the control protocol of Hausknecht et al. *(9)*. Instead of specifying direction for the entire link, the intersection manager specifies the direction for each cell. This requires that vehicles are always in contact with an intersection manager. However, that is not a significant limitation because AVs would have to contact the intersection manager to request a reservation. If the link is sufficiently long that vehicles might be outside the range of

wireless communications from the intersection manager, relay stations could be created along the link. Frequent changes in lane direction require frequent communication of future lane directions to vehicles, but this is not an issue for vehicles always in contact with an intersection manager. As with the reservation protocol, AVs must comply with the lane directions specified by intersection managers. Therefore, the technology necessary to implement cell-based DLR is a small extension of the technology used in the reservation protocol.

Hausknecht et al. *(9)* also studied a bi-level program to optimize lane reversal for static traffic assignment (STA). However, STA is designed for steady state conditions, and their formulation cannot respond to time-varying demand. Therefore, we use DTA in our models.

Since most studies have relied on micro-simulation models, they have been restricted to small networks or have made significant simplifications in the modeled behaviors, reducing their traffic efficiency *(18, 19)*. Levin & Boyles *(25)* proposed a more tractable model of reservation control to solve DTA on city networks, but DLR adds an additional level of complexity. Although we demonstrate our DLR model with small networks, using small networks is consistent with previous work. Future work will explore heuristics for DLR in larger networks, and DLR with UE instead of SO routing.

3. METHODOLOGY

Assumptions

AV behavior using current road technology has yet to be well-defined. Additionally, behaviors using proposed technologies that exist only in concept such as reservation-based intersections or DLR are even less established. Therefore, we make the following assumptions about vehicle behavior in this model:

1) All vehicles are AVs, and have vehicle to infrastructure communications. The additional complexities of DLR with human drivers are outside the scope of this paper and will be left for future work.

2) SO behavior. As mentioned previously, AVs already follow substantial communications and behavior protocols. They may also be required to follow an assigned route in order to optimize system performance in a previously unachievable manner. This assumption is beneficial because it implies that the locations of vehicles in the network can be predicted and the lane configuration can be solved as an optimization problem. The UE assumption presents a greater challenge that will be the subject of future work.

3) Required lane changing. We assume that vehicles may be required to change lanes up to κ times per timestep. For example, a common CTM timestep of 6 seconds with free flow speed of 48 km per hour results in a cell length of 80 m. Thus, a 6 second timestep should be sufficient for at least one lane change.

4) Perfect information of demand. Finding the SO assignment requires some knowledge of future demand. We assume demand is known perfectly. This is reasonable for peak hours, during which DLR has the greatest potential to reduce congestion. During peak hours, the departure time for travelers leaving home for work, or leaving work for home, is fairly consistent, and the origin/destination may be specified in advance. Additionally, a centralized network manager may log vehicle travel in a consistent manner to predict demand.

For simplicity of modeling lane changing and turning movement behavior, we model all lanes in one direction as being contiguous. Therefore, the lane direction problem reduces to specifying the number of lanes in each direction for each pair of cells. For any link $[a, b]$, we say it is *paired*

1   with link $[b, a]$ if $[a, b]$ and $[b, a]$ have the same length and free flow speed. This would result in
2   each link in the pair having the same number of cells, with each cell $i \in [a, b]$ having a
3   corresponding cell $\bar{\imath} \in [b, a]$ in the opposite direction. Establishing the pairing of cells and links is
4   necessary to determine the number of lanes available for allocation.

Formulation

6   The MILP is based on the SO linear program (LP) for CTM by Ziliaskopoulos [14] for a single
7   destination and Li et al. (2003) for more general networks. The SODTA formulation by
8   Ziliaskopoulos has been widely applied in a number of research applications [15]. CTM more
9   realistically propagates traffic than alternative approaches relying on link performance functions. It
10   faces challenges due to the size of the linear program, the "holding back" phenomenon [16] , and
11   in multi-destination applications, FIFO violations [17]. While addressing these issues is beyond the
12   scope of the current work, it is possible that in a network comprised solely of AVs, the latter two
13   could represent realistic behavior.
14   The addition of the number of lanes per cell, assumed to be integer, requires an MILP as
15   opposed to an LP. In preparation for the formulation, let C be the set of cells and E the set of cell
16   connectors. Let $C_R \subset C$ and $C_S \subset C$ be the sets of origin and destination cells, respectively. Let T
17   be the set of discrete time intervals. Without loss of generality, and for simplicity of notation, let
18   the timestep be 1. To define cell transitions, let $\Gamma^-(i)$ and $\Gamma^+(i)$ be the sets of preceding and
19   succeeding cells to cell i. For the fundamental diagram, let N_i^t be the maximum number of vehicles
20   that can fit in cell i *per lane* at time t and let Q_i^t be the capacity *per lane* for cell i at time t. As with
21   Daganzo's [10] CTM, this model uses the trapezoidal fundamental diagram $\Psi_i^t(x) =$
22   $\min\{x, Q_i^t, w(N_i - x)\}$, where w is backwards wave speed. Let d_{rs}^t be the demand for $(r, s) \in C_R \times$
23   C_S at time t. Let P be a set of all pairs of corresponding cells (a, b).
24   The decision variables are cell density $x_{rs,i}^t$, cell transition flows $y_{rs,ij}^t$ from $i \in C$ to $j \in C$
25   per origin-destination pair (r, s) at time t, and the number of lanes per cell l_i^t. Including the number
26   of lanes as a decision variable is one of the advantages of this model.

27   The objective of the DLR-SODTA model is to minimize total system travel time, which due
28   to the CTM assumptions, is simply the summation of the density of each cell over all time steps.
29   This results in the following MILP:

$$\min Z = \sum_{(r,s) \in C_R \times C_S} \sum_{t \in T} \sum_{i \in C \setminus C_S} x_{rs,i}^t \tag{1}$$

s.t.

$$x_{rs,j}^{t+1} = x_{rs,j}^t + \sum_{i \in \Gamma^-(j)} y_{rs,ij}^{t,} - \sum_{k \in \Gamma^+(j)} y_{rs,jk}^t \qquad \begin{matrix} \forall_{(r,s) \in C_R \times C_S}, \\ \forall_{j \in C \setminus (C_R \cup C_S)}, \\ \forall_{t \in T} \end{matrix} \tag{2}$$

$$x_{rs,j}^{t+1} = x_{rs,j}^t + \sum_{i \in \Gamma^-(j)} y_{rs,ij}^{t,} \qquad \begin{matrix} \forall_{(r,s) \in C_R \times C_S}, \qquad \forall_{j \in C_S}, \\ \forall_{t \in T} \end{matrix} \tag{3}$$

$$\sum_{t \in T} \sum_{i \in \Gamma^-(s)} y_{rs,is}^t = \sum_{t \in T} d_{rs}^t \qquad \forall_{(r,s) \in C_R \times C_S} \tag{4}$$

$$\sum_{\forall j \in \Gamma^+(i)} y_{rs,ij}^t \leq x_{rs,i}^{t,} \qquad \begin{array}{c} \forall_{(r,s)\in C_R \times C_S},\\ \forall_{i\in C(C_R \cup C_S)}\\ \forall_{t\in T} \end{array} \qquad (5)$$

$$\sum_{\forall r \in C_R} \sum_{\forall s \in C_S} \left(\sum_{i \in \Gamma^-(j)} y_{rs,ij}^t + \delta x_{rs,j}^t \right) \leq \delta N_j l_j^t \qquad \begin{array}{c} \forall_{j\in C\backslash(C_R\cup C_S)},\\ \forall_{t\in T} \end{array} \qquad (6)$$

$$\sum_{\forall r \in C_R} \sum_{\forall s \in C_S} \sum_{\forall i \in \Gamma^-(j)} y_{rs,ij}^t \leq Q_j^t l_j^t \qquad \begin{array}{c} \forall_{j\in C\backslash(C_R\cup C_S)},\\ \forall_{t\in T} \end{array} \qquad (7)$$

$$\sum_{\forall r \in C_R} \sum_{\forall s \in C_S} \sum_{\forall j \in \Gamma^+(i)} y_{ij}^t \leq Q_i^t l_i^t \qquad \begin{array}{c} \forall_{i\in C\backslash(C_R\cup C_S)},\\ \forall_{t\in T} \end{array} \qquad (8)$$

$$x_{rs,r}^{t+1} - x_{rs,r}^t + \sum_{j \in \Gamma^+(r)} y_{rs,rj}^t = d_{rs}^t \qquad \begin{array}{c} \forall_{(r,s)\in C_R \times C_S},\\ \forall_{r\in C_R},\\ \forall_{t\in T} \end{array} \qquad (9)$$

$$x_{rs,i}^0 = 0, y_{rs,ij}^0 = 0 \qquad \begin{array}{c} \forall_{(r,s)\in C_R \times C_S},\\ \forall_{(i,j)\in E},\\ \forall_{t\in T} \end{array} \qquad (10)$$

$$y_{rs,ij}^t \geq 0 \qquad \begin{array}{c} \forall_{(r,s)\in C_R \times C_S},\\ \forall_{(i,j)\in E},\\ \forall_{t\in T} \end{array} \qquad (11)$$

$$l_i^{t+1} \leq l_i^t + \kappa \qquad \forall_{i\in C}\forall_{t\in T} \qquad (12)$$

$$l_i^{t+1} \geq l_i^t - \kappa \qquad \forall_{i\in C}\forall_{t\in T} \qquad (13)$$

$$l_{i+1}^{t+1} \leq l_i^t + \kappa \qquad \forall_{i\in C}\forall_{t\in T} \qquad (13)$$

$$l_{i+1}^{t+1} \geq l_i^t - \kappa \qquad \forall_{i\in C}\forall_{t\in T} \qquad (14)$$

$$l_a^t + l_b^t = L_{ab} \qquad \forall_{(a,b)\in P} \qquad (15)$$

$$l_i^t \geq 0 \qquad \forall_{i\in C}\forall_{t\in T} \qquad (16)$$

where δ is the ratio of backwards wave speed to free flow speed. Constraints (2) through (9) define the cell transition flows. Constraints (5), (6), and (7) have been modified from the original multi-destination CTM linear programming model to account for the explicit representation of multiple lanes as a decision variable. Constraints (11) through (14) bound the number of lanes that can be reversed per time period by κ, and constraint (15) defines the number of lanes available to any pair of cells as L_{ab}, the total number of lanes available to both cells, which is an input to the model. Note that all available lanes must be allocated during all time periods, which will at times result in an arbitrary lane configuration.

Analysis

Let Z^* be the optimal value of the objective function. Also, let $\bar{Z} = Z$ solved with the additional constraints

$$l_i^t = \bar{l}_i \qquad\qquad \forall_{i \in C} \forall_{t \in T} \quad (16)$$

1 for some $\bar{l}_i$'s satisfying $\bar{l}_a + \bar{l}_b \leq L_{ab}$ and $l_i \geq 0$ $\forall_{i \in C}$. Let $\bar{Z}^*$ be the optimal solution with
2 corresponding flow and lane assignment $(\bar{y}^*, \bar{l})$. $\bar{Z}^*$ reduces to solving the SO problem with a fixed
3 lane configuration $\bar{l}$. Clearly, $(\bar{y}^*, \bar{l})$ is a feasible solution to the original problem since the fixed
4 configuration constraint (14) satisfies constraints (11) through (13). This results in the following
5 observation:

6 **Proposition 1. $Z^* \leq \bar{Z}^*$.**

7

8 **4. DEMONSTRATION AND ANALYSIS**
9 This section presents the DLR-SODTA model results on a small corridor example and a larger grid
10 network. The DLR results are compared with the fixed-lane results. The DLR-SODTA problem
11 was solved using the AMPL programming interface to the CPLEX solver.

12 **Two link demonstration**
13 The DLA-SODTA model is initially demonstrated on a simple two-link example in order to closely
14 analyze the relationship between dynamic lane allocation and dynamic traffic demand patterns.
15 Both links are of length 650 m with a free flow speed of 50 kph. Each link has two lanes with a
16 capacity of 1800 vehicles/hour/lane. Figure 1 illustrates the demonstration network.


(a)

(b)
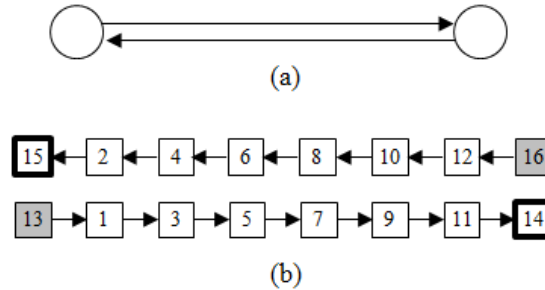
17
18 **FIGURE 1   (a) simple two link network and (b) cell network representation**
19

20 Using a time increment of 6 seconds, the each link is comprised of 8 cells with $N_i = 13.2$ vehicles
21 and $Q_i = 3$ vehicles. In all cases, κ, the number of lanes which may change direction during a time
22 period, is 1. We examine four demand cases and compare the DLR and fixed lane SODTA results.
23 Demand case I is illustrated in Figure 2.

900 vphpl

3000 vphpl
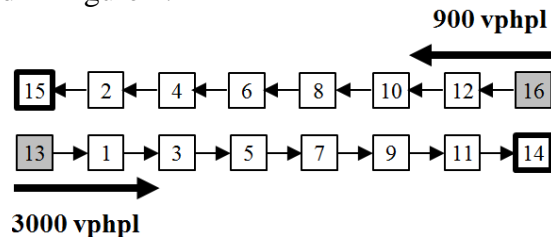
24
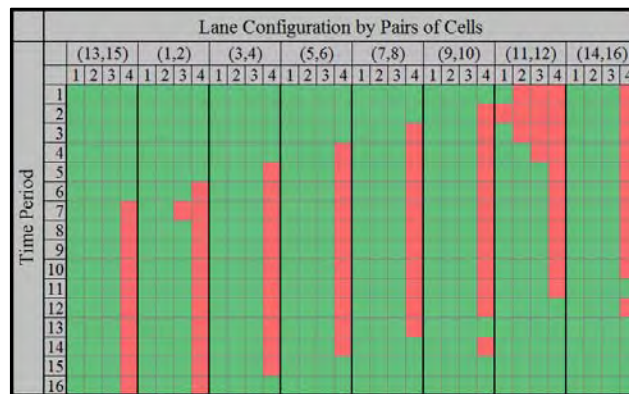25 **FIGURE 2   Demand case (I)**
26

27 In case (I), the vehicle flow is much higher in one direction. In the traditional fixed lane network,
28 this situation will result in congested conditions. The SODTA model considered 30 time steps, or

1   3 minutes of simulation. Demand for the first ten time steps was assumed to be $d_{13,14}^{0...9} = 10$
2   vehicles and $d_{16,15}^{0...9} = 3$ vehicles respectively. The demand follows a uniform departure time
3   profile.
4   The DLR model resulted in a total travel time of 5166 seconds and 18 time increments for all
5   vehicles to exit the network. The fixed-lane approach was higher with a total travel time of 6834
6   seconds and 23 time-increments for all vehicles to exit.
7   Figure 3 shows a detailed representation of the lane configuration for pairs of cells. Each
8   vertical column represents the four lanes that are shared by a pair of cells. The green shows that a
9   lane is assigned to the first cell in the pair, while the red represents a lane assignment to the second
10   cell in the pair. For example, under pair (13,15), all four lanes are assigned to cell 13 until time
11   period 7. In demand case I, the vehicle flow was unbalanced and therefore a majority of the lanes
12   were able to be utilized by the direction with a higher volume of flow. Also note that when there
13   is no vehicle demand for the cell or cell connector, the lane is assigned arbitrarily.
14

15
16   **FIGURE 3   Lane Configuration in demand case (I)**
17
18   In the second case, the flow from both directions is more equal, as Figure 4 shows. This is a
19   common case for congested network corridors, even during peak hours. Demand for the first ten
20   time steps was assumed to be $d_{13,14}^{0...9} = 9$ vehicles and $d_{16,15}^{0...9} = 5$ vehicles.
21
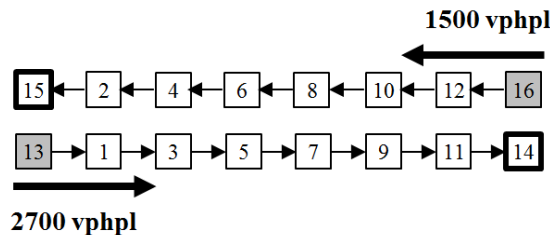
22
23   **FIGURE 4   Balanced Demand case (II-IV)**
24
25   In the fixed lane case, the model requires 16 time periods for all the flow to exit the network while
26   the DLR model requires 20 time-increments. The total travel time in the fixed case was 7230
27   seconds and in the DLR case was 6756 seconds. Again, the DLR model was able to reduce the total
28   travel time. However, because there were more vehicles from both directions, the reduction was not
29   as great.
30   Demand case III examines the impact of time dependent demand, which an important
31   consideration for network operators. In this case, the total vehicle demand is the same (90 vehicles/3

minutes) but the departure times are different. In this scenario, the departure time are more spaced out and we assume $d_{13,14}^{0...4} = 18$ vehicles and $d_{16,15}^{10...14} = 10$ vehicles.

Both the fixed-lane and the DLR models require 25 time periods for all vehicles to exit the network. However, the total travel time in the fixed case was 9084 seconds and in the DLR case was 7488 seconds.

In addition, Figure 5 shows the detailed lane configuration in demand case III. This demand scenario may be particularly conducive to dynamic lane allocation because the first wave of demand from (13,14) had sufficient time to exit the network before the second wave of demand from (16,15) entered the network.

FIGURE 5   Lane Configuration in demand case (III)

Finally, we examine the "peak" demand case where the total demand at each departure time is no longer uniform.

TABLE 1 Peak departure pattern demand

Time Period	(14,13)	(16,15)
0	5	0
1	15	0
2	10	0
3	30	0
4	30	0
5	0	5
6	0	5
7	0	20
8	0	18
9	0	2
Total	**90**	**50**

The total travel time for the fixed case is 8958, while the total travel time for the DLR-SODTA is 8718. The vehicles exited the network in 22 time-steps versus 18 time-steps. Table 2 summarizes the results from the four demand cases. Additionally, Table 2 presents the results for the case in

which only two of the four lanes are available to change directions as DLR[1]. This would ensure that for all time periods, each direction has at least one lane available which could be another possible dynamic lane configuration.

TABLE 2 Summary of results for the two-link network

	Total Demand	Departure Profile	# Departure Periods	Fixed (s)	DLR (s)	DLR[1] (s)
I	100, 30	Uniform	10	7464	5796	5796
II	90, 50	Uniform	10	7230	6756	6756
III	90, 50	Uniform	5	9084	7488	8220
IV	90, 50	Peak	5	8958	8718	8718

Finally, we examined a 30 minute CTM simulation period, which is 300 time steps. We loaded demand at the same rate (9 and 5 vehicles per timestep respectively) for 15 minutes, or 150 time steps. In this case, we placed a constraint that required that there be at least one lane in each direction during all times periods (called DLR[1]). There was a total of 1,350 vehicles between (13,14) and 750 between (16,15).

The DLR solution assigned 3 lanes to the direction with a greater volume of vehicles and then switched to a 2 lanes in each direction configuration after 108 time increments. This relatively static assignment of lanes is expected because of the uniform demand profile. If the demand were to arrive in more of a heavy-slow pattern, we would expect there to be more changes in lane configuration as more capacity was switched to the favored direction of travel.

The total travel time in the fixed case was 108.9 hours. The DLR model reduced the travel time to 69.4 hours, which represented 36% of the travel time.

Grid network demonstration

Finally, this work presents the results for the SODLR model on a demonstration network with a grid structure and multiple OD pairs. A grid network results in additional paths available between each OD and may have a significant impact on the performance of dynamic lane management. Furthermore, the additional constraint (4) is necessary to ensure that the total demand between each origin-destination is maintained.

Figure 6 shows the demonstration network with four zones (i.e., A, B, C, D) that act as both origins and destinations. The OD pairs considered are A-D, D-A, B-C, and C-B with a demand of 3300 vph, 300vph, 2700 vph, and 600 vph respectively. Links have identical properties and the same as the previous example (i.e., two lanes available in the fixed case, a free flow speed of 50 kph and length of 650 m). In this network, we expect each OD pair to have three primary paths through the network. The majority of demand will favor the most direct path through for each OD, but as congestion increases, the paths on the outside links will become more favorable.
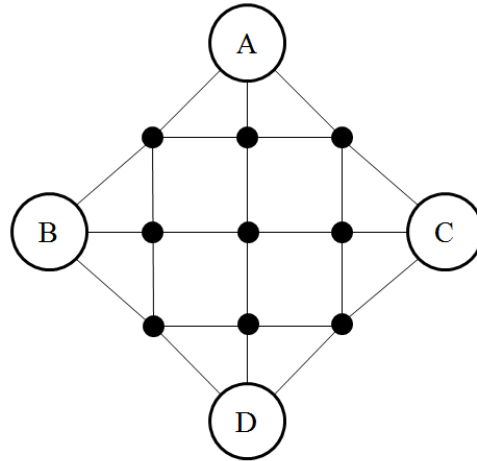
FIGURE 6   Grid demonstration network with four OD pairs

We explore three different demand cases, similar to the two link example, and each case has the same amount of total demand. Case I has a uniform departure profile for ten departure time periods. Case II features a peak pattern of departure over five time periods, while Case III has a more pronounced peak over three departure time periods. The peak periods were chosen such that the departure time periods for opposing OD pairs (i.e., A-D and D-A) were overlapping.

Table 3 shows the results for the three demand cases on the grid shaped demonstration network. The total demand is shown for OD pairs (A-D, D-A, B-C, C-B). Table 3 shows the results for the fixed case where there are required to be two lanes in each direction for all time periods and the SODLR case, where the lane management can be optimized. In each case, the reduction in total travel time is between 12-15%. This is a significant reduction for the relatively short simulation period shown and suggests that dynamic lane reversal may be able to significantly reduce travel time. However, for the case where the demand is overlapping in all directions, the reduction in total travel time may be less.

TABLE 3 Summary of results for grid network demonstration

Demand Case		Total demand	# Departure periods	Fixed (min)	DLR (min)	Reduction
I	Uniform	83,8,68,15	10	238.74	200.95	15.8%
II	Medium Peak	83,8,68,15	5	261.09	227.65	12.8%
III	High Peak	83,8,68,15	3	279.18	245.55	12.0%

5. CONCLUSION AND FUTURE DIRECTIONS

The presence of autonomous vehicles will give network operators the chance to increase the efficiency of traffic streams using previously impossible approaches. This work investigates the concept of dynamic lane reversal, where the direction vehicles are allowed to travel on a lane is changed at very short time intervals.

We proposed a mixed integer linear programming model based on a Li et al.'s model of system optimal dynamic traffic assignment *(13)* that propagates traffic using the cell transmission model. The number of lanes in each cell is explicitly considered as a decision variable, allowing for

real time network design in response to time-varying travel demand. Results illustrate the importance of accounting for time-varying demand profiles when exploring the DLR concept. However, due to the integer representation of lanes, this approach will face significant computation challenges when using traditional optimization techniques. Although the model presented here supports the possibility of dynamic lane reversal, of course there are still a number of practicalities that were not accounted for, but will be the subject of future research.

As advances in technology make autonomous vehicles an increasingly likely proposition, research exploring their impact on transport planning and operations is of great importance. The issue of dynamic lane reversal and the corresponding network design problem present numerous opportunities. The model proposed here can be improved in the future by addressing some of the known issues with the linear relaxation of the CTM (holding back, FIFO), as well as studying tractable heuristics for large city networks.

REFERENCES

(1) Dresner, K., & Stone, P. (2006a, July). Traffic intersections of the future. In Proceedings of the National Conference on Artificial Intelligence (Vol. 21, No. 2, p. 1593). Menlo Park, CA; Cambridge, MA; London; AAAI Press; MIT Press; 1999.

(2) Fajardo, D., Au, T. C., Waller, S. T., Stone, P., & Yang, D. (2011). Automated Intersection Control. Transportation Research Record: Journal of the Transportation Research Board, 2259(1), 223-232.

(3) Zhang, X. M., An, S., & Xie, B. L. (2012, October). A Cell-Based Regional Evacuation Model with Contra-Flow Lane Deployment. In Advanced Engineering Forum (Vol. 5, pp. 20-25).

(4) Wang, J. W., Wang, H. F., Zhang, W. J., Ip, W. H., & Furuta, K. (2013). Evacuation planning based on the contraflow technique with consideration of evacuation priorities and traffic setup time. Intelligent Transportation Systems, IEEE Transactions on, 14(1), 480-485.

(5) Dixit, V., & Wolshon, B. (2014). Evacuation traffic dynamics. Transportation research part C: emerging technologies, 49, 114-125.ajardo, D., Au, T. C., Waller, S. T., Stone, P., & Yang, D. (2011). Automated Intersection Control. Transportation Research Record: Journal of the Transportation Research Board, 2259(1), 223-232.

(6) Zhou, W. W., Livolsi, P., Miska, E., Zhang, H., Wu, J., & Yang, D. (1993, October). An intelligent traffic responsive contraflow lane control system. In Vehicle Navigation and Information Systems Conference, 1993., Proceedings of the IEEE-IEE (pp. 174-181). IEEE.

(7) Xue, D., & Dong, Z. (2000). An intelligent contraflow control method for real-time optimal traffic scheduling using artificial neural network, fuzzy pattern recognition, and optimization. Control Systems Technology, IEEE Transactions on, 8(1), 183-191.

(8) Meng, Q., Khoo, H. L., & Cheu, R. L. (2008). Microscopic traffic simulation model-based optimization approach for the contraflow lane configuration problem. Journal of Transportation Engineering, 134(1), 41-49.

(9) Hausknecht, M., Au, T. C., Stone, P., Fajardo, D., & Waller, T. (2011, October). Dynamic lane reversal in traffic management. In Intelligent Transportation Systems (ITSC), 2011 14th International IEEE Conference on (pp. 1929-1934). IEEE.

(10) Daganzo, C. F. (1994). The cell transmission model: A dynamic representation of highway traffic consistent with the hydrodynamic theory. Transportation Research Part B: Methodological, 28(4), 269-287.

(11) Daganzo, C. F. (1995). The cell transmission model, part II: network traffic. Transportation Research Part B: Methodological, 29(2), 79-93.

(12) Braess, P. D. D. D. (1968). Über ein Paradoxon aus der Verkehrsplanung. Unternehmensforschung, 12(1), 258-268.

(13) Li, Y., et al. (2003). "A decomposition scheme for system optimal dynamic traffic assignment models." Networks and Spatial Economics 3(4): 441-455.

(14) Ziliaskopoulos, A. K. (2000). A linear programming model for the single destination system optimum dynamic traffic assignment problem.*Transportation Science,34*(1), 37-49.

(15) Shen, W., & Zhang, H. M. (2014). System optimal dynamic traffic assignment: Properties and solution procedures in the case of a many-to-one network. Transportation Research Part B: Methodological, 65, 1-17.

(16) Carey, M., Bar-Gera, H., Watling, D., & Balijepalli, C. (2014). Implementing first-in–first-out in the cell transmission model for networks. Transportation Research Part B: Methodological, 65, 105-118.

(17) Doan, K., & Ukkusuri, S. V. (2012). On the holding-back problem in the cell transmission based dynamic traffic assignment models. *Transportation Research Part B: Methodological, 46*(9), 1218-1238.

(18) Carlino, D., Depinet, M., Khandelwal, P., & Stone, P. (2012, September). Approximately orchestrated routing and transportation analyzer: Large-scale traffic simulation for autonomous vehicles. In *Intelligent Transportation Systems (ITSC), 2012 15th International IEEE Conference on* (pp. 334-339). IEEE.

(19) Carlino, D., Boyles, S. D., & Stone, P. (2013, October). Auction-based autonomous intersection management. In *Intelligent Transportation Systems-(ITSC), 2013 16th International IEEE Conference on* (pp. 529-534). IEEE.

(20) Dresner, K., & Stone, P. (2004, July). Multiagent traffic management: A reservation-based intersection control mechanism. In *Proceedings of the Third International Joint Conference on Autonomous Agents and Multiagent Systems-Volume 2* (pp. 530-537). IEEE Computer Society.

(21) Dresner, K., & Stone, P. (2006a, July). Traffic intersections of the future. In *Proceedings of the National Conference on Artificial Intelligence* (Vol. 21, No. 2, p. 1593). Menlo Park, CA; Cambridge, MA; London; AAAI Press; MIT Press; 1999.

(22) Dresner, K., & Stone, P. (2006b, May). Human-usable and emergency vehicle-aware control policies for autonomous intersection management. In *Fourth International Workshop on Agents in Traffic and Transportation (ATT), Hakodate, Japan.*

(23) Fajardo, D., Au, T. C., Waller, S., Stone, P., & Yang, D. (2011). Automated intersection control: Performance of future innovation versus current traffic signal control. *Transportation Research Record: Journal of the Transportation Research Board*, (2259), 223-232.

(24) Kesting, A., Treiber, M., & Helbing, D. (2009). Enhanced Intelligent Driver Model to Access the Impact of Driving Strategies on Traffic Capacity. *arXiv preprint arXiv:0912.3613*.

(25) Levin, M. W., & Boyles, S. D. (2015). Intersection Auctions and Reservation-Based Control in Dynamic Traffic Assignment. In *Transportation Research Board 94th Annual Meeting* (No. 15-2149).

(26) Li, Z., Chitturi, M., Zheng, D., Bill, A., & Noyce, D. (2013). Modeling Reservation-Based Autonomous Intersection Control in VISSIM. *Transportation Research Record: Journal of the Transportation Research Board*, (2381), 81-90.

(27) Schakel, W. J., Van Arem, B., & Netten, B. D. (2010, September). Effects of cooperative adaptive cruise control on traffic flow stability. In *Intelligent Transportation Systems (ITSC), 2010 13th International IEEE Conference on* (pp. 759-764). IEEE.

(28) Schepperle, H., & Böhm, K. (2007). Agent-based traffic control using auctions. In *Cooperative Information Agents XI* (pp. 119-133). Springer Berlin Heidelberg.

(29) Shladover, S., Su, D., & Lu, X. Y. (2012). Impacts of cooperative adaptive cruise control on freeway traffic flow. *Transportation Research Record: Journal of the Transportation Research Board*, (2324), 63-70.

(30) Van Arem, B., Van Driel, C. J., & Visser, R. (2006). The impact of cooperative adaptive cruise control on traffic-flow characteristics. *Intelligent Transportation Systems, IEEE Transactions on*, *7*(4), 429-436.

(31) Vasirani, M., & Ossowski, S. (2010). *A market-based approach to accommodate user preferences in reservation-based traffic management*. Technical Report ATT.

(32) Vasirani, M., & Ossowski, S. (2012). A market-inspired approach for intersection management in urban road traffic networks. *Journal of Artificial Intelligence Research*, 621-659.

(33) Levin, M. W., & Boyles, S. D. (2015). Effects of Autonomous Vehicle Ownership on Trip, Mode, and Route Choice. In *Transportation Research Board 94th Annual Meeting* (No. 15-2149).

Bus Routing Problem for KIPP Charter Schools
Michael W. Levin
Stephen D. Boyles

Abstract

KIPP provides school bus service to the majority of students over a relatively large geographic region. We applied Clarke and Wright's (1964) heuristic to quickly find routes that adhere to capacity and travel time constraints. These routes improved transportation spending and reliability significantly over their previous routes.

Key words: school bus routing; vehicle routing problem; public transit

KIPP is a system of free college preparatory schools to promote higher education in low socio-economic status students. In Austin, as of 2014, KIPP had over 3000 students enrolled, and due to student demographics, the majority of students relied on school buses for transportation. Because Austin has only two campuses, KIPP's students may not live in nearby neighborhoods, necessitating city-wide bus service. Currently, bus routes are determined by hand.

Because KIPP is committed to providing free, quality education, transportation costs cannot be passed on to students, so the problem is to minimize cost while maintaining a minimum level of service. This falls within the class of vehicle routing problems (Toth and Vigo, 2001). Although commercial software packages are available for school bus routing, due to the associated costs and their relatively small problem size, KIPP decided instead to work with the Data-Supported Transportation Operations and Planning Center, which combines research in transportation with education to disseminate research findings for practical implementation.

The bus routing problem faced by KIPP is sufficiently complex to benefit from broad sensitivity analyses in algorithm choice, estimating demand, and selecting constraints on travel time and other performance criteria. However, such analyses fall outside the interests and scope of KIPP as well as the problems faced by many smaller organizations. The goal of this practice summary is not to describe these analyses – as their outcome may depend on the specific problem – but to demonstrate how reasonable choices for these questions culminating in a simple software package can result in significant improvements in cost and reliability. We hope that other similar organizations for which complex commercial software is not cost-effective might also benefit by similar methods. These results might also encourage practitioners to offer low-cost, simple alternatives to existing commercial software targeted to small school districts.

We used Clarke and Wright's (1964) heuristic in a custom software package incorporating demand and travel time estimations to create a routing solution. The Clarke-Wright heuristic finds separate routes for each stop then merges routes greedily to minimize an objective. The Clarke-Wright heuristic has been previously applied to school bus routing by Russell and Morrel (1986), who developed a modified "many-to-several" heuristic for bus service for a small number of special-education students. This paper discusses the potential benefits of using the original Clarke-Wright heuristic for a much larger problem size. During the 2013-2014 term, KIPP buses served nearly 1600 students in three age groups traveling to two separate campuses. Observations from using our method in the 2014-2015 term show significant improvements in total transportation spending and reliability despite 25% greater demand.

Solving this problem required consideration of several practical details. Minimizing bus operating time was chosen as the objective function because school start and end times for KIPP are close to peak hours for congestion and time-based driver salaries comprise a significant fraction of bus operating costs. To estimate travel times, we calculated average travel times per

road segment from models of AM and PM peak hour traffic in VISTA (Ziliaskopoulos et al., 2000), which solves dynamic traffic assignment. To avoid confusion to students, routes optimized for the AM peak were used for the PM peak after verifying they met all constraints.

The quality of service required two constraints. First, students should not be on the bus for more than an hour each way. Second, buses should have seating for all students served. Since around 60% of students take the bus, we had to estimate maximum ridership per stop. Because of the geographically large area that KIPP provides service to, bus stops are major locations, such as libraries, schools, or stores, that are easy to find, and at which 20-30 students can congregate. However, ridership specific to neighborhoods is not known, and while student counts at each stop can be collected, these change from day to day due to weather conditions, after-school activities, changes in parental-work patterns, or other unusual events. Therefore, we estimated demand by finding the closest bus stop for each student address through Google Maps API, and reducing the demand at each stop to 60%. This was reasonable because of the nearly uniform low socio-economic demographic of the student population.

We implemented our solution in Java, creating an application with two parts: estimating demand, and generating bus routes. This was used to generate routes for the 5 schools that KIPP operates in Austin. For simplicity and due to bus capacity that varies with student age group, we found routes for each age group separately. Computation for the Clarke-Wright heuristic required less than a second for each school on modern hardware, making this tractable for analyzing different demand scenarios. Using our travel time and ridership data, we compared our 45 routes for the 2013-2014 year with KIPP's hand-created routes for 1578 students over 62 stops. Overall, the predicted total operating time was reduced by 9.8% in the morning and 9.4% in the afternoon, with the differences due to time-dependent traffic conditions. Most of the improvements in total operating time came from greater use of the constrained resources. For most routes the maximum student travel time was close to the constraint of 1 hour or the bus capacity was mostly utilized.

KIPP began using our software for routing at the start of the 2014-2015 school year, and student demand increased 25% necessitating significant changes to the routing. Therefore we do not have direct observations in operating time reductions. However, our routing made several notable improvements in reliability. Overall, on-time arrivals in October increased from 82.9% in 2013 to 91.7% in 2014. In addition, the total number of complaints decreased by 21.4% despite the greater demand. Since we better adhered to demand constraints, KIPP was also able to eliminate "follow-along buses" for when student demand on a route exceeded the capacity of a single bus. As a result of the new routing, KIPP estimates that they saved $57,800 in transportation costs from August to October 2014, around 8.4% of their total spending.

Acknowledgements

References

Clarke, G. U., and J. W. Wright. "Scheduling of vehicles from a central depot to a number of delivery points." *Operations research* 12.4 (1964): 568-581.

Russell, R. A., & Morrel, R. B. (1986). Routing special-education school buses. *Interfaces*, *16*(5), 56-64.

Toth, Paolo, and Daniele Vigo, eds. *The vehicle routing problem*. Siam, 2001.

Ziliaskopoulos, Athanasios K., and S. Travis Waller. "An Internet-based geographic information system that integrates data, models and users for transportation applications." *Transportation Research Part C: Emerging Technologies* 8.1 (2000): 427-444.